Effect of Process Parameters and Double Gas Shielding on Mechanical and Metallurgical Behaviour during Gas Metal Arc Welding of Austenitic with Duplex Stainless Steel

A Dissertation Submitted
In Partial Fulfillment of the Requirements
for the Degree of

Master of Engineering

in

Production Engineering

By

RAMESH KUMAR
(Registration No. 801282016)

to the

MECHANICAL ENGINEERING DEPARTMENT

THAPAR UNIVERSITY, PATIALA

July, 2014

CERTIFICATE

I hereby declare that the thesis entitled **Effect of Process Parameters and Double Gas Shielding on Mechanical and Metallurgical Behaviour during Gas Metal Arc Welding of Austenitic with Duplex Stainless Steel** is an authentic record of my study carried out as requirements for the award of the degree of **Master of Engineering** in **Production Engineering** at **Thapar University, Patiala** under the supervision of **Anirban Bhattacharya**, Assistant Professor, Mechanical Engineering Department, Thapar University, Patiala during July, 2013 to July, 2014. The matter embodied in this report has not been submitted in partial or full to any other university or institute for the award of any degree.

Date: 18/07/2014

Ramesh Kumar

It is certified that the above statement made by the student is correct to the best of my/our knowledge and belief.

(ANIRBAN BHATTACHARYA)
Assistant Professor
Mechanical Engineering Department
Thapar University, Patiala - 147004

Countersigned by

Dr. AJAY BATISH
Professor & Head
Mechanical Engineering Department
Thapar University, Patiala - 147004

Dr. S.K MOHAPATRA
Dean of Academic Affairs
Thapar University, Patiala - 147004

Dedicated to

My Grand Father & Grand Mother

Acknowledgements

With deep sense of gratitude i express my sincere thanks to my guide **Anirban Bhattacharya,** Assistant Professor for their valuable guidance, proper advice and constant encouragement during the my work on this seminar.

I also feel very much obliged to **Dr. Ajay Batish**, Professor and Head of mechanical Engineering Department.

A very special thanks and reward to non-teaching staff members **Mr. M. Suri, Mr. Surender, Mr. Rath, Mr. Roshan, Mr. Rajinder, Mr. Narender,** of Central Workshop, Thapar University, Patiala for their help during this period of work.

My very special thanks go to all my family members. Their love, affection and patience made this work possible and the blessings and encouragement of my beloved parents greatly helped me in carrying out this research work. I am also thankful to my friends **Sanchit Singla, Shanky Garg** for his help and cooperation.

I am also thankful to **School of Physics and Material Science** Department for providing microhardness test machine for our research work.

I am also wish to record my sincere thanks to the **TEQIP-II** for providing the financial support.

Finally, but most importantly, I thank Almighty God, my Lord for giving me the will power and strength to make it this far when I didn't see a light.

RAMESH KUMAR

Registration No. 801282016

iii

Abstract

Austenitic and duplex stainless steel constitutes the largest stainless family in terms of alloy type and usage. One of the most important issues, in the case of dissimilar welds, is the evaluation of proper process parameters for welds between duplex and austenitic stainless steels. The aim of present study was to investigate the effects of process parameters i.e. current, voltage, filler wire, gas flow rate, type of gas and effect of double layer or single layer shielding on desired response in gas metal arc welding of dissimilar metal joining of stainless steels. The response measured were change in weld quality by tensile strength, impact strength, microhardness, weld distortion, visual inspection of cracks and metallurgical analysis of dissimilar metal joining of AISI 304 and AISI 316 with Duplex 2205. The effect of all the input parameters are analysed using the Taguchi experimental analysis. Tensile strength of the welded specimen were studied and found that current, voltage, filler wire and flow rate were significant parameters. Toughness of the weld specimen were studied and found that more toughness is achieved with increase in voltage and current. It was also seen that more toughness is achieved by using filler wire of Duplex 2205. For dissimilar metal joining of AISI 316 and Duplex 2205 maximum value of toughness (132.435 Joules) was obtained in the welded joint of parameters 160 A, 16 V, 14 L/min, filler wire of AISI 316, He and double layer shielding with flow rate of 8 L/min. For AISI 304 and Duplex 2205 maximum value of toughness (63.765 Joule) was observed under (trial 16). Microhardness test showed that for joining of dissimilar materials for AISI 304 and AISI 316 with DUPLEX 2205 the value of hardness was mainly dependent on welding current and shielding gas flow rate. Weld distortion of the weld specimen were studied and concluded that voltage, filler wire and interaction of current × voltage were the most dependent parameters leads to change in weld distortion. Weld distortion tends to decrease with decrease in current and voltage and by using filler wire of AISI 316. The surface morphology of the welded plates was characterized by scanning electron microscopy. The effect of heat input and flow rate of shielding gas on the microscopy is discussed. Dye penetrant test showed that welding was of very good quality and there was some defects shown when using pure Helium as a shielding gas. Joint quality result showed that for both the materials in welded region there were no major flaws and inclusion except a crack observed in a particular sample of dissimilar metal joining of AISI 304 and AISI 316 with Duplex 2205.

Table of Contents

List of Figures

List of Tables

Acronyms

ANOVA	Analysis of Variance
CTWD	Contact Tip to Work Distance
DCEN	Direct Current Electrode Negative
DCEP	Direct Current Electrode Positive
DF	Degree of Freedom
GMAW	Gas Metal Arc Welding
GTAW	Gas Tungsten Arc Welding
HAZ	Heat Affected Zone
OA	Orthogonal Array
ODPP	Optimal Design Process Parameter
SAW	Submerged Arc Welding
SEM	Scanning Electron Microscope
SMAW	Shielded Metal Arc Welding
SS	Sum of Square

Chapter 1

Introduction

1.1 Introduction

Welding processes are essential for the manufacturing for large range of components that can vary from large structures like aeroplanes, bridge to small and precise componenets such as components for micro-electronics applications.

First use of arc welding is done in year 1880's by the industries. But idea of arc welding was first patented in 1881 by the Russian inventor Slavianoff. Development of coating electrodes is done in the year 1920 and after that arc welding is accepted for fabrication of critical components. Now welding is commonly used at large scale for fabrication of heavy items like ships, bridge construction and pressure vessels.

Welding is a process of joining that include two or more parts of metals which are permanently joined by heating the work piece with the help of arc and/or by applying the pressure or without pressure. During heating in welding process metallurgy of the metals or component may be affected [Norrish, 2006].

Many of the materials are joined by various welding processes in which some processes are easy to weld than other processes. So to compare these processes term 'weldability' is used. Weldability of a material depends upon the various factors like metallurgy of a material, gas absorption and evolution by the material, crack propagation of welded parts and extent of oxidation etc. If the percentage of carbon is less than 0.12 in a material the weldability of a material is good otherwise poor. Welding processes are used in the various industries include oxy acetylene welding, shielded metal arc welding (SMAW), submerged arc welding (SAW), gas metal arc welding (GMAW), gas tungsten arc welding (GTAW) etc. All processes have their own significance like resistance welding is used in automobile industry, GMAW is used for welding low carbon steels, GTAW is used for welding nuclear power plant, SAW is used in cold pressure welding whereas gas welding and shielded metal arc welding are used for general purpose welding processes on large scale.

1.2 Arc Welding

Arc welding is a joining process in which coalescence between two parts is produced by heating the work piece with the help of an electric arc, by applying the pressure or without pressure and/or with or without using filler metal. Usage of filler metal depends upon the thickness of work piece or base metal. In arc welding some processes use shielding gas and some processes use flux as a coating material on the electrode. Shielding gas and flux is used to protect the weld pool from the contamination of atmospheric air.

Generally in mechanism of arc welding arc electrons are emitted from the cathode and reaches to anode after passing from hot ionized gas. Electrons are emitted from cathode with large current and less voltage i.e. from 100 A to 2000 A current and voltage from 10 V to 80 V. For analysis purpose arc is divided into five consecutive parts such as first is cathode spot, cathode drop zone, arc plasma, anode drop zone and last is anode spot. A brief description about all these five parts and after that various processes of arc welding are discussed.

Cathode spot is that negative part of the arc from which electrons are emitted. There are generally three types of cathode spot which has been observed. These are:

a) Mobile cathode spot mode
b) Thermionic cathode spot mode
c) Normal mode

Cathode drop zone is the region after cathode spot. This region is in the gaseous form. Voltage drop in this zone is drastically of 8 V at 100 A current and increases as the current decreases.

The portion which is visible in the arc is known as arc column. That portion of arc has high temperature with low potential gradient. Potential gradient is lower than that of cathode spot and anode drop zone and varies between 0.5–5 V/mm. Anode and anode drop zone is not a fixed spot region. It is larger than cathode spot and smaller than maximum diameter of arc column. Voltage drop in anode drop zone is of the order of 1 to 3 V and with a depth of 10^{-1} to 10^{-2} mm. also when electrons reach at anode they lose their heat of condensation. That zone has a very low current density of only 200 A current.

1.2.1 Shielded Metal Arc Welding

Shielded metal arc welding is the most popular arc welding process used in industries and in general purpose worldwide. In India about 90% of the total work of welding is done with the help of shielded metal arc welding. Through the use of SMAW is decreasing due to

advancement in new welding processes like GMAW, GTAW, and SAW etc. but it is impossible to be omitted from short run jobs. Main reason for indispensable of this process is that its low running cost and less skill required for its usage.

Shielded metal arc welding is a joining process in which coalescence between two mating parts is produced by applying heat to the work piece with the help of an arc, by applying the pressure or without pressure or with or without using filler metal (as shown in Fig. 1.1). Usage of filler metal depends upon the thickness of work piece or base metal. In arc welding some processes use shielding gas and some processes use flux as a coating material on the electrode. Use of flux and shielding gas is to protect the weld bead from the contaminated atmospheric air. In SMAW process heat required for welding is obtained from the arc stuck between the coated electrode and workpiece. For the adjustment of heat required on the base metal or work piece welding current is used. If large heat is required to fuse the base metal than current is increased and arc distance is shortened while if less heat is required for diffusion than current will be lowered or arc distance will be increased.

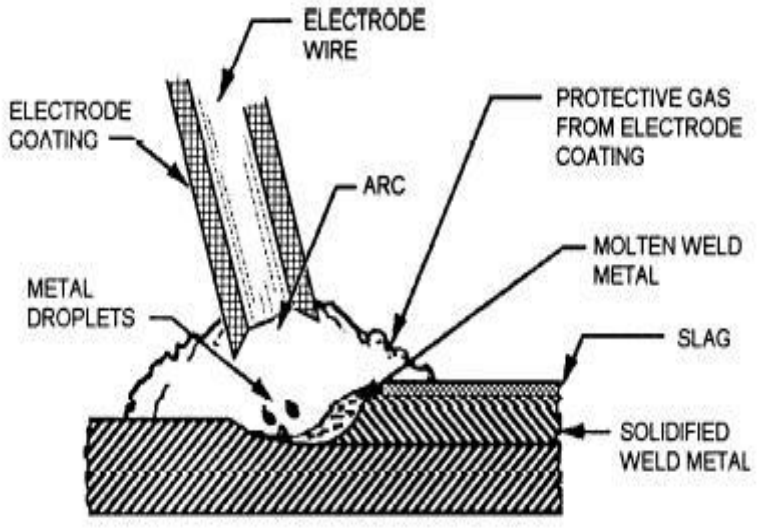

Figure 1.1: Flux shielded manual metal arc welding operation
[http://www.corrosionist.com]

During SMAW arc will heat the electrode and work piece and due to that heating electrode and work piece melts than droplets from the tip of electrode drag onto the surface of work piece and deposited at that point where welding is to be required. Flux which is coated on the electrode produces a slag to prevent the weld bead from the surrounding atmosphere air.

For a new operator there is one difficulty may arise to ignite the arc between the electrode and work piece. Generally there are two methods are used to strike the arc one is by touching

the coated electrode tip to the workpiece material and momentarily taking it away from the base metal or work piece and other is by scratching the electrode on the surface of work piece in the arc of circle. Last method is mostly used by the new operators because this method reduces the sticking of electrode from the work piece.

1.2.2 Gas Tungsten Arc Welding

GTAW process is well established as a high quality fusion welding technique. Developments in the process have extended the potential application range and offer improved process control. In 1920 a new idea comes in the mind of researchers to weld the metal with the help of non- consumable electrodes. But after a gap period of 10 years this idea was patented in USA. This process is used with the argon and helium as a shielding gas. But due to high cost of helium gas this process has not got much importance but again in 1940 in the period of Second World War this process is used for joining aluminium, magnesium and other alloys. Inert gas is used in this process so it is also known as TIG. Now a days this process is popular because it not only give good strength welding but also give good quality and smooth welding on the upper surface of base metal [Norrish, 2006].

GTAW is a joining process where coalescence between two mating parts is produced by applying the heat to the work piece with the help of electric arc between the tungsten electrode and metallic part. Shielding gas is also used for the protection of weld bead from the contaminated atmospheric air (as shown in Fig. 1.2). In this process arc is stuck with the help of high frequency unit or by touching the electrode with a scrap piece of tungsten metal. In the second method a high frequency current is super- imposed on the welding current. Than a welding torch is put near the work piece and a spark is set up between the electrode and work piece through ionised gap. Where as in second method arc is initially struck on a scrap piece and then broken by increasing the arc gap. This procedure is repeated two three times until the electrode is warm up and then finally arc is struck between the electrode and cleaned work piece. This procedure of striking the arc will avoid breaking of electrode tip, work piece contamination and tungsten loss. After striking the arc it is allowed to imping on the surface of work piece where welding is to be done. Welding is done by moving the torch as such it is used in oxy acetylene welding. In the end of welding arc is broken by increasing the gap between the work piece and electrode.

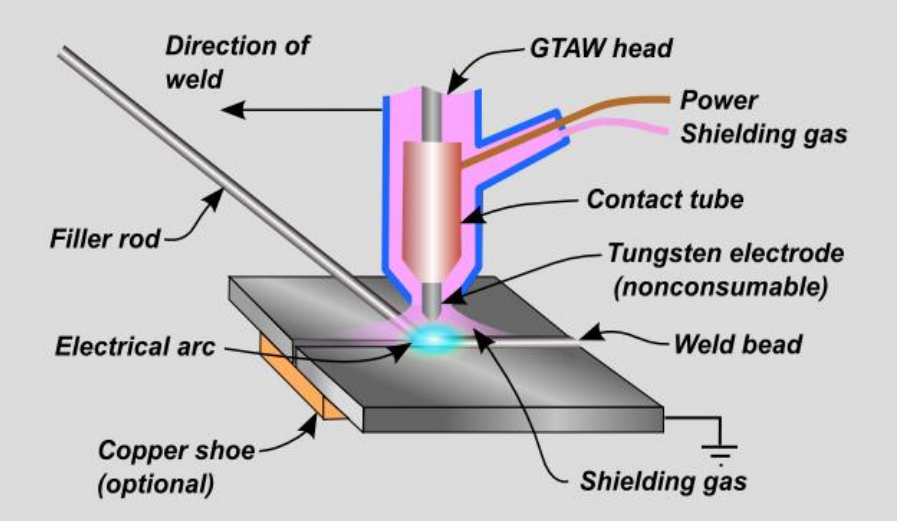

Figure 1.2: Gas tungsten arc welding operation [http://www.burnsstainless.com]

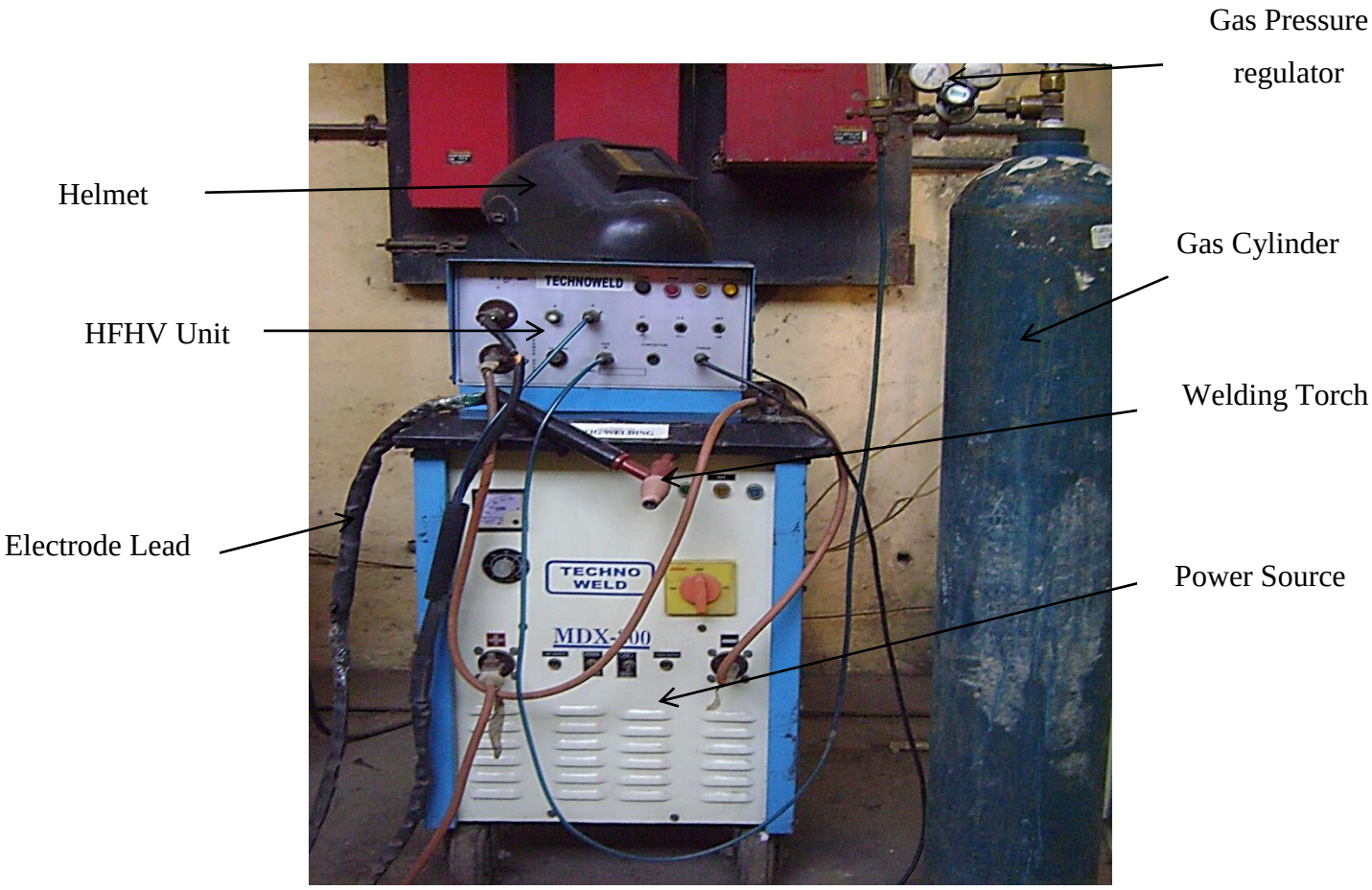

Figure 1.3: GTAW set up (**Courtesy:** Central Workshop, Thapar University, Patiala)

In GTAW welding filler wire and torch are kept at angle of 10–20 degree and 70–80 degree respectively with the flat work piece.

Torches used in GTAW welding are of two types one is water cooled torches and other is air cooled torches. When the current range is up to 200 A, air cooled torches are used and when the current range is 1000 A, water cooled torches are used.

A collet is used to hold the electrode in a GTAW torch, size of collet depend upon the diameter of electrode. Gas nozzle is weak part of GTAW it is generally made of ceramic to bear high temperature of arc.

DC Power source used for GTAW is similar as used in shielded metal arc welding with the same rating but the AC power source is de rated to 25% to compensate for current rectification. Operating current range is 3 A to 200 A and range for voltage is 10 V to 35 V with a 60% duty cycle. DC power source of electrode negative is used generally but for welding aluminium and magnesium direct current electrode negative is used for cathode cleaning to takes place [Parmar, 2011]. Tungsten rod is used as electrode for the GTAW with a melting point of 3400 ^{0}C. They provide the desired properties of high melting point, ability to emit electrons, good heat conductivity and low electrical resistance. These electrodes are classified into four types as listed in Table 1.1 below.

Table 1.1: Tungsten electrode specification for GTAW

AWS Classification	Material	Thorium %	Zirconium %	Tip colour
EWP	Pure tungsten	-	-	Green
EWTh-1	Tungsten+1%Th	0.8-1.2	-	Yellow
EWTh-2	Tungsten+2%Th	1.7-2.2	-	Red
EWZr	Tungsten+ Zirconium	-	0.15-0.40	Brown

Diameter of these electrodes range between 0.5 and 6.4 mm and length varies from 75 to 610 mm. Electrode size of GTAW depends upon the current and type of the material. If the diameter of electrode is less and current value is large than electrode inclusion will takes place in the material. If the electrode diameter is large and current is low than arc will wander erratically over electrode tip [Parmar, 2011].

1.2.3 Submerged Arc Welding

Submerged arc welding is also an joining process in which coalescence between two parts is produced with an electric arc that is set up between the bare electrode and the work piece by applying the heat and with or without applying pressure. In this process electrode and weld pool are hidden in the flux as shown in Fig. 1.4. Flux is acting as blanket for weld pool and

electrode and flux may be in the form of granular material. Electrode used is in bare form i.e. no coating is done on the electrode and is continuously feed in the weld pool and act as a filler rod. No external pressure is applied in SMAW process. This process is also pronounced as SAW.

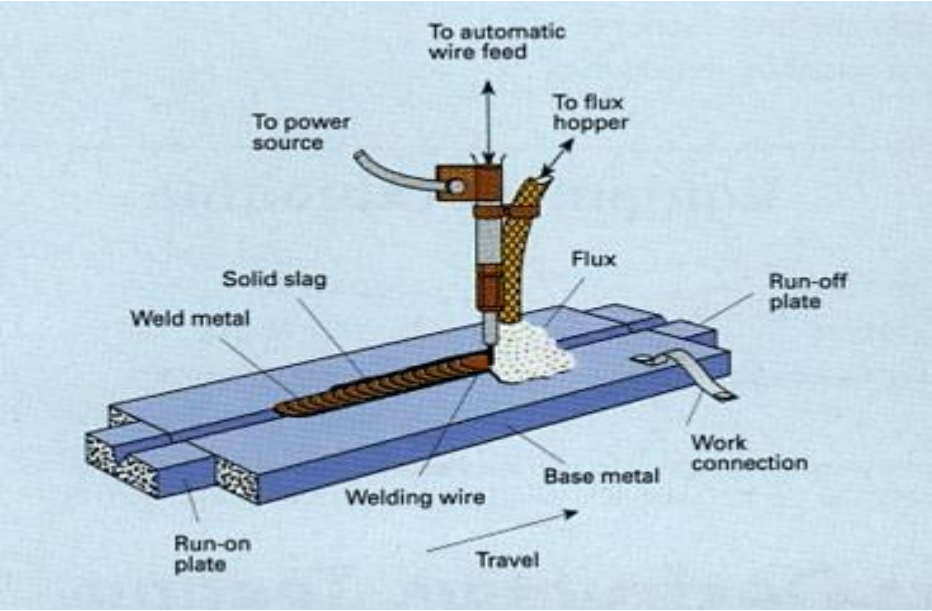

Figure 1.4: Submerged Arc Welding Operation [http://www.twi.co.uk]

In the operation of SAW trigger from the hopper is pulled than flux starts flowing from the hopper and falling on weld pool and electrode where joint is to be welded. During initiation of arc flux is non-conducting and arc is initiated by placing the steel wool in between the bare electrode and metallic part. After the initiation of arc flux will melt and deposit on the weld pool and become conductive and arc is continuously maintained through this flux. The flux which is visible on the weld bead and in the atmosphere can be reuse again. One thing should be noted that flux used on weld pool is of sufficient depth so as to reduce spatter and protect it from contamination in the atmosphere. These result in smooth weld bead. The molten flux which is deposited on the weld pool forms a slag on top of weld bead. The slag which is deposited on the weld pool peels off of its own otherwise it is removed with the help of chipping hammer. If the depth of layer is less on the weld pool than it will result in arcing and flash through the flux and it is injurious to eyes. If the flux is too large then humping of weld pool is the result and due to which narrow bead will be obtained. If flux is more than desire able quantity can cause surface pitting due to which gases cannot escape from the weld pool which is some time referred to as ‘pock marks’.

Filler rod used in SAW is of standard size of 1.6 mm to 13 mm. filler rod may be coated with copper to increase its life and provide good electrical conductivity. SAW is characterised by its high welding current of 1000 A which is 5 to 6 times higher than shielded metal arc welding and leads to high rate of material deposition. Due to its high current capacity large thickness plates can be welded up to 16 mm without any edge preparation. High deposition of material leads to high welding speed than shielded metal arc welding. Welding with DCEP produces deeper penetration than DCEN.

Welding current, I_w, is given by,

$$I_w = P/K \quad (1.1)$$

Where P is depth of penetration and k is proportionality factor.

The value of k depends upon flux used, wire diameter, electrode polarity and kind of current. For butt joint its value is in the range of 1.25 to 1.75 and for surfacing by SAW lies in the range of 1.0 to 1.15.

1.2.4 Gas Metal Arc Welding

Now a day's gas metal arc welding is dominating over other gas welding processes for the fabrication of parts. In the race period of 60 years many research work is done and progresses so far and good results are obtaining with high quality.

Gas metal arc welding is a joining process where joint between two mating parts is produced by heating with an electric arc with a continuously fed filler wire and the work piece. There is no flux used for GMAW and coated electrode but shielding gas is used to provide a shield around the weld pool to protect it from contamination of atmosphere. Generally direct current positive polarity is provided to the electrode.

GMAW Parameters

GMAW is a semi-automatic welding process in which a welding gun is hold by the operator and he can operate it according to its desire. For the initiation of welding arc it is essential to set the process parameters like welding current, arc voltage, feed rate of filler wire, travelling speed, electrode stick out, shielding gas, flow rate of gas, welding position etc. So these parameters are discussed as below. The welding current drawn by the GMAW depends upon the interactions of process parameters such as voltage, gas flow rate and electrode stick out. To achieve constant penetration than it is necessary to maintain a constant stick out distance.

Arc Voltage

Flat characteristic power source is used in GMAW by setting the open circuit voltage. There is slight drop in the V-I characteristic when there is difference in open circuit voltage and actual value of arc voltage. When arc voltage is changed it lead to change in bead geometry, also led to change in microstructure. When the arc voltage is too low the metal transfer is either by short-circuit mode or by dip transfer mode. These mode leads to successful processes and they take place at lower metal temperature with least loss of alloying element.

Wire Feed Rate

In GMAW of flat characteristic power source with constant voltage wire feed rate varies with the welding current. Graph between these variable is shown in Fig. 1.5. From Fig. 1.5 it is realized that graph is linear initially at lower feed rate and melting rate become non-linear if wire feed speed is further increased. For the same wire feed rate increase leads to increase in welding current. An increase in welding current, with other variable constant, results in increase depth of penetration and weld depth, increased deposition rate and increase in weld bead size at a given cross section.

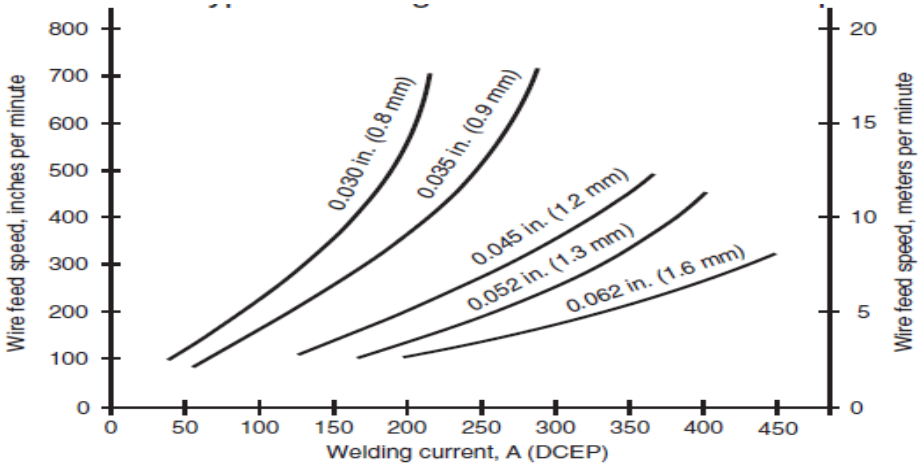

Figure 1.5: Graph showing typical welding currents vs. wire feed speeds [Kobe Steel, 2011]

Travel Speed

Weld penetration is increase or decrease with increase or decrease in travel speed. From the pilot work it is seen that with increase in welding speed there is decrease in weld bead width

and vice versa. By reducing the speed sometime leads to decrease in penetration due to sliding of excessive molten metal from the weld bead and result in shallow weld bead. So increasing heat input rate due to reduced speed shows itself in the form of increased weld width and the reverse is true for the increase in welding speed. Figure 1.6 shows the normal weld bead formed at appropriate speed and humping weld bead at faster speed.

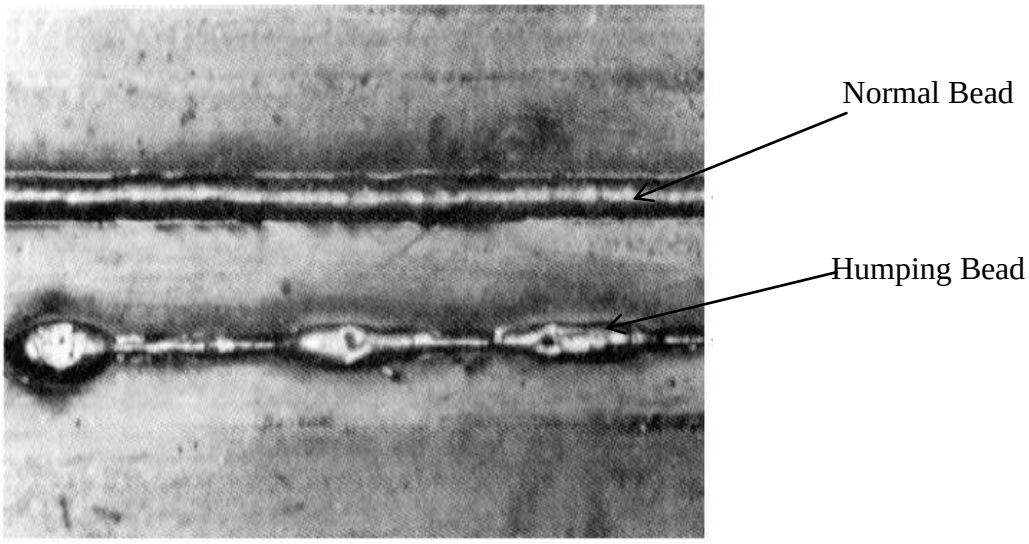

Figure 1.6: Weld Bead at Low Speed and High Speed [Kobe Steel, 2011]

Electrode Stickout

Electrode stick out is the distance between the tip to tip of the nozzle and electrode filler wire. Electrode stick out is also known as contact tip to work surface distance (CTWD) as shown in Fig. 1.7. For the metal deposition rate and the bead geometry it is the important parameter. When stick out electrical resistance is increasing it results in preheating of electrode filler wire, results in lower requirement of welding current at any feed rate. If stick out distance is more which result in excessive metal being deposited and spatter on the material surface. To short distance of electrode stick out result in damage of nozzle and large distance decreases nozzle efficiency.

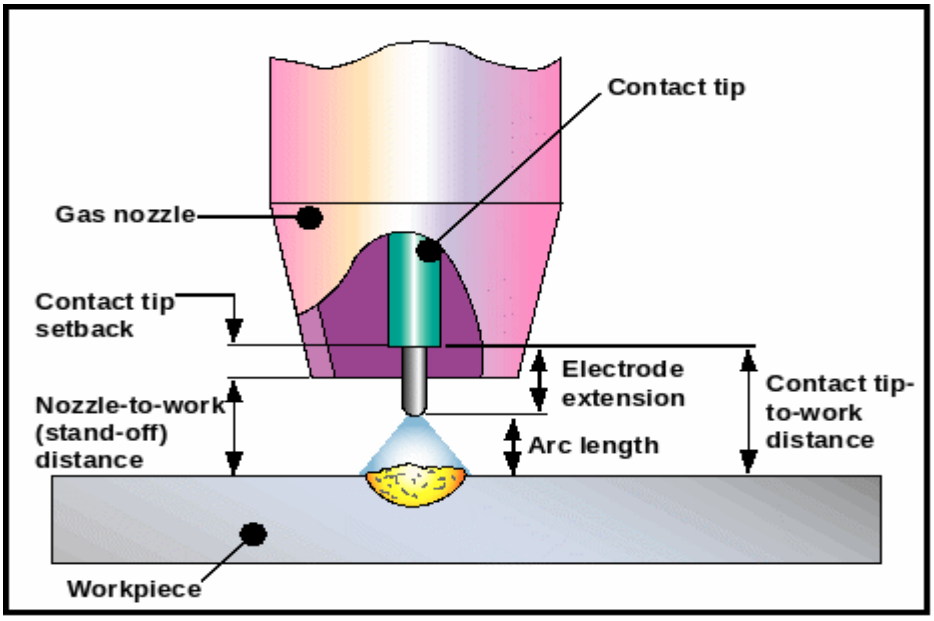

Figure 1.7: Contact tip to work distance [http://dc347.4shared.com/]

Stick out is usually kept between 5-15 mm for short-circuiting transfer and 16–25 mm for other type of metal transfer. Normal nozzle to work distance should be approximately 1-1.5 times the inner diameter of gas being used.

Gas Flow Rate

Another important parameter in GMAW is gas flow rate. Proper gas flow rate is necessary to get defect free welds. If gas flow rate is less than requirement porous bead is obtained and also if it is more than requirement than blowing of metal from the weld pool takes place (as shown in Fig. 1.8). If nozzle to work piece distance is more than more gas flow rate is required and if distance is less than less gas flow rate is required.

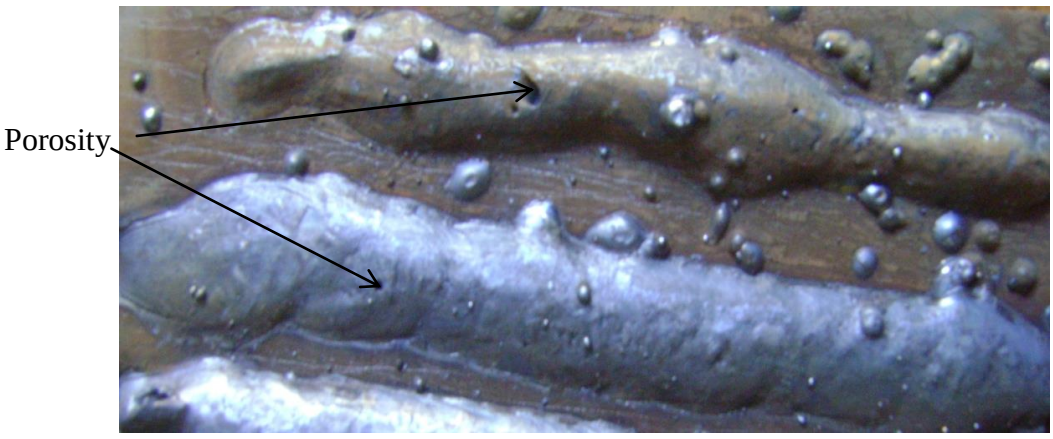

Figure 1.8: Porosity in material due to lack of shielding gas

Proper location of grounding is necessary to minimize the arc blow especially for ferromagnetic materials. So it is necessary to weld always away from the grounding of the work piece table.

Welding Position

Geometry of the weld bead is dependent on the position of the work piece with respect to the welding gun or nozzle. Most commonly used welding process is down hand welding position and gives the most satisfactory bead shape. In this welding position all modes of metal transfer can be easily utilised. Sometimes overhead and vertical welding positions require the metal transfer either by spray transfer or short circuit transfer mode. Filler wire diameter of 1.22 mm diameter is recommended to be used for these positions as otherwise the weld pool size becomes too large to control easily. Bead size is also small in these positions.

Electrode to Work Angle

From the pilot work done on duplex stainless it is concluded that electrode to work angle also affect the weld bead geometry. In automatic welding gun is usually perpendicular to work piece, whereas in semi-automatic welding gun is kept at some angle to the work piece with forehand and backhand welding position. If the plate thickness is more than backhand welding is used and if the plate thickness is less than forehand welding technique is used.

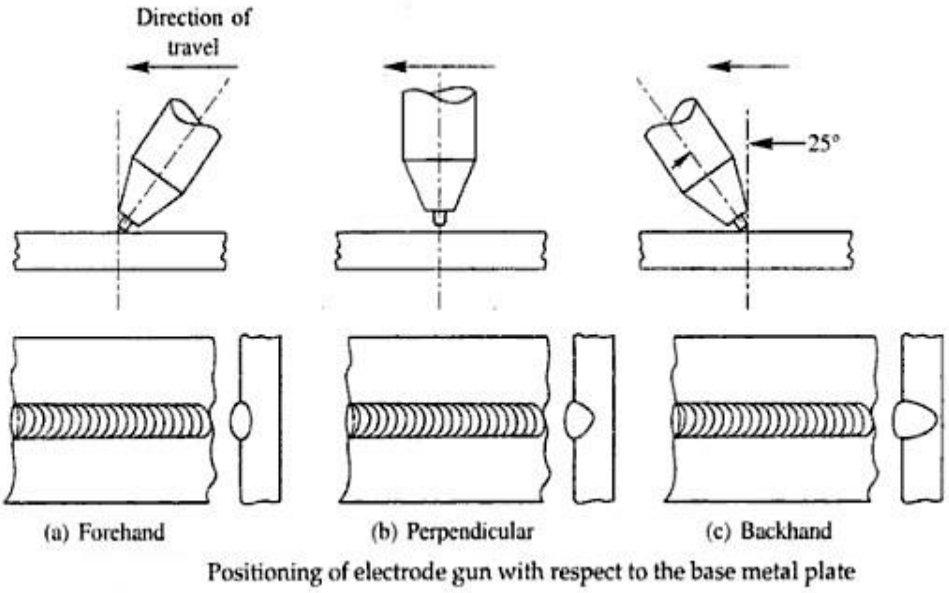

Figure 1.9: Different welding technique [http://www.zirconium-tungsten-electrode.com]

The forehand welding position shows in Fig 1.9 results in weld with shallow penetration but wider bead. The backhand welding gives a narrow weld with deep penetration. 60 to 80

degree electrode to work angle is recommended for backhand welding and for forehand welding 75 degree angle is recommended.

Electrode Size

Filler wire of GMAW process also affect the weld bead geometry for the same current. Filler wire of Lower diameter gives the more penetration. By using filler wire of larger diameter shallow penetration and wider bead is obtained.

Filler wire with smaller diameter is used because of following reasons.

a) For the adjustment of arc length.

b) Deposition of molten metal with spray transfer.

c) Easy to handle and spool of filler wire.

d) To obtain the high deposition efficiency.

With number of advantages of the use of thin wires it is to be kept in mind that the feeding problem increases considerably with the decrease in diameter and that the welding current range, over which a wire can be used. Also smaller diameter wires are more costly on weight bases. From the above parameters it is selected that a trial run of bead is made before starting a final operation and adjust the parameters according to it. After finalizing the parameters easy arc initiation is achieved with smoother weld pool of fewer spatters. Electrode movement is perhaps the last major operator control to achieve good quality weld in GMAW. Most commonly method used is drag and stringer bead pattern in which gun is moved with oscillation in a straight path. To stop the work it is necessary to withdraw the welding gun by increasing the nozzle to work piece distance so that in the end proper crater is obtained.

1.3 Filler Wire and Shielding Gases in GMAW

In GMAW filler wire and shielding gases are used as consumables. To weld different materials with the help of GMAW than it is necessary to select carefully electrode wire and shielding gas. The electrode wire and shielding gas selected is such that they should provide best compatibility in between base metal and filler wire. Much research work has been done so far to get good compatibility between base metal and filler wire. Also there are many national and international guidelines to follow these standards.

Filler wires are generally sold in spools of 12.5 kg each with a careful layer winding to feed into the gun with least risk of snagging. If tempering is more in wire then there is

feeding difficulties and springing action. Filler wires are friction loaded on reels so as to unwind under slight tension. Mechanical locking arrangement is provided in the machine so as to avoid over feeding of the wire. An arc is created between the work piece and a continuously consumable filler wire. The need of operator is to only focus on directing the GMAW nozzle at the position where welding is to be done with proper motion and speed. Filler wires are available with different diameter from 0.8 to 1.2 mm diameter.

Welding Wire/Method Recommendations

Table 1.2: Wire type with consideration

Type of filler wire	Consideration
Solid Carbon-Steel ER70S-6	Used with carbon dioxide or mixture of argon and carbon Carbon dioxide provides deeper penetration 75% Argon/25% CO_2 has fewer spatters than CO_2.
Flux Cored/ Carbon-Steel E71T-GS	Shielding gas is not required. Good for outdoor conditions. Suitable for dirty, rusty, painted materials. More temperature than solid wires.
Solid Aluminium ER-4043 ER-5356	Must be used with Argon or other Argon/ Helium mixes. ER-4043 recommended to be used with spool guns for best results. Strong welds and easier feeding is difficult with ER-5356.
Solid Stainless Steel ER308/308L	Use with Helium/Argon/CO_2 mixtures. For austenitic stainless steel base metals.

AWS GMAW Electrode/Rod Classification System – Stainless Steel

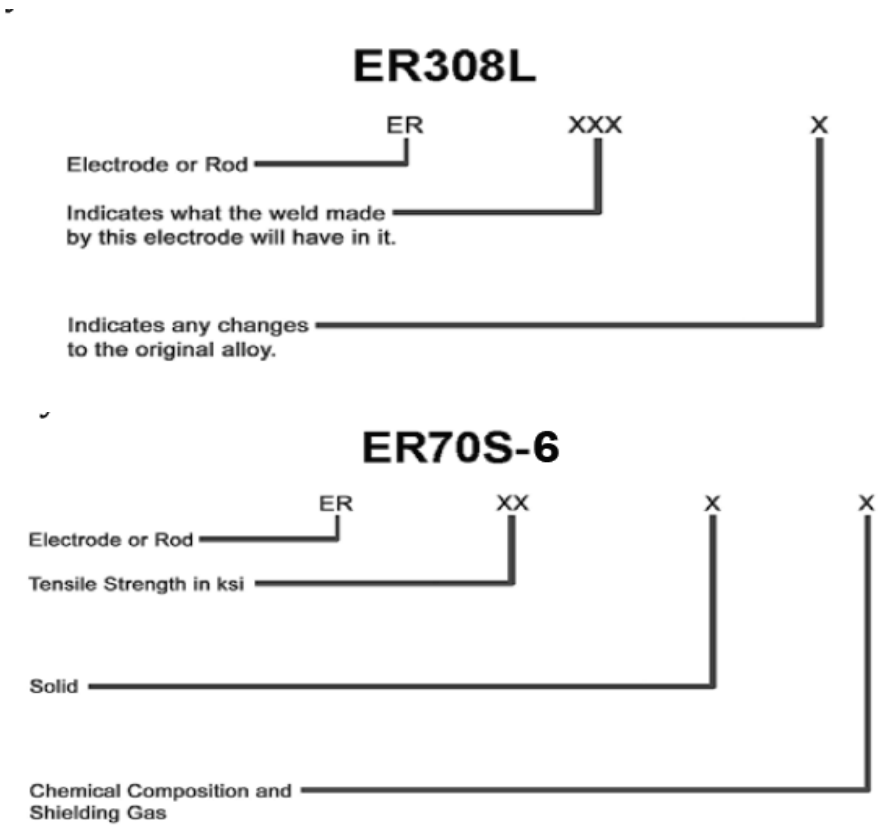

Figure 1.10: Coding of filler wire

Figure 1.10 shows the coding of filler wire, ER308L code we can conclude the properties of stainless steel. In the above symbol ER designate for the electrode or rod. XXX indicates what the weld made by this electrode will have in it and X indicates any change to original alloy. Whereas in the second code ER indicates electrode or rod, XX indicates tensile strength, X indicates solid and another X after hyphen indicates chemical composition and shielding gas.

Shielding Gases

Most commonly shielding gases used for arc welding processes such as GTAW, GMAW and plasma arc welding processes are argon, helium and carbon dioxide. There are some gases also such as oxygen; hydrogen and nitrogen are used in mixture with above gases. So these gases are classified into two groups

a) Inert gases like argon and helium.
b) Reactive gases such as carbon dioxide, hydrogen, oxygen and nitrogen these gases dissolve and react with metals.

Inert or semi-inert shielding gases are commonly used in several welding processes, So GMAW and GTAW, also known as metal inert gas and tungsten inert gas. Purpose of shielding gas is to protect the weld area from contamination of atmospheric gases and water vapour. Atmospheric gases lower down the quality of the weld and make the welding process more difficult. Other arc welding processes like submerged arc welding process use other methods of protecting the weld from the atmospheric gases for example, uses of flux.

Argon

Argon is a shielding gas which is non-combustible, non-explosive obtained from the atmospheric air by refrigeration and fractionation. Argon is 1.23 times heavier than atmospheric air. This gas is stored in cylinders of black colour in gaseous state. Cylinders for argon gas are painted black at bottom and painted white at top. When cylinder is full of gas it is kept at a pressure of 150 atmospheres. A pressure regulator for argon gas is painted black in colour. To adjust the flow rate of gas flow meter is attached to the pressure regulator. Flow rate for shielding gas can be varied from 4-40 L/min. but generally flow rate of 10 to15 L/min is used.

Argon gas is specified by its grades which are discusses as:

Grade A (99.99 % pure or more) argon is used for welding active and rare metals.

Grade B (99.96 % pure) used for welding of magnesium and aluminium alloy.

Grade C (99.9 % pure) argon is used for welding stainless steel and high strength alloy.

Helium

Helium is chemically inert, has a lower density than air and requires a higher arc voltage (at the same current and arc length) than argon. The resultant increase in power produces increased heat input and fusion area although lower depth-to-width ratios are normally experienced. The cost of helium is considerably higher than that of argon, but the welding speeds that are usually obtained make it a viable option, particularly for high-conductivity materials. One problem with helium is that due to its lighter weight it can deviate its path from the weld pool so to eliminate this problem high flow rate of shielding gas is maintained in case of helium. With helium it is possible to weld 30-45% faster than using argon gas.

Carbon Dioxide

Carbon dioxide is chemically active, but has a higher density than air. It can dissociate in the arc to release oxygen and carbon monoxide and this can result in a reduction in the weld metal content of elements such as silicon, manganese and titanium and an increase in carbon. Because of its chemical activity its use is restricted to GMAW welding of steel. The arc voltage is 1–2 V higher in CO_2 (for an equivalent current and arc length) than that found in

argon-based mixtures and the heat input is slightly higher resulting in increased fusion. Transfer behaviour, operating tolerances and arc stability are generally poor, especially at high currents [Norrish 2006]. Carbon dioxide is prepared by calcination of coke or anthracite in specially designed boilers and collected from natural resources. Penetration characteristics of CO_2 are similar to helium gas due to similarity in weights of the gases. CO_2 where used should be free from moisture because in the presence of moisture it forms hydrogen and result in porous bead. Due to greater electrical resistance, current should be higher for CO_2 than the helium and argon.

Other Gases

Oxygen is odourless, colourless gas which combines with other gases to form oxides for example it combines with CO_2 and form CO which may get entrapped in weld pool and result in void. So to avoid this problem Mn and Si are added in it.

Hydrogen is the lightest gas which is added in maximum up to 3% in the argon or helium. It can also present in arc atmosphere due to the presence of moisture. From the study of research papers it is concluded that with increasing in hydrogen in other gases lead to more penetrated weld pool.

Nitrogen is another gas used as shielding gas. It is available in atmosphere in large amount. This is soluble in molten steel but solubility is less at room temperature. Addition of nitrogen in the weld pool results in good strength and hardness of weld. But too much increase in hardness results in lack of ductility due to which there are more chances of cracking.

Different Colours Used on Cylinders for Different gases

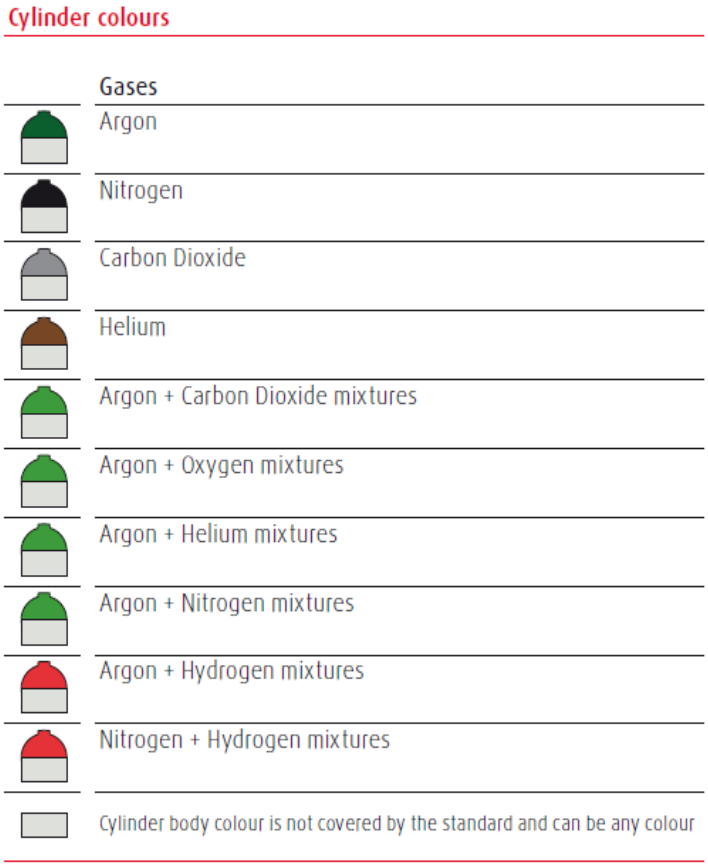

Figure 1.11: Different colours used on cylinders for different gases [http:/www.boconline.co.uk]

Most commonly gases used for GMAW welding is argon (Ar) or helium (He), or a mixture of both these inert gases. Sometimes, oxygen (O_2), hydrogen (H_2) or carbon dioxide gas is used as it stabilizes the arc, increase penetration depth, increase the welding speed improve the fluidity and help to increases the many more mechanical properties of materials.

The Table 1.3 indicates the different choice of shielding gas for GMAW welding, considering different types of materials and arc types.

Table 1.3: comparison of shielded gas and base materials [http:/www.smt.sandvik.com]

Material → / Gas type↓	Austenitic stainless steel	Duplex stainless steel	Super-duplex stainless steel	Ferritic stainless steel	High-alloy austenitic stainless steel	Nickel alloy
Argon	▪	▪	▪ a	▪	▪	▪
Helium	▪	▪	▪ a	▪	▪	▪
Argon + Helium	▪	▪	▪ a	▪	▪	▪
Argon + 3% O_2	▪ b	▪ b	▪ b	▪ b	▪ c	-
Argon + 3% CO_2	▪ e	▪ e	▪ e	▪ e	▪ c	-
Argon + 30% Helium + 3% O_2	▪ f	▪ f	▪ f	▪ f	▪ c	-
Argon + 30% Helium + 3) CO_2	▪ f	▪ f	▪ f	▪ f	▪ c	-
Argon + 30% Helium + 2% N_2	-	-	▪	-	▪ g	-

Effect of different shielding gas on the different metallic materials is pointed as:

a) Argon is most preferred in GMAW welding.
b) More fluidity as compared to argon.
c) Argon is prefferable.
d) Not suitable for spray-arc welding with low carbon.
e) More fluidity as compared to argon. Suitable for short-arc transfer mode.
f) More fluidity as compared to argon. Suitable for short-arc transfer mode.
g) For alloys in which nitrogen is present.

1.4 Applications, Merit and Demerits of GMAW

For every welding process it may be arc welding, friction welding, and resistance welding or whatever there is always some advantages, disadvantages and limitation are discusses as follow:

Merits

a) Lower cost of electrodes.
b) Due to continuously feed of electrode much faster process than GTAW.
c) Deeper penetration can be obtained.
d) Both thin and thick material can be welded.
e) Higher travel speed with GMAW reduces distortion.
f) Reduce weld fume generation.

g) Generally lower metal deposition with GMAW as compared to other open arc welding processes.

Demerits

a) More complex welding equipment's are required as compared to other welding processes.
b) In some shielding gases air draft may be dispersed so it cannot be well suited for outdoors.
c) Cooling rate of weld metal is higher than other processes and results in slag deposition over weld metal.
d) GMAW process is complex than other processes like GTAW because numbers of parameters are required to be controlled effectively to achieve good results.

Limitations

a) The lower heat input with short-circuit transfer mode restricts its use to thin materials.
b) Higher heat input with axial spray transfer mode restricts its use to thick materials.
c) Higher heat input with axial spray transfer mode restricts its use to flat and horizontal welding positions.
d) The use of helium as a shielding gas is more expensive.

1.5 Stainless Steels

Stainless steel are iron based steel which contains at least 10.5% chromium. They are mostly characterised by its chromium content. Main aim of chromium is to provide a thin layer of itself on surface of steel and prevent it from oxidation and corrosion, chromium alloyed steels absorbs O_2 from the atmospheric gases and provides a layer on steel surface. A steel mechanical properties characterised by its microstructure. So based on the microstructure steels can be classified into following groups:

a) Austenitic stainless steel
b) Ferritic stainless steel
c) Duplex stainless steel
d) Martensitic stainless steel
e) Precipitation hardening stainless steels

These above steels are discussed in details with their chemical composition, properties and applications.

1.5.1 Austenitic Stainless Steel

Austenitic stainless steel includes the series of 200 or 300 series. From survey in market it has been concluded that 304 grade steel is mostly used. Steels of these series are characterised by its chromium and nitrogen content. The austenitic stainless steels contain 18–20% Cr, 12–20% Ni, up to 0.10% C and small amounts of a few other elements such as molybdenum, nitrogen, phosphorus, sulphur etc. The balance between the Chromium and Nickel is normally adjusted to provide a microstructure of austenitic stainless steel. Nickel and nitrogen act as a austenitic stabilizer. Austenite stainless steels are characterized by good tensile strength and more toughness over a large temperature range and oxidation resistance to over 538 °C. This group include the series of 300. For welding of austenitic steel filler metal used is same as that of base metal means both are austenitic in nature [TMR Stainless, 2009].

1.5.2 Ferritc Stainless Steel

The ferritic stainless steels contain 11 to 28% Cr, up to 0.18% C and some ferrite promoters Al, Nb, Ti and Mo. They are ferritic over a wide range of temperature so they are not transform to austenite steels and are not harden able by heat treatment. This group includes the series of 400. Ferrite stainless steels are characterized by grain growth at HAZ and lower toughness. Filler wire of higher chromium content is used to weld ferritic stainless steels. [TMR Stainless, 2009].

1.5.3 Martensitic Steel

Martensitic steels contain 11–18% Cr and more than 1% C. These steels are characterised by its high carbon content than other steels. On heating these steels can be transformed to austenite and then upon rapid cooling turns into martensitic. Due to large carbon content they are harder in nature. They are majorly found in the 400 series. They have large tendency of cracking during cooling. Filler wire of same Cr and CO_2 is always used with the base metal. [TMR Stainless 2009].

1.5.4 Duplex Stainless Steel

Duplex steels come in the categories of both austenitic and ferrite phases i.e. they have good corrosive resistance as well as strength and ease of fabrication. Duplex stainless steels have the tendency to solidify as fully ferrite, but during the cooling of duplex stainless steel half of

the ferrite converts into austenite approximately at 1040 °C. There is always lower amount of nickel and chromium content as compared to the austenitic stainless steel. Nitrogen upto 0.15% is added to transform the ferrite structure to austenitic structure. Duplex stainless steels are ferromagnetism in nature. These steels have combined the properties of both austenitic and ferritic stainless steel. The most common grade is DUPLEX2205 consisting of 15% Cr, 8% Ni, 3% Mo and 0.15% N [TMR Stainless, 2009].

1.5.5 Precipitation Hardening Stainless Steel

Precipitation hardening stainless is categorized into three steels–martensitic, semi austenitic and austenitic steel. The martensitic stainless steels can be obtained by quenching from the austenitic temperature. These steels contain less than 0.10% C, so they are not hard in nature but hardness is obtained by aging of these materials at 550 °C. The semi austenitic stainless steels will not transform to martensitic when cooled from the austenitic temperature because the martensitic transformation temperature is below room temperature. This removes alloy elements from solution, thereby destabilizing the austenite, which raises the martensitic transformation temperature so that a martensitic structure will be obtained on cooling to room temperature. Aging the steel is done at 550 °C that will relieve stresses and temper the martensitic structure to increase toughness [TMR Stainless, 2009].

1.6 Weldability Issues of Stainless Steel

Weldability also referred to as join ability means ability of a material to weld. There are some materials which can be weld easily and some processes are difficult to weld. So term weldability is used to check welding process, we are use is capable for welding or not.

The weldability of steel, with addition of hydrogen leads to cold cracking and reduces the hardness of the steel, which ensures the formation of martensite during treatment process. Material which have high carbon content and other alloying element leads to more hardness. Harder the material leads to poor weldability. So for the adjustment of alloying elements a term carbon equivalent is used. Carbon equivalent compare their properties to Plain carbon steel. The effect on weldability of elements like chromium and vanadium, while not as great as carbon, is more significant than that of copper and nickel, for example. As the equivalent carbon content rises, the weldability of the alloy decreases.

1.6.1 Schaeffler Diagram

A Schaeffler diagram (as shown in Fig. 1.12) can be used to find out the effect of the composition of two elements on the structure obtained after cooling from 1050 °C to room temperature. In Schaeffler diagram two elements such as chromium and nickel is used because chromium is ferrite stabilizer and nickel is austenitic stabilizer. This diagram by calculating the proportion of chromium and nickel equivalents shows the limits of the austenitic, ferritic and martensitic

Schaeffler diagram does not allow determination of the composition and volume of the carbide phase. Furthermore, for a carbon content lower than 0.12%, the agreement of predictions with actual system is reduced due to consumption of carbon by the carbide formation process. Schaeffler diagram is suited for the prediction of structure of steels.

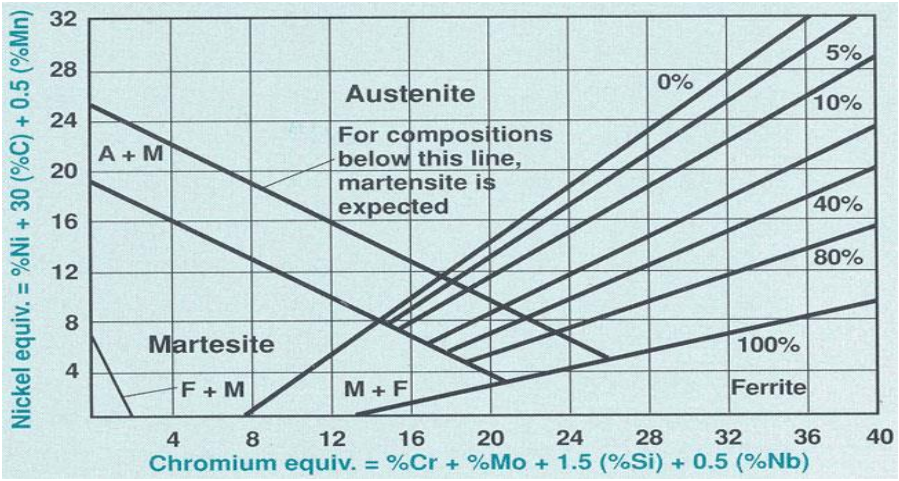

Figure 1.12: Schaeffler Diagram [http://www.nhml.com]

1.6.2 Precautions during Welding

During welding of stainless steel following precautions need to be taken.

a) Do not weld stainless steel with mild steels.
b) Do not use same brush which is used to clean mild steel.
c) Use high purity argon gas while purging otherwise oxide formation will takes place.
d) Use correct welding parameters.
e) Before welding clean the material with acetone.

1.6.3 Pre-heating and Post-heating

Generally pre heating or post heating of stainless steels is not required. Fully austenitic steel are sometime leads to formation of hot cracks so heat input is controlled carefully and dilution should be kept minimum. So preheating up to 100 $^{\circ}$C is done sometime.

While in the case of duplex no post heating is done if post heating of duplex is done it will lead to the distortion. Sometime pre heating is done up to temperature of 100 $^{\circ}$C to remove the moisture from duplex in very cold conditions.

Chapter 2

LITERATURE REVIEW

2.1 Introduction

A lot of research work has been done so far for predicting the effect of different variables on the strength and properties of different kinds of steel by joining them with GMAW. Literature survey is categorized in the following broad areas:

- Effects of mixture of shielding gas on steel properties.
- Welding parameter selection for optimization in welding.
- Effects on microstructure.

2.2 Review of Literature

2.2.1 Effect of Shielding Gas Mixture on Mechanical Properties

Kang et al. [2009] studied the effect of mixture of shielding gas and alternate supply of shielding gas on the AISI 304 austenitic stainless steel using GTAW process and find the variations of different shielding gases on welding distortion and welding speed.

In this research study, AISI 304 is joined with filler rod of grade ER308 by using alternate supply of He and Ar as a shielding gas. A mixture of Ar and 67% He is also used for welding to study its effect on fusion zone of weld metal. By using these shielding gases welding was done with the help of GTAW machine. After welding of specimens, study of various process parameters had done such as welding speed, weld distortion and alternate supply of shielding gases and it had been concluded that

Lowest degree of distortion is achieved in alternate method of Ar and He as a shielding gases rather than Ar and Ar + 67% He. By comparing conventional method of welding using Ar + 67% He and alternate method using argon and He showed that with same welding speed without compromising the weld shape the alternate method using Ar and He as a shielding gas solve the problem of the increase in gas cost and welding distortion.

Durgatlu [2004] investigated the effects of mixture of hydrogen and argon as a shielding gas on the austenitic steel with 4 mm thickness by using GTAW process with welding wire of same material. In this study he used mixture of hydrogen and argon gas as

the shielding media in different proportions and pure argon. Microstructure, mechanical properties and penetration effects were examined by using these shielding gases.

In this research work first of all a austenitic steel is cut in dimensions of 200×80×4 mm making chamfer of 30° and then welded by filler wire of 2.5 mm with gas tungsten arc welding. Parameters such as gas flow rate of 10 L/min, welding speed 100 mm/min and current intensity of 115 A was selected. Tensile test, bending test, micro hardness test and penetration were examined on material by selecting the different values of these parameters and results are obtained such as good tensile strength is obtained from Ar + 1.5% H_2 when used as a shielding gas. By using these shielding gases cracks, tearing and surface defection were not examined with naked eyes. Microhardness of weld metal is lower than that of HAZ and base metal by using these shielding gases. It was also seen that penetration is increasing by increasing the amount of hydrogen content in the argon shielding gas. Mean grain size was also increases with increase in hydrogen content in argon shielding gas. It was noticed that more hydrogen content more increase in deviation in orientation of grain size.

Gulenc et al. [2005] studied the effect of proportions of hydrogen in argon as a shielding gas for welding AISI 304 by using GMAW welding. Influence of hydrogen was that tensile strength, penetration of weld metal and toughness was increases by mixing it with Ar as a shielding gas. It was also influenced that when hydrogen is added it argon it increases the volume of molten metal in the weld region because of higher thermal conductivity of mixture of gases of hydrogen and argon.

In this research work austenitic steel of grade 304 sizes 140×75×10 mm thick is welded by using GMAW welding using diameter 1.2 mm with different shielding gases and current parameters. After welding, study of mechanical properties and microstructure properties of weldment is studied. From this study it has been concluded that high tensile strength was obtained with shielding gas of Ar-1.5% H_2 as a welding current of 240 A. Best toughness value was obtained when welding is done with Ar-5% H_2 and current of 240 A. Bending test does not show any tearing, cracking and any other defect. Base metal has high hardness and strength than other zone such as HAZ. Grain size of weld metal increases with increases in heat input because of increasing hydrogen addition to shielding gases. Penetration profile width and height also increases with increases in hydrogen content.

Ebrahimnia et al. [2009] studied the effects of four different shielding gas compositions. They investigated the influence of mixture of the shielding gas composition on

the welding of the steel ST 37-2. In this study, they realised the first function of the shielding gas is used to protect the molten metal from the contamination of atmospheric gases such as nitrogen and oxygen as the weld pool is being formed. Other function of this shielding gases to form the stable arc and uniform metal transfer. Yield strength and and ultimate strength of this alloy is 340 MPa and 540 MPa. Filler wire used for welding of this material is ER70S-6. Mixture of shielding gas in four different compositions was used in this process. Constant gas flow rate of 10 L/min is used for the shielding gas. Automatic GMAW process is used with constant voltage type transfer mode. After the experimental study they have concluded that with increase in amount of carbon dioxide in shielding gas with argon there is decrease in the amount of inclusion and porosity. Toughness of the material increases first with increase in the amount of carbon dioxide in shielding gas and then remains constant. Hardness of weld metal increases as there is increase in amount of carbon in shielding gas.

Pires et al. [2007] investigated that the development of shielding gases mixture for two main reasons: first is to improve productivity and process parameters and second is to reduce fumes emissions to reduce the health and safety hazards. In this study argon, carbon dioxide and oxygen is used in some definite proportions as a shielding gas mixture. This study also aiming at the stability if arc during welding process.

After conducting experiments on above setup it has been concluded that: in some gas mixture spray transfer mode of arc is generated due to increase in thermal conductivity and in some cases repelled transfer occur due to active components in the mixture. When shielding gas is used with ternary mixture spray and short circuit transfer mode will occur. It has also been concluded that with increase in amount of oxygen and carbon dioxide in shielding gas fume formation rate is increasing and also leadsto increase in arc temperature and instability.

2.2.2 Welding Parameter Selection for Optimization in Welding

Lothongkum et al. [1999] studied the welding parameters of gas tungsten arc welding at AISI 304L stainless steel sheet with a thickness of 3mm in flat, vertical and overhead positions of welding. The shielding gases used for this research work were pure argon and a mixture of argon and nitrogen. After conducting the experiments it has been concluded that in vertical and overhead positions of welding gravitational force come into play and results in fall down of molten metal from the weld pool and leads to undercut after solidification. This gravitational effect can be eliminated by selecting the proper welding parameters.

Juang and Tarng [2002] studied the process parameters for obtaining optimal weld pool geometry in the GTAW welding of stainless steel is presented. In this research paper the weld bead geometry had many quality characteristics. Modify Taguchi technique is used to optimize these quality characteristics in the selection of process parameters. From the study it has been concluded that the optimal weld pool geometry has four smaller-the-better quality characteristics, i.e. the front height, front width, back height and back width of the weld pool. The modified Taguchi method is adopted to solve the optimal weld pool geometry with four smaller-the better quality characteristics.

Lu et al. [2013] proposed the effect of double layer shielding gas in GTAW using Helium as the inner layer shielding gas, mixture of helium and CO_2 as the outer layer shielding gas and realised that weld efficiency with this process was increased as compared with that of the common gas tungsten arc welding process. CO_2 gas is used as an outer shielding gas because it can decompose into oxygen in the welding process and also cheaper than oxygen. In this paper, CO_2 was used instead of O_2, and He is used as inner layer shielding with mixture of helium and carbon dioxide as double layer shielding in GTAW welding of Cr13Ni5Mo material. Function of He as inner layer shielding is to protect the electrode from CO_2 and function of CO_2 is to decompose into oxygen and increase the penetration depth and weld efficiency. From the above study it has been concluded that with new method of gas tungsten arc welding using mixture of helium and carbon dioxide as an outer layer shielding depth of penetration is increasing and welding efficiency is also increases.

Tiwari et al. [2010] studied the effects of welding process parameters on the welding of Mild Steel material with thickness of 6 mm welded by metal arc welding. Welding parameters selected for this process are welding current, arc voltage heat input and speed of welding. Butt joints are prepared first of all using metal arc welding process and effect of process parameters like welding speed and rate of heat input are investigated on depth of penetration. After conducting and examine the study optimum process parameters obtained were current 105 A, arc voltage is 24 V. From the above study results that are concluded are

- Deepest penetration was obtained at welding speed of 110.39 mm/min.
- When heat input rate was 1369.68 J/mm than maximum depth of penetration was obtained.

It has also been concluded that with increase in speed at constant current and arc voltage depth of penetration is increasing up to optimal value and if speed is further increased depth of penetration starts decreasing.

Ibrahim et al. [2012] studied that the effects of process parameters on depth of penetration, microstructure changes and microhardness measurement on plate of 6 mm thickness of base metal by using the robotic gas metal arc welding. The process parameter considered for this study is welding current, arc voltage and welding speed. The arc voltage and welding current were chosen with 3 level of each in range from 22 to 30 V and 90 to 210 A respectively. The welding speed considered for this process is 20, 40 and 60 cm/min. After conducting the experiments depth of penetration, microstructural changes and microhardness is observed for each trial condition. From the above study it is concluded that with increase in current and voltage depth of penetration increases. Optimum parameters that are found from the research is 22 V at 210 A at the welding speed 60 cm/min. It has also been seen that hardness is maximized at 90 A and it slowly dropped to 150 A and at 210 A it small increased than 150 A. The higher value of hardness is 26 V at 90 A at welding speed 60 cm/min. When welding parameters are changed grain size is increase from coarse grain size to fine grain size.

Suben and Tusek [2001] studied the effects of melting rate, high productivity arc welding process, shielding gas and their characteristics. He realised that in industrial application of GMAW welding processes, various type of shielding gases or their mixture are used. The quality of weld required is the main criterion for selection of these suitable gases. A mathematical model for prediction of a melting rate is used in this study. Based on the investigation of the high productivity gas shielded arc welding in various shielded media, following conclusion may be drawn; the melting rate in welding with a cored wire is higher than in welding with a solid wire at same condition.

2.2.3 Effect on Microstructure

Elsawy [2001] studied the characterization of the GTAW fusion line phase for super ferritic stainless steel weldment by taking a sample of 6.35 mm thick plate for welding in the annealed and quenched condition. The welding process parameters used were welding current of 300 A, straight polarity 120 A , pure argon as shielding gas with flow rate of 24 L/min. microstructure observations are taken at the fusion line near the root pass. Main objective of this study were :

- Welding of29Cr–4Mo–2Ni alloy with filler material of Inconel 626.
- Find out the reason behind brittle fracture at the fusion line.

From this study it is concluded that in tensile test, fracture occurred at the weld fusion line with very slight plastic deformation. Attempt to weld the 29Cr–4Mo–2Ni alloy with Inconel 626 filler material is unsuccessful due to formation of excess phase at the fusion line. The excess phases as identified by SEM/XEDS and X–ray diffraction were identified as mixture of austenite and sigma phase on broken face of tensile specimen**.**

Ruan et al. [2012] studied the effect of Twin wire GMAW (metal inert gas arc welding) arc welding and applied the SiO_2 activating flux applied on half of the surface. From the above study they concluded that: no much difference in the microstructural changes by using SiO_2 as a activating flux. HAZ of the joint with the SiO_2 flux was observed to be slightly wider than that of the joint without flux. By using flux of SiO_2 deeper penetration is obtained up to 26% because it leads to increase in temperature. There is no much effect of the flux on the tensile strength of a material.

Karadeniz et al. [2007] investigated the effect of various welding process parameters on depth of weld penetration welded by robotic GMAW. Process parameters selected for the research work was welding current, arc voltage and welding speed. The welding currents were selected in a range of 95 to 115 A, arc voltages were selected as 22 to 26 V and the welding speeds were chosen as 40, 60 and 80 cm/min for all trial conditions. From the results obtained from robotic GMAW welding following conclusion can be drawn: with increase in the current depth of penetration increased. Deepest penetration was obtained at the weldig speed of 60 cm/min. The effect of welding current is 2.5 times greater than that of arc voltage and welding speeds on penetration.

Li et al. [2010] designed two pipeline structures in the welding torch. Pure inert gas passes though the inner pipeline which keeps the arc stable and protects the tungsten electrode. A mixed gas containing an active gas passes through the outer pipeline. The active element which is decomposed from the active gas dissolves in the weld pool so as to change the Marangoni convection from an outward to an inward direction. After experiments they have concluded that: It is an effective way to obtain a relatively deep and narrow weld pool shape by adding an active gas to the outer layer of the double shielded GTAW method. The

Marangoni convection changes from the outward to the inward direction as the oxygen content in the weld pool exceeds a certain concentration so as to make the depth/width ratio relatively high. The weld depth under the double shielded GTAW welding method is about 2~3 times larger than found in conventional GTAW welding. It is easy to generate heavy oxide layer on the weld pool surface as the oxygen addition in the shielded gas under the single layer shielding method. The heavy oxide layer may inhibit the heat flow on the weld pool surface, and reduce the depth/width ratio. By adjusting the process parameters the double shielded GTAW welding can completely avoid the oxidation of the electrode tip. This will increase the electrode life in the welding.

Abbasi et al. [2011] studied the effect of increased pressure on automatic GMAW machine using a mixture of Ar and CO_2 as a shielding gas. Variation in process parameters like wire feed rate, travelling speed, arc voltage and arc pressure were observed on depth of penetration. In this study all the above parameters are studied with different proportions of gas mixture of argon and carbon di oxide as a shielding gas. From the study of different parameters it has been concluded that Using Ar/CO_2 mixture it was possible to make bead on plate welds with the GMAW. With increase in voltage and pressure good quality of weld bead is obtained up to an optimal value but when voltage and pressure is increased further more spatter was produced, this being particularly marked with higher feed speeds. Fumes density are also increased with increase in pressure and results in the deposits of dust in all tests and prevented the detailed observation of the arc.

2.3 Summary of Literature View

A lot of research work was done in the field of austenitic steel or other steel with different shielding gases and their mixture by using gas tungsten arc welding or gas metal arc welding. Some investigator studied the effect of various parameters on the mechanical properties and microstructure [Lothingkum et al., 1999; Juang and Tarng, 2002; Lu et al., 2013; Palani and Murugan, 2006; Tiwari et al., 2010]. Some of the research work is carried out in the metallurgical aspects and microstructural properties of the base metal before and after welding in the base metal, weld metal and HAZ [Park et al. 2011, Elsway, 2001; Ruan et al., 2012; Karadeniz et al., 2007; Li et al., 2010; Kacar and Kokemli, 2005; Feng et al., 2012]. Research work has also been carried out by varying the shielding gas composition like mixture of hydrogen and helium in argon during the gas tungsten arc welding process in order to study its

effect on the various mechanical properties and microstructure of base metal [Kang et al., 2009; Durgatlu, 2004; Gulenc et al., 2005; Ebrahimnia et al., 2009; Pires et al., 2007]. It can be concluded from literature review that the main process parameter which affect the properties of welded joints are welding current, shielding gas, gas flow rate, electrode chosen composition of base metal and filler metal. In some research paper it has been seen that effect of double shielding gas is studied on the material by analysing its metallurgical behaviour and mechanical properties.

2.4 Scope and Objectives of the Present Work

AISI/SAE304 is being commonly used in routine structural work because of economic consideration but research work carried on this material is less while joining with AISI/SAE 316 and Duplex 2205 stainless steel. Little work has been reported so far for joining the materials AISI/SAE 316 with Duplex 2205 and AISI/SAE304 with Duplex 2205. Effect of argon and its mixture with H_2 and CO_2 has been reported by many but that of Ar and He is less. Quality of the welded joint is greatly influenced by the type of gas shielding and flow rate. Inert gas shielding proves a better quality joint but shielding region may be small and high chance of fly away from the being welded region. A double layer shielding could be an effective way to provide a continuous and better shielding during welding. Very less work has been done with double shielding gases during dissimilar metal joining. Based on the above scope the following objectives are identified for the present work.

- To study the effect of process parameters like current, voltage and filler wire on mechanical properties like tensile strength, impact test, microhardness and weld distortion during joining of AISI 304 and Duplex 2205.
- Effect of gas flow rate, shielding gas (Ar, He and their mixture), single layer and double layer shielding (CO_2 as outer layer shielding with different flow rate) during joining of AISI 304 and Duplex 2205.
- Analysis the SEM and metallurgical behaviour of dissimilar metal joining of AISI 304 and DUPLEX 2205.
- To study the effect of process parameters like current, voltage and filler wire on mechanical properties like tensile strength, impact test, microhardness and weld distortion during joining of AISI 316 and Duplex 2205.

- Effect of gas flow rate, shielding gas (Ar, He and their mixture), single layer and double layer shielding (CO_2 as outer layer shielding with different flow rate) during joining of AISI 316 and Duplex 2205.
- Analysis the SEM and metallurgical behaviour of dissimilar metal joining of AISI 304 and DUPLEX 2205.

Based on the above discussion following tests and analysis are carried out such as:

- Tensile strength
- Toughness test
- Indentation microhardness test
- Weld distortion measurement
- Dye penetration test
- Scanned electron microscopy
- Joint quality

Chapter 3

Design of Experimental Study

3.1 Introduction

In this chapter all the detailed information of experimental data is provided like materials, machine, selection of parameters and measurement setup. In this chapter it has also been explained about pilot work done for selecting the various parameters, setup used for measurements, fabrication of setup.

3.2 Welding Setup and Consumables

Before starting of some experiment for welding there is requirement of welding setup and consumables required for welding purpose. Which are described as:

3.2.1 Welding Machine

GMAW welding was carried out on metal inert gas welding machine (TORNADO GMAW 350 Make: Ador Fontech Ltd,) available at Central Workshop, Thapar University, Patiala as shown in the Fig. 3.1. The main parts of the machine are power source, welding torch, GMAW welding setup, gas regulator, and gas cylinder. The welding current and voltage can be regulated and displayed on GMAW welding setup of the welding machine and has a range of 0–400 A and voltage in the range of 0–40 V. The function of welding torch is to carry the filler wire and shielding gas and direct the supply of shielding gas in the welding region. Addition setting such as crater voltage, crater current and arc force are also available to set the arc. In this machine filler wire of 0.8, 1.0 and 1.2 diameters can be used.

Table 3.1: Main technical parameter of welding machine

S.no.	Welding parameter	Range
1.	Welding Current (A)	0–400
2.	Welding Voltage (V)	0–40
3.	Electrode Diameter (mm)	0.8–1.2

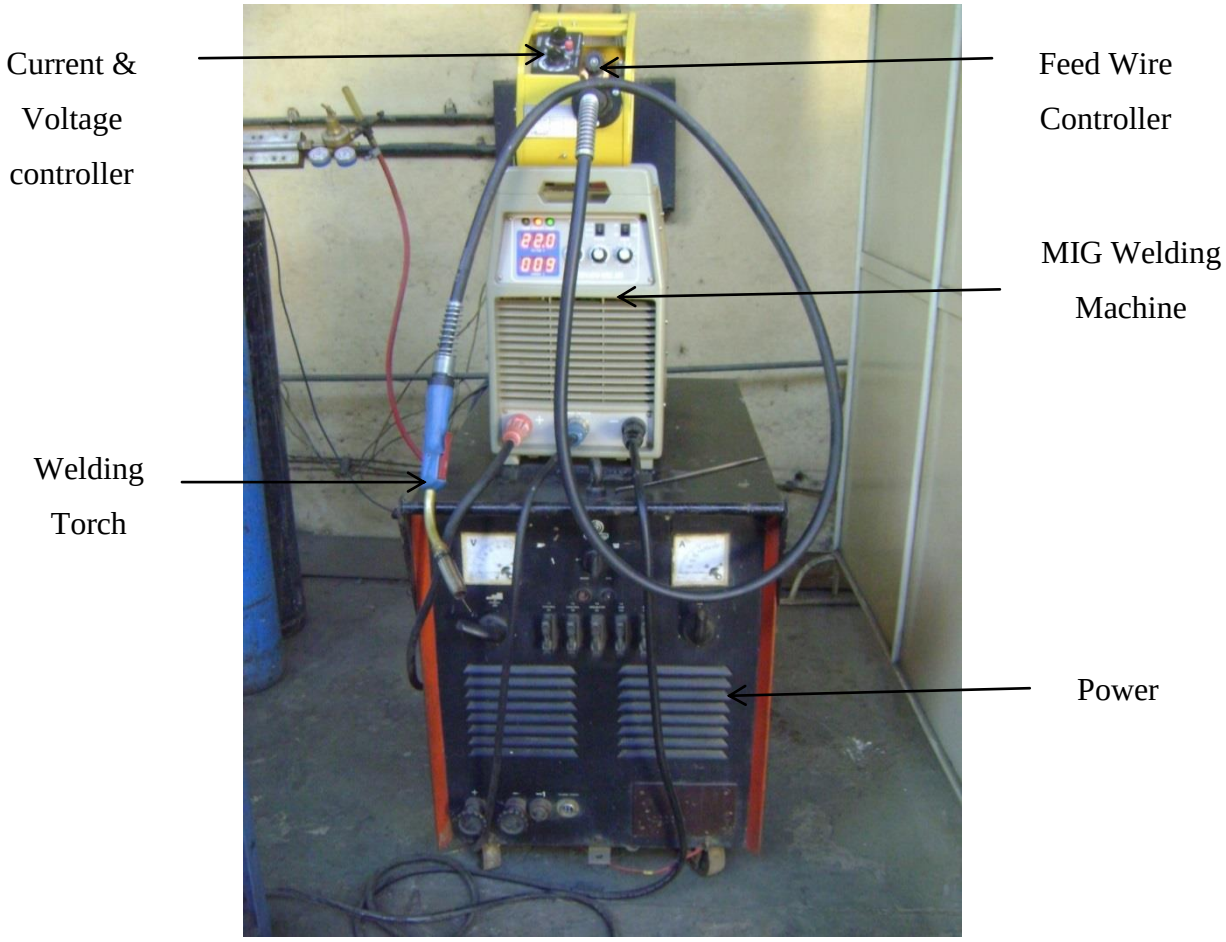

Figure 3.1: Gas metal arc welding setup
(**Courtesy:** Central Workshop, Thapar University, Patiala)

3.2.2 Shielding Gases and Nozzles

Most commonly shielding gases used for arc welding processes such as GTAW, GMAW and plasma arc welding processes are argon, helium and carbon dioxide. There are some gases also such as oxygen; hydrogen and nitrogen are used in mixture with above gases. In GMAW filler wire and shielding gases are used as consumables. To weld different materials with the help of GMAW than it is necessary to select carefully electrode wire and shielding gas. The electrode wire and shielding gas selected is such that they should provide best compatibility in between base metal and filler wire. Much research work has been done so far to get good compatibility between base metal and filler wire. Also there are many national and international guidelines to follow these standards.

Filler wires are generally sold in spools of 12.5 kg each with a careful layer winding to feed into the gun with least risk of snagging. If tempering is more in wire then there is feeding difficulties and springing action. Filler wires are friction loaded on reels so as to unwind under slight tension. Mechanical locking arrangement is provided in the machine so as to avoid over feeding of the wire. An arc is created between the work piece and a continuously consumable filler wire. The need of operator is to only focus on directing the GMAW nozzle at the position where welding is to be done with proper motion and speed. Filler wires are available with different diameter from 0.8 to 1.2 mm diameter.

For the present experimental work a double shielding gas nozzle is designed for double shielding gas effect. In which one gas is coming from inner layer and other gas would come from outer layer to protect the weld pool from atmospheric air.

Figure 3.2: Double shielding gas nozzle

3.2.3 Filler Wires

In the GMAW TORNADO 350 filler wires are used of different diameters i.e. in a range 0.8 to 1.2 mm diameter. Filler wires chosen for welding of present study is of two grades of stainless steel are of grade AISI 316, AISI 304 and one of duplex 2205 of size Ø1.2 mm diameter rolled in a spool of 12.5 kg each is obtained from (Ador Frontech Ltd.) as shown in Fig. 3.3. Filler wire is used as a three level design with combination of materials such as (AISI 304 and duplex 2205) and (AISI 316 and duplex 2205).

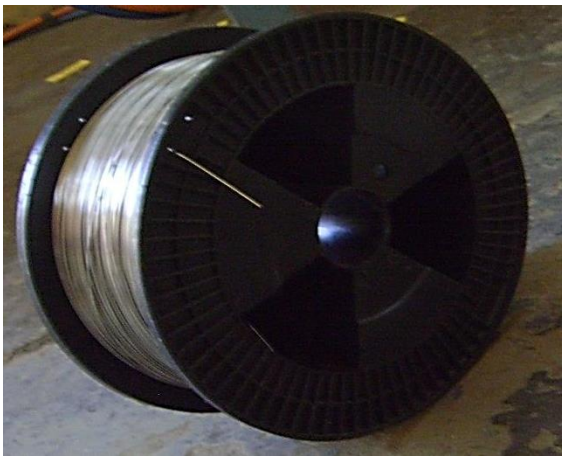

Figure 3.3: ER 304L grade filler wire spool

3.3 Work piece Materials

Materials to be used in present study are as follows:

Stainless steel 304, Stainless AISI 316, Duplex 2205

These above steels come in the category of austenitic steel and duplex steel are discussed as follow:

Stainless steel AISI 304, Stainless AISI 316

Austenitic stainless steel includes the series of 200 or 300 series. From survey in market it has been concluded that 304 grade steel is mostly used. Steels of these series are characterised by its chromium and nitrogen content. The austenitic stainless steels contain 18–20% Cr, 12–20% Ni, up to 0.10% C and small amounts of a few other elements such as molybdenum, nitrogen, phosphorus, sulphur etc. The balance between the Chromium and Nickel is normally adjusted to provide a microstructure of austenitic stainless steel. Nickel and nitrogen act as a austenitic stabilizer. Austenite stainless steels are characterized by good tensile strength and more toughness over a large temperature range and oxidation resistance to over 538 °C. This group include the series of 300. For welding of austenitic steel filler metal used is same as that of base metal means both are austenitic in nature [TMR Stainless, 2009].

Table 3.2: Chemical composition of AISI 304 and AISI 316

Metal	Chemical composition %									
	Fe	C	Si	Mn	P	S	Cr	Mo	Ni	Cu
AISI 304	69.0	0.05	0.33	0.978	0.049	0.008	18.2	0.912	10.14	0.382
AISI 316	70.0	0.07	0.29	0.36	0.06	0.009	17.9	0.005	9.02	1.42

Duplex steels come in the categories of both austenitic and ferrite phases i.e. they have good corrosive resistance as well as strength and ease of fabrication. Duplex stainless steels have the tendency to solidify as fully ferrite, but during the cooling of duplex stainless steel half of the ferrite converts into austenite approximately at 1040 °C. There is always lower amount of nickel and chromium content as compared to the austenitic stainless steel. Nitrogen upto 0.15% is added to transform the ferrite structure to austenitic structure. Duplex stainless steels are ferromagnetism in nature. These steels have combined the properties of both austenitic and ferritic stainless steel. The most common grade is DUPLEX2205 consisting of 15% Cr, 8% Ni, 3% Mo and 0.15% N [TMR Stainless, 2009].

Table 3.3: Chemical composition of Duplex 2205

Metal	Main chemical composition									
	Fe	C	Si	Mn	P	S	Cr	Mo	Ni	Cu
Duplex 2205	66.2	0.1	0.327	1.46	0.020	0.005	23.1	3.26	4.92	0.198

3.4 Selection of Various Factors

From the study of literature review and pilot work on base materials of thickness 5 mm range of various parameters are selected which can be used with GMAW welding.

Welding current 160–200 A

Voltage 16–20 V

Filler wire AISI 304, AISI 316, Duplex 2205

Gas flow rate 12–16 L/min

Type of gases Argon, helium and their mixture

Shielding layer Single layer or double layer shielding

3.4.1 Welding Current

TONADO GMAW 350 welding machine has a current range from 0 to 400 A. when a pilot study is conducted to identify the value of welding current as it is the most important parameter during GMAW welding (because GMAW welding works on the flat characteristics). It shows that there was start of the arc and a weld bead was formed at 150 A and then current was raised in the steps of 25 A each and later on at 200 A. It was also seen that metal fused completely and blow hole takes place because of high heat generated at this temperature in case of AISI 304 grade stainless steel as shown in Fig. 3.4.

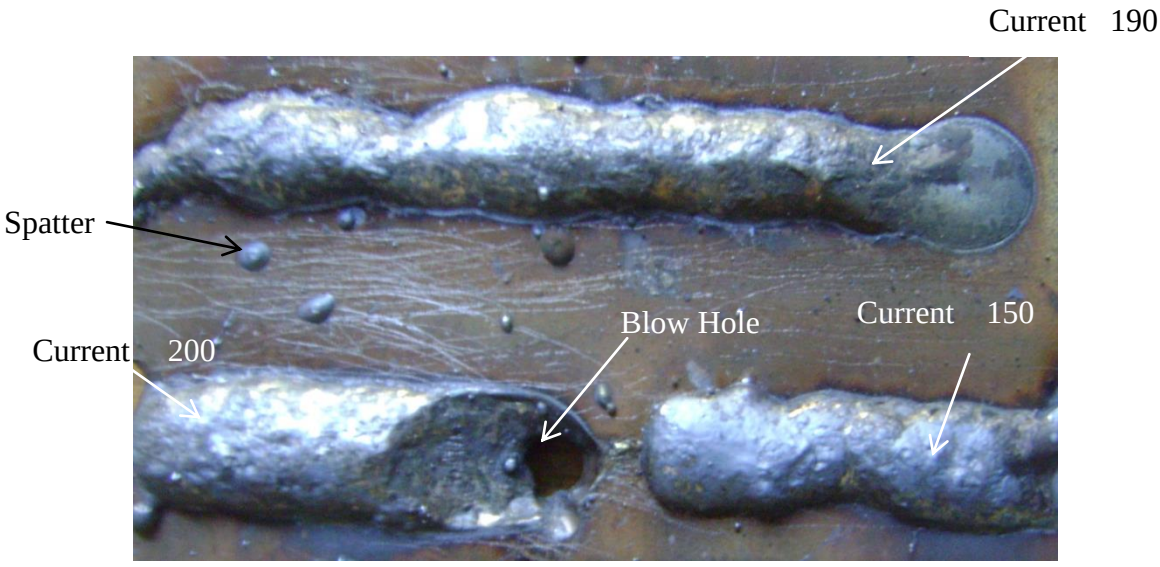

Figure 3.4: Pilot work on stainless steel 304 at different current

Figure 3.5: Pilot work on Duplex 2205 at different current

Similar study was also carried on AISI 316 grade and duplex 2205 stainless steel and results are shown in the figure 3.3. On the basis of this study values of current were chosen as 150 A, 190 A for the present research work. From the figures of pilot study it has been concluded that at 200 A current arc blows and more spatter will takes place.

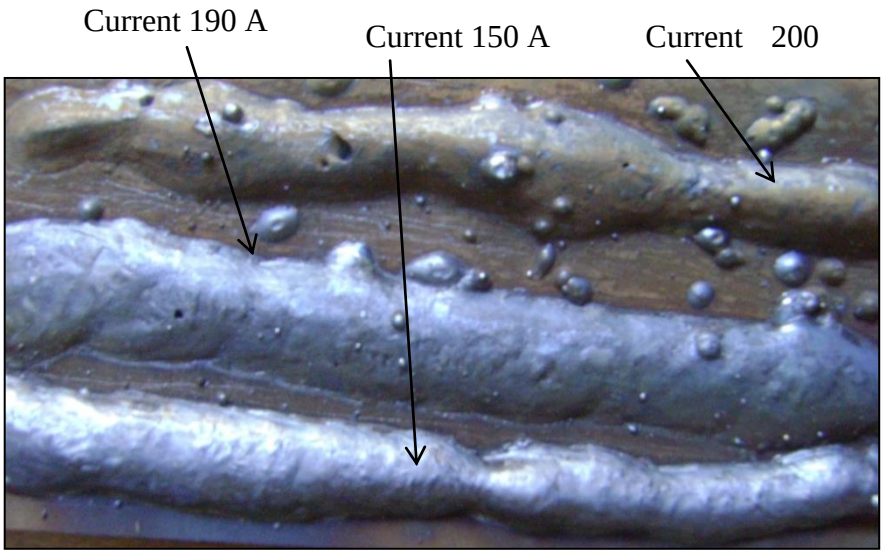

Figure 3.6: Pilot work on stainless steel AISI 316

3.4.2 Welding Voltage

From the pilot study it has been seen that there is no problem with arc when welding is carried out in a range of 20-25 V. but when the voltage is increased above 24 V wandering of arc takes place and it is difficult to weld the material. Also it has been seen that arc is not judged at the correct place while welding above 25 V. Parameter welding voltage is selected after conducting pilot work on stainless steel of 304 grades. From pilot study it has been concluded that welding voltage above 24 V results in burning of metal completely and deposited on other side as shown in figure 3.4.

Figure 3.7: Pilot work on mild steel show burning of metal

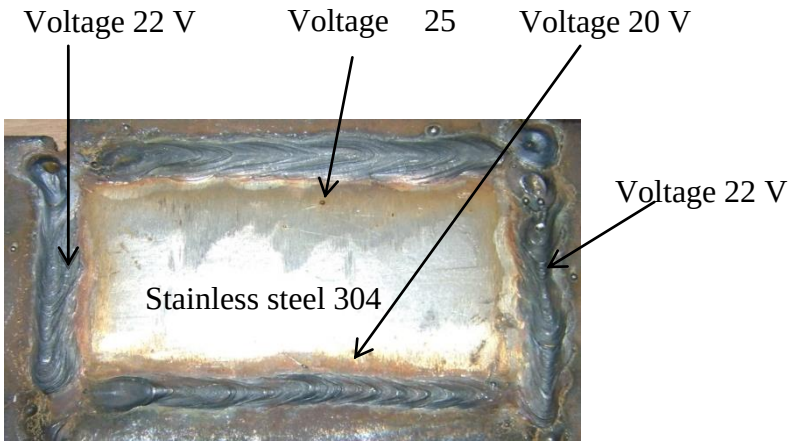

Figure 3.8: Pilot work on stainless steel at different voltage (I = 160 A)

Pilot study for welding voltage was also carried out to know the effect of different gas composition on it. AISI 304 stainless steel plates of size 100 mm×50 mm×5 mm were used as the test specimen. Welding current for pilot study was chosen as 150 A and gas flow rate as 12 L/min.

3.4.3 Shielding Gas and Gas Flow Rate

Most commonly shielding gases used for arc welding processes such as GTAW, GMAW and plasma arc welding processes are argon, helium and carbon dioxide. There are some gases also such as oxygen; hydrogen and nitrogen are used in mixture with above gases. So these gases are classified into two groups:

a) Inert gases like argon and helium.
b) Reactive gases such as carbon dioxide, hydrogen, oxygen and nitrogen these gases dissolve and react with metals.

Shielding gases used for the present study are pure Argon, mixture of Argon and Helium i.e. 70% Ar + 30% He and pure Helium. Flow rate of shielding gas plays an important role in case of GMAW. Flow rate of gas generally in between 10 to 15 L/min. Proper flow rate of shielding gas maintain the stability of arc. For the present study flow rate of shielding gas is maintained 12 to 16 L/min. with 3 levels.

3.5 Design of Experiment

In any experimental research, when experimental test procedure is time consuming to satisfy the need design objectives with the least number of trials are an important requirement. In this case, Taguchi experimental technique provides an efficient and systematic approach for experiments to determine near optimum value of process parameters for its performance. Taguchi technique involves laying out the experimental conditions using specially

constructed tables known as ‘orthogonal arrays’. Orthogonal arrays significantly reduce the number of experimental configurations to be trial. The results given by small scale experimental trial are valid over the entire experimental region spanned by the control factors. The most important stage in Taguchi technique is the design of experiment lies in the selection of the control factors. So, a large number of factors are included initially so that non-significant variables can be excluded at the earliest opportunity. Literature review reveals that parameters viz., current, voltage, gas flow rate, gas type, filler wire, single or double layer shielding of gas largely influence the welding parameters. Thus, the impacts of six process parameters are studied using L_{27} orthogonal array design. The control factors and the parameter settings for welding are given in Table 3.4. Table 3.4 presents the selected levels for various control factors. The tests are conducted as per the experimental design given in Table 3.5. The standard linear graph, as shown in Fig. 3.9, is used to assign the factors and interactions to various columns of the orthogonal array

Table 3.4: Process parameters and three levels for the welding of AISI 304, AISI 316 and Duplex 2205

S.no	Parameter	Symbol	Units	Levels		
				1	2	3
1.	Welding current	*A*	A	160	180	200
2.	Welding voltage	*B*	V	16	18	20
3.	Shielding gas	*C*	------	Pure Argon	Pure Helium	70% Ar + 30% He
4.	Gas flow rate	*D*	L/min	10	12	14
5.	Filler wire	*E*	-------	AISI 304	AISI 316	Duplex 2205
6.	Single layer or double layer shielding	*F*	L/min	Single layer	Double layer $(CO_2)_1$	Double layer $(CO_2)_2$

($(CO_2)_1$: double layer shielding with gas flow rate of 8 L/min**,** $(CO_2)_2$: double layer shielding with gas flow rate of 12 L/min)

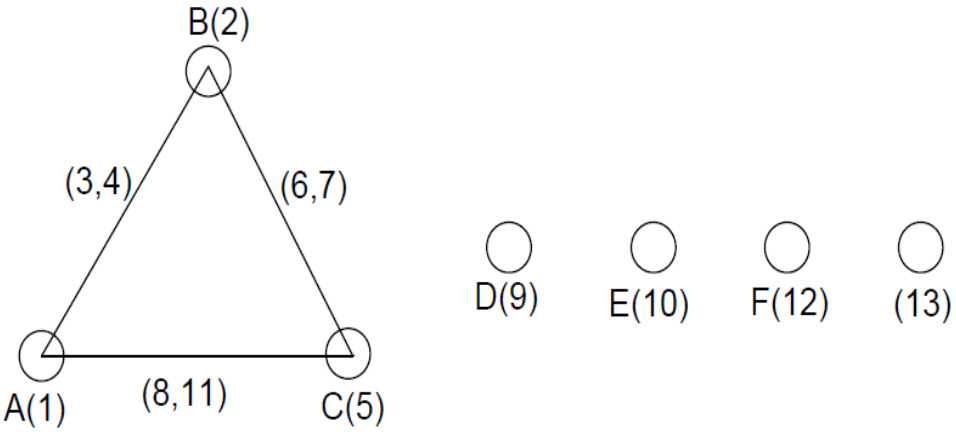

Figure 3.9: Linear graph for L_{27} orthogonal array

The selected parameters viz., current, voltage, gas flow rate, filler wire, gas type, single or double layer shielding of gas each at three levels, are considered in this study. These six parameters each at three levels would require 36 = 729 runs in a full factorial experiment whereas Taguchi's experimental approach reduces it to 27 runs only offering a great advantage. The plan of the experiments as shown in Table 3.5, columns are assigned to current (*A*), voltage (*B*), gas flow rate (*C*), filler wire (*D*), gas type (*E*) and single or double layer shielding (*F*) respectively.

Calculation of DOF

DOF denotes the number of the independent comparisons that can be made in any experiment. The number of factors considered for experimentation, their respective levels determine the total degree of freedom required for designing OA. Mathematically, DOF for each factor is calculated as,

DF= n-1, where n is the level of each factor

Table 3.5: Factors and degrees of freedom

Sr. no.	Factors	Degree of freedom
1	Welding current	2
2	Voltage	2
3	Gas flow rate	2
4	Filler wire	2
5	Pre-heating	2
6	Post-heating	2

Response characteristics

The response variables are listed below in the table.

Table 3.6: Response Characteristics

Response Name	Response Type	Units
Tensile Strength	Higher the better	MPa
Toughness	Higher the better	kg
MicroHardness	Nominal the better	HVN
Distortion	-	mm
Joint Quality (Visual Inspection)	-	-

Table 3.7: Orthogonal array for GMAW of AISI 304 and Duplex 2205

Exp. No.	Current (A)	Voltage (V)	Flow rate (L/min)	Filler wire	Gas type	Single or double layer
1	160	16	12	AISI 304	Ar	Single Layer
2	160	16	14	AISI 316	He	$(CO_2)_1$
3	160	16	16	Duplex 2205	70% Ar + 30% He	$(CO_2)_2$
4	160	18	12	AISI 316	He	$(CO_2)_2$
5	160	18	14	Duplex 2205	70% Ar + 30% He	Single Layer
6	160	18	16	AISI 304	Ar	$(CO_2)_1$
7	160	20	12	Duplex 2205	70% Ar + 30% He	$(CO_2)_1$
8	160	20	14	AISI 304	Ar	$(CO_2)_2$
9	160	20	16	AISI 316	He	Single Layer
10	180	16	12	AISI 316	70% Ar + 30% He	$(CO_2)_1$
11	180	16	14	Duplex 2205	Ar	$(CO_2)_2$
12	180	16	16	AISI 304	He	Single Layer
13	180	18	12	Duplex 2205	Ar	Single Layer
14	180	18	14	AISI 304	He	$(CO_2)_1$
15	180	18	16	AISI 316	70% Ar + 30% He	$(CO_2)_2$
16	180	20	12	AISI 304	He	$(CO_2)_2$
17	180	20	14	AISI 316	70% Ar + 30% He	Single Layer
18	180	20	16	Duplex 2205	Ar	$(CO_2)_1$
19	200	16	12	Duplex 2205	He	$(CO_2)_2$
20	200	16	14	AISI 304	70% Ar + 30% He	Single Layer
21	200	16	16	AISI 316	Ar	$(CO_2)_1$
22	200	18	12	AISI 304	70% Ar + 30% He	$(CO_2)_1$
23	200	18	14	AISI 316	Ar	$(CO_2)_2$
24	200	18	16	Duplex 2205	He	Single Layer
25	200	20	12	AISI 316	Ar	Single Layer
26	200	20	14	Duplex 2205	He	$(CO_2)1$
27	200	20	16	AISI 304	70% Ar + 30% He	$(CO_2)_2$

($(CO_2)_1$: double layer shielding with gas flow rate of 8 L/min**,** $(CO_2)_2$: double layer shielding with gas flow rate of 12 L/min)

. **Table 3.8** Orthogonal array for GMAW of AISI 316 and Duplex 2205

Exp. No.	Current (A)	Voltage (V)	Flow rate (L/min)	Filler wire	Gas type	Single or double layer
1	160	16	12	AISI 304	Ar	Single Layer
2	160	16	14	AISI 316	He	$(CO_2)_1$
3	160	16	16	Duplex 2205	70% Ar + 30% He	$(CO_2)_2$
4	160	18	12	AISI 316	He	$(CO_2)_2$
5	160	18	14	Duplex 2205	70% Ar + 30% He	Single Layer
6	160	18	16	AISI 304	Ar	$(CO_2)_1$
7	160	20	12	Duplex 2205	70% Ar + 30% He	$(CO_2)_1$
8	160	20	14	AISI 304	Ar	$(CO_2)_2$
9	160	20	16	AISI 316	He	Single Layer
10	180	16	12	AISI 316	70% Ar + 30% He	$(CO_2)_1$
11	180	16	14	Duplex 2205	Ar	$(CO_2)_2$
12	180	16	16	AISI 304	He	Single Layer
13	180	18	12	Duplex 2205	Ar	Single Layer
14	180	18	14	AISI 304	He	$(CO_2)_1$
15	180	18	16	AISI 316	70% Ar + 30% He	$(CO_2)_2$
16	180	20	12	AISI 304	He	$(CO_2)_2$
17	180	20	14	AISI 316	70% Ar + 30% He	Single Layer
18	180	20	16	Duplex 2205	Ar	$(CO_2)_1$
19	200	16	12	Duplex 2205	He	$(CO_2)_2$
20	200	16	14	AISI 304	70% Ar + 30% He	Single Layer
21	200	16	16	AISI 316	Ar	$(CO_2)_1$
22	200	18	12	AISI 304	70% Ar + 30% He	$(CO_2)_1$
23	200	18	14	AISI 316	Ar	$(CO_2)_2$
24	200	18	16	Duplex 2205	He	Single Layer
25	200	20	12	AISI 316	Ar	Single Layer
26	200	20	14	Duplex 2205	He	(CO2)1
27	200	20	16	AISI 304	70% Ar + 30% He	$(CO_2)_2$

($(CO_2)_1$: double layer shielding with gas flow rate of 8 L/min**,** $(CO_2)_2$: double layer shielding with gas flow rate of 12 L/min)

3.6 Measurement Setup

After selecting the parameter for welding it is necessary to investigate the results from these parameters. To calculate or study the results from these parameters measurement setup are required. For measurement setup required is atomic absorption spectrometer, microhardness test machine, SEM, distortion measurement etc. Brief introduction of these measurement setup are as follow:

- Impact Test
- Indentation Microhardness Test
- Distortion Measurement
- Dye penetration test.
- SEM and EDX analysis
- Joint quality
- Tensile strength test

3.6.1 Impact Test

Impact strength of a material is defined as the resistance offered by the material against the suddenly applied load. It is also defined as the maximum amount of energy absorbed by the material when subjected to sudden load. Impact test on the weld specimen is performed on the impact testing machine (Make: Alfred J. Amsler & Co., Switzerland) having a range of 0–30 k-gm or 0–300 joules as shown in the Fig. 3.10. For impact test initial energy to the hammer was given as 15 Kg–m or 147.15 Joules. Specimens were prepared according to ASTM standards A-370 (2010).

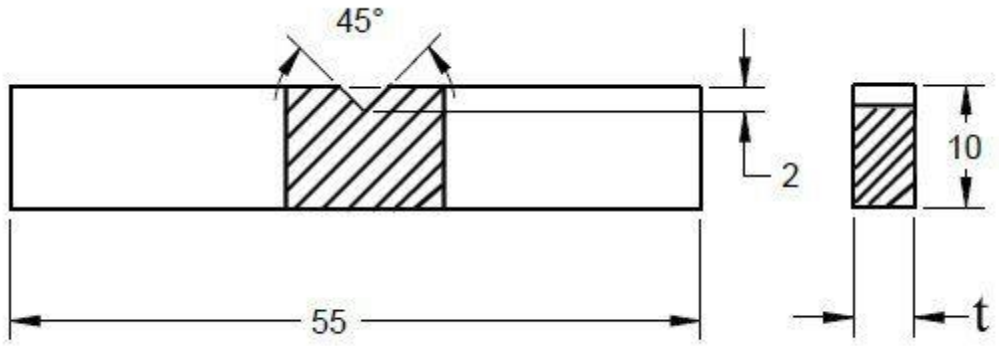

(Where thickness = 5mm, all dimensions are in mm)

(a)

(b)

Figure 3.10: (a) Standard size of impact test specimen according to ASTM standard A-370
(b) Impact testing machine
(**Courtesy:** Solid Mechanics Lab, MED, Thapar University, Patiala)

3.6.2 Indentation Microhardness Test

Indentation hardness tests are used to determine the hardness of a material to deformation. Several such tests exist, wherein the examined material is indented until an impression is formed; these tests can be performed on a macroscopic or microscopic scale. Micro hardness of the weld region was measured by using the computer interfaced micro hardness tester (Make: optical technologies, Madras, India) as shown in Fig. 3.12. The measurement was dependent on the size of indentation on the samples. The hardness values obtained were useful indicators of material properties. The load applied on the indenter was 500 gm. and the dwell time was 20 sec. The samples measuring for micro hardness were firstly ground on the belt grinder, shown in Fig. 3.11 then rubbed with emery paper size no. 400, 600, 800, 1000, 1500 & 2000 and then polished on polishing wheel.

Figure 3.11: Weld grinder (**Courtesy:** Machine Tool Lab, Thapar University, Patiala)

Figure 3.12: Microhardness test machine
(**Courtesy:** School of Physics and Material Science, Thapar University, Patiala)

3.6.3 Distortion Measurement Setup

During all welding on one side of a part will cause much more distortion than if the welds are alternated from one side to the other. During this heating and cooling cycle, many factors affect shrinkage of the metal and lead to distortion, such as physical and mechanical properties that change as heat is applied. So to measure the distortion of weld metal setup is prepared by self. In this setup a metallic block is taken from the raw material after that all edges are finished on the weld grinder after grinding on weld grinder milling operation is done on its surface to cut the slot up to 10 mm deeper as shown in Fig. 3.13.

Figure 3.13: Slot cutting on distortion setup with milling machine
(**Courtesy:** Central Workshop, Thapar University, Patiala)

After milling operation thru holes are made on perpendicular surface to slot surface. Thru holes are made with the help of drilling machine as shown in Fig. 3.14. After making holes, threads are made with the help of tappet in the holes to hold the weld plate for distortion measurement. Nut and bolt arrangement is use to hold the weld plate. After holding the weld piece a dial gauge indicator is used to measure the distortion.

Figure 3.14: Drilling on distortion setup with bench drilling machine
(**Courtesy:** Central Workshop, Thapar University, Patiala)

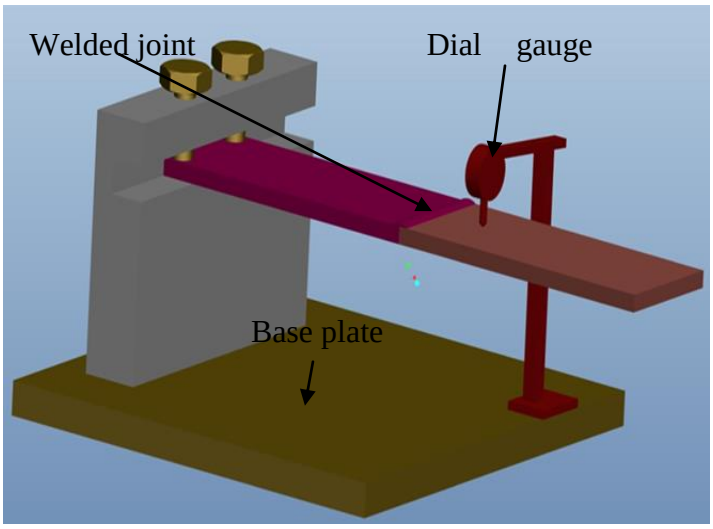

Figure 3.15: Distortion measurement setup

3.6.4 Dye Penetration Test

DPT (dye penetration test) test was performed on the welded region to detect the surface cracks and porosity. For performing test, three solutions namely developer ORION 115D, Penetrant Remover ORION 115PR and Red Dye Penetrant ORION 115P (Make: The Oriental Chemical Works, Kolkata) were used as shown in the Fig. 3.16.

Figure 3.16: Checkmate's cleaner, penetrant & developer used for DPT test of specimens

3.6.5 Scanning Electron Microscope

A scanning electron microscope (SEM) as shown in Fig. 3.17 is a type of electron microscope that produces images of a sample by scanning it with a focused beam of electrons. SEM is used mainly for imaging of surfaces and analysis of small surface features. It provides magnification up to 240,000 and high spatial resolution. For the present experimentation work, SEM of samples was investigated on three magnification ranges, namely,500× and 1000×.

Figure 3.17: Scanning electron microscope
(**Courtesy:** SAI Lab, Thapar University, Patiala)

3.6.6 Visual Inspection of Cracks

All the polished specimens prepared above for micro hardness testing were seen under optical (which uses a light beam to view the object) microscope (as shown in Fig. 3.18) at 100X to find the joint quality in terms of internal defects like crack, porosity, blow hole etc.

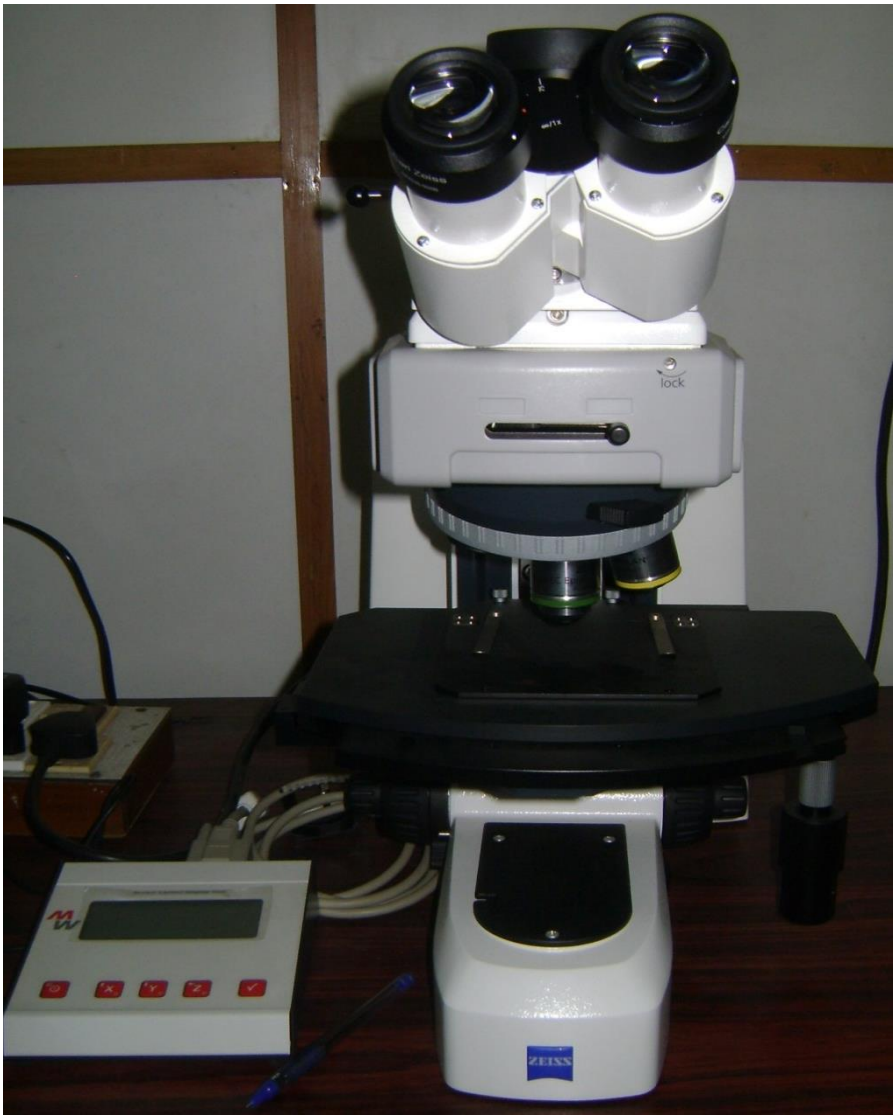

Figure 3.18: AXIO optical microscope
(**Courtesy:** Metrology lab, Thapar University, Patiala)

3.6.7 Tensile Strength

Flat specimens are firstly prepared before performing the tensile strength. The dimension of the flat specimen is 200 mm × 50 mm × 5 mm and an axial load is applied from both the ends. The ASTM standard test method for tensile properties of metallic material has the designation E8/E8M–09. In the present work, this tensile test is performed in the universal testing machine (Make: HEICO Ltd.–New Delhi, India, Load capacity – 60×10^3 N) as shown in Fig. 3.19.

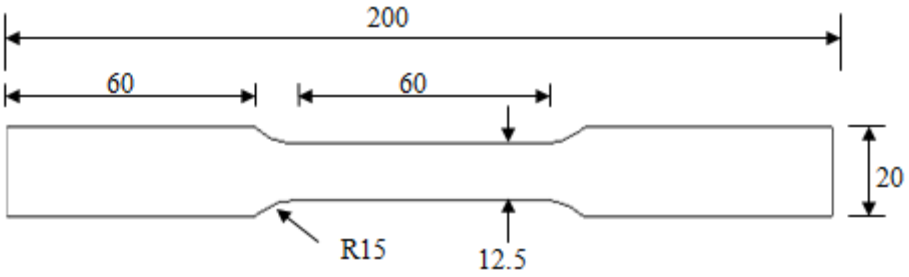

(All dimensions in mm)

Figure 3.19: Tensile Test specimen according to ASTM E8/E8M–09

Chapter – 4

Results and Discussions

4.1 Introduction

This chapter presents the effect of selected process parameters such as current, voltage, shielding gas type, gas flow rate, filler material, and single or double layer shielding gas on the responses like tensile strength, impact strength, microhardness, weld distortion, dye penetration and microstructural observations by SEM. Taguchi experimental designs is used to study the effect of six different process parameters each varied at three level and their interactions using L_{27} orthogonal array having 27 trials for the different set of materials. After conducting the experimental study using L_{27} orthogonal array, various tests are performed and the results are analysed using analysis of variance (ANOVA), response table, main effect plots, interaction plot and optimal design is obtained. From the analysis of results effect of significant parameters on responses and their behaviour are also discussed.

4.2 Tensile Strength

Tensile strength of a material is defined as the maximum amount of tensile stress that a material can take before its failure. The tensile test is performed on dog bone shaped specimens. The ASTM standard E8/E8M–09 is used for tensile properties of metallic material. In the present work, this test is performed on the computerised universal testing machine (Make: HEICO Ltd.–New Delhi, India, Load capacity – 60×10^3 N) and the results obtained are used to calculate the tensile strength of samples.

4.2.1 Tensile Strength in Welding of AISI 304 and Duplex 2205

The results of tensile strength carried out on joints performed as per L_{27} orthogonal array on the welding of materials AISI 304 and Duplex 2205 are given in Table 4.1.

Table 4.1: Results of tensile strength for joints between AISI 304 and Duplex 2205

Exp. No.	Current (A)	Voltage (V)	Flow rate (L/min)	Filler wire	Gas type	Single or double layer	Tensile strength (MPa)
1	160	16	12	AISI 304	Ar	Single Layer	204.32
2	160	16	14	AISI 316	He	$(CO_2)_1$	373.12
3	160	16	16	Duplex 2205	70% Ar + 30% He	$(CO_2)_2$	196.16
4	160	18	12	AISI 316	He	$(CO_2)_2$	561.12
5	160	18	14	Duplex 2205	70% Ar + 30% He	Single Layer	635.84
6	160	18	16	AISI 304	Ar	$(CO_2)_1$	392.32
7	160	20	12	Duplex 2205	70% Ar + 30% He	$(CO_2)_1$	587.04
8	160	20	14	AISI 304	Ar	$(CO_2)_2$	452.04
9	160	20	16	AISI 316	He	Single Layer	243.12
10	180	16	12	AISI 316	70% Ar + 30% He	$(CO_2)_1$	106.40
11	180	16	14	Duplex 2205	Ar	$(CO_2)_2$	452.96
12	180	16	16	AISI 304	He	Single Layer	122.72
13	180	18	12	Duplex 2205	Ar	Single Layer	492.48
14	180	18	14	AISI 304	He	$(CO_2)_1$	543.54
15	180	18	16	AISI 316	70% Ar + 30% He	$(CO_2)_2$	278.24
16	180	20	12	AISI 304	He	$(CO_2)_2$	770.88
17	180	20	14	AISI 316	70% Ar + 30% He	Single Layer	587.01
18	180	20	16	Duplex 2205	Ar	$(CO_2)_1$	732.32
19	200	16	12	Duplex 2205	He	$(CO_2)_2$	271.04
20	200	16	14	AISI 304	70% Ar + 30% He	Single Layer	260.00
21	200	16	16	AISI 316	Ar	$(CO_2)_1$	254.12
22	200	18	12	AISI 304	70% Ar + 30% He	$(CO_2)_1$	166.24
23	200	18	14	AISI 316	Ar	$(CO_2)_2$	301.42
24	200	18	16	Duplex 2205	He	Single Layer	470.40
25	200	20	12	AISI 316	Ar	Single Layer	265.44
26	200	20	14	Duplex 2205	He	(CO2)1	734.40
27	200	20	16	AISI 304	70% Ar + 30% He	$(CO_2)_2$	557.28

($(CO_2)_1$: double layer shielding with gas flow rate of 8 L/min**,** $(CO_2)_2$: double layer shielding with gas flow rate of 12 L/min)

Figure 4.1: Specimen after tensile strength of joints between AISI 304 and Duplex 2205

Analysis of Variance for Tensile Strength

To find out the significance of various factors like current, voltage, filler material, gas flow rate, gas type and single or double layer shielding on tensile strength ANOVA is performed at measured data with 90% confidence level. *F*-test is used to find out the most significant factor correspond to each input parameter. *F*-test is based on the principle that larger the value of *F* calculated, greater the effect on that parameter. Table 4.2 and Table 4.3 shows the results obtained from the ANOVA and response table for the tensile strength of AISI 304 and Duplex 2205. From Table 4.2 it is observed that current, voltage, flow rate, filler, interaction of current × flow rate and interaction of voltage × flow rate are statistically the most significant parameter that affects the tensile strength.

Table 4.2: ANOVA for tensile strength of joints between AISI 304 and Duplex 2205

Source	Symbol	DF	SS	Variance	*F*-value	Percentage contribution
Current (A)	*A*	2	36219	18109	27.29	3.63
Voltage (V)	*B*	2	406484	203242	306.31	40.76
Flow rate (L/min)	*C*	2	76509	38255	57.66	7.67
Filler wire	*D*	2	149448	74724	112.62	14.98
Gas	*E*	2	31022	15511	23.38	3.11
Single layer or double layer	*F*	2	25392	12696	19.13	2.54
Current × Voltage	*A* × *B*	4	149674	37418	56.39	15.00
Current × Flow rate	*A* × *C*	4	109141	27285	41.12	10.94
Voltage × Flow rate	*B* × *C*	4	11954	2989	4.50	1.19
Residual Error		2	1327	664		0.133
Total		26	997172			100

(DF: degree of freedom, SS: sum of squares)

Table 4.3 shows the response table of various input parameters with the rank in term of their relative significance. From the Table 4.3 it is found that voltage is the most significant factor with rank 1 and single or double layer shielding gas is least significant factor assigned with rank 6.

Table 4.3: Response Table for tensile strength of joints between AISI 304 and Duplex 2205

Level	Current (A)	Voltage (V)	Flow rate (L/min)	Filler	Gas	Single or double layer
1	405.0	249.0	380.6	385.5	394.2	364.6
2	454.1	426.8	482.3	330.0	454.5	432.2
3	364.5	547.7	360.7	508.1	374.9	426.8
Delta	89.6	298.7	121.5	178.1	79.6	67.6
Rank	4	1	3	2	5	6

Figure 4.2 shows the main effect plot to show the influence of process parameters on joints between AISI 304 and Duplex 2205 in which X-axis shows process parameters and Y-axis shows the tensile strength with mean line. Figure 4.2 shows that with increase in current and voltage, tensile strength increases because increase in these parameters leads to increase in heat input. More heat input means more fusion of base material with filler wire results in high tensile strength but too much increase in current results in spatter of arc. Due to which proper bead is not formed. Tensile strength is also affected by flow rate of shielding gas because stable arc is produced with suitable flow rate of shielding gas when laminar flow is observed. But if gas flow rate is not proper than stability in arc will not takes place and results in porosity in weld bead. Duplex 2205 filler material shows more tensile strength

because they are more resistance to hot cracking and have high thermal conductivity with low coefficient of thermal expansion as compared to AISI 316. Tensile strength is not much influenced by gas type and single or double layer shielding. Figure 4.3 shows the interaction plot between significant factors current × voltage and voltage × flow rate. With increase in current and voltage spray transfer mode takes place. In this mode arc is in the form of droplet are directed axially from electrode to weld bead, result in good surface bead, more uniform penetration and tensile strength. Another interaction between current and flow rate shows that by increasing current and flow rate thermal conductivity of weld metal increase and result in good tensile strength.

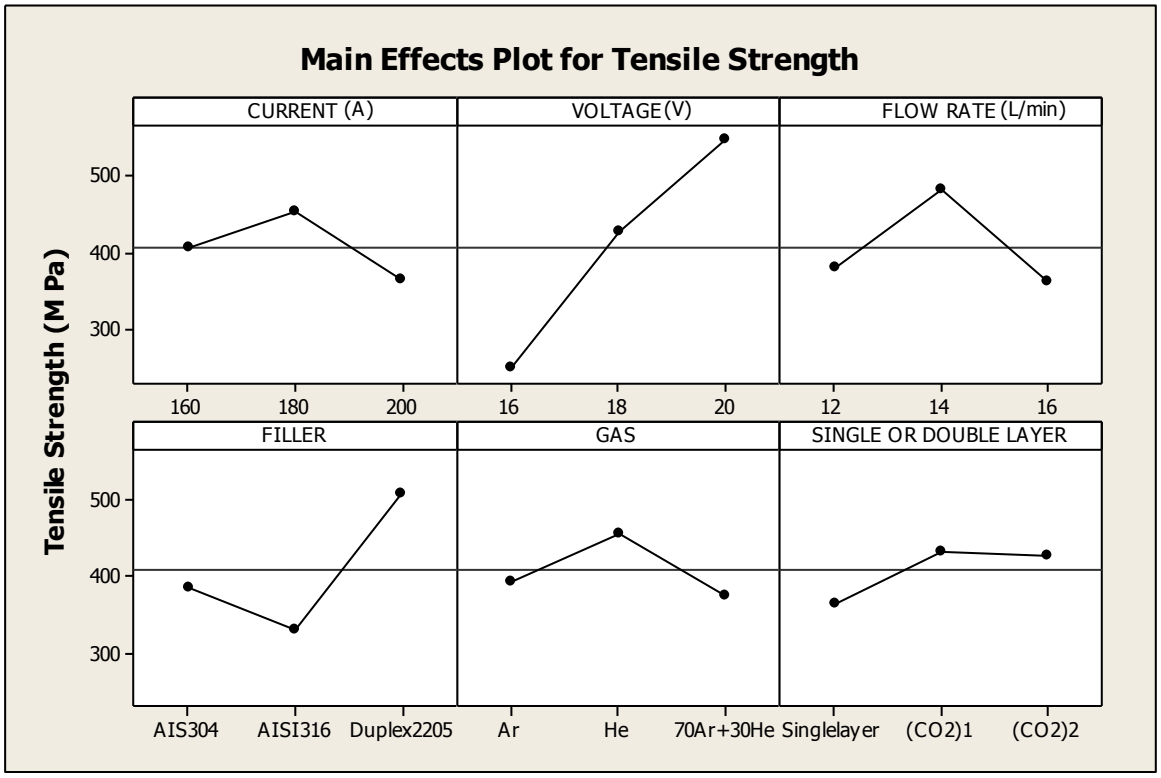

Figure 4.2: Main effect plot to show the influence of process parameters on tensile strength of joints between AISI 304 and Duplex 2205

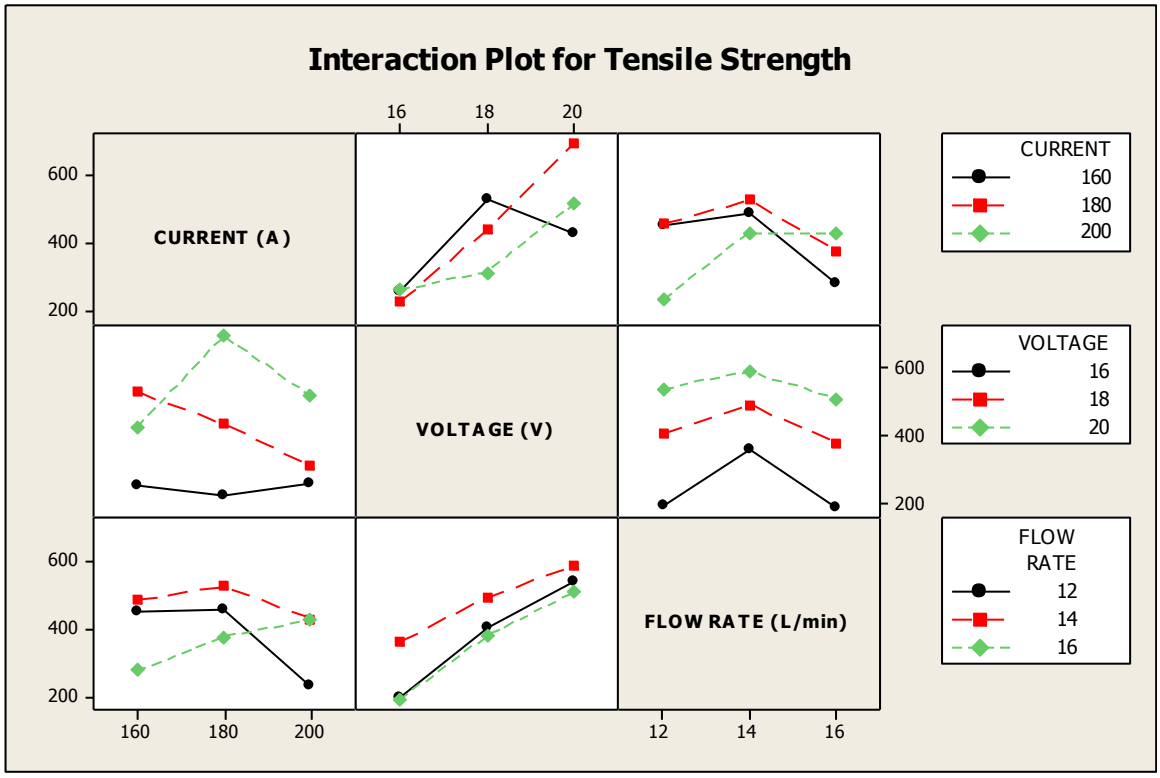

Figure 4.3: Interaction plot for tensile strength of joints between AISI 304 and Duplex 2205

Optimal Design

From the main effect plot and interaction plot in Fig. 4.2 and Fig. 4.3 is used to estimate the maximum tensile strength with optimal design parameters conditions with "higher the better" type of response. From Table 4.2 considering higher *F*-value and corresponding percentage contribution current, voltage, flow rate, filler and interaction between current × voltage and current × flow rate are observed significantly influencing the tensile strength. The levels of these factors gives the maximum tensile strength are noted from main effect plot (Fig. 4.2) and the corresponding tensile strength for at these levels of $\overline{A_2}$, $\overline{B_3}$, $\overline{C_2}$, $\overline{D_3}$ are obtained directly from the Table 4.3. For interactions, levels of current × voltage ($A\times B$) and current × flow rate ($A\times C$) are decided from the interaction plot (Fig. 4.3) and maximum tensile strength is observed at ($\overline{A_2 \times B_3}$), ($\overline{A_2 \times C_2}$). To obtain the best estimate of a mean when an interaction is present, the trial that include that treatment condition should be averaged. Average tensile strength for these two interactions are obtained by taking the average of three trials (trial 15, 16, 17) for ($\overline{A_2 \times B_3}$) and average of trials (trial 11, 14, 17) for ($\overline{A_2 \times C_2}$). Maximum value of current, voltage and flow rate is selected because tensile strength is 'higher the better' type response. Desired mean value in this case is estimated as:

$$\mu_{A_2,B_3,C_2,D_3,A_2\times B_3,A_2\times C_2} = \overline{A_2} + \overline{B_3} + \overline{C_2} + \overline{D_3} + \overline{A_2 \times B_3} + \overline{A_2 \times C_2} - 5\,\overline{T} \qquad (4.1)$$

$= 454.1 + 547.7 + 482.3 + 508.1 + 696.73 + 527.83 – 2039.25$

$= 1177.51$ MPa

Confidence interval is calculated as under

$$CI = \sqrt{\frac{F_{\alpha,\nu_1,\nu_2} V_e}{n_{eff}}} \quad (4.2)$$

Where Fα, ν_1, ν_2 = *F* ratio

α = 0.1 (risk)

Confidence = 1 – α

ν_1 = DF for mean (always 1)

ν_2 = Total DF (=26)

$\overline{T}$ = Average of all experimental trial

n_{eff} = Number of tests under that condition using the participating factors

$$n_{eff} = \frac{N}{1 + DF_{A,B,C,D,A\times B,A\times C}} = \frac{27}{1+16} = 1.588$$

N is the number of trial in the experiment

V_e = Variance of error

$$CI = \sqrt{\frac{2.91 \times 664}{1.588}} = \pm 34.82 \text{ MPa}$$

Thus the calculated value of tensile strength is (1177.51 $\pm$ 34.82) MPa

The value of population (μ) is 1177.51 MPa which is very large than expected value due to influence of some random variable where some parametric combination resulted in very poor joint result in low tensile strength (like experiment number. 3, 10, 12, 22). This leads to reduction in trial average ($\overline{T}$). So optimum value selected from trial (trials 16, 18, 26) by taking their mean is 745.86 MPa.

Thus the optimum value of tensile strength is (745.86 $\pm$ 34.82) MPa

4.2.2 Tensile Strength in Welding of AISI 316 and Duplex 2205

The results of tensile strength carried out on joints performed as per L_{27} orthogonal array on the welding of materials AISI 316 and Duplex 2205 are given in Table 4.4.

Table 4.4: Results of tensile strength for joints between AISI 316 and Duplex 2205

Exp. No.	Current (A)	Voltage (V)	Flow rate (L/min)	Filler Wire	Gas Type	Single or Double Layer	Tensile strength (MPa)
1	160	16	12	AISI 304	Ar	Single Layer	480.80
2	160	16	14	AISI 316	He	$(CO_2)_1$	388.80
3	160	16	16	Duplex 2205	70% Ar + 30% He	$(CO_2)_2$	333.76
4	160	18	12	AISI 316	He	$(CO_2)_2$	299.04
5	160	18	14	Duplex 2205	70% Ar + 30% He	Single Layer	377.60
6	160	18	16	AISI 304	Ar	$(CO_2)_1$	494.88
7	160	20	12	Duplex 2205	70% Ar + 30% He	$(CO_2)_1$	780.96
8	160	20	14	AISI 304	Ar	$(CO_2)_2$	423.04
9	160	20	16	AISI 316	He	Single Layer	268.16
10	180	16	12	AISI 316	70% Ar + 30% He	$(CO_2)_1$	139.04
11	180	16	14	Duplex 2205	Ar	$(CO_2)_2$	316.80
12	180	16	16	AISI 304	He	Single Layer	371.28
13	180	18	12	Duplex 2205	Ar	Single Layer	425.76
14	180	18	14	AISI 304	He	$(CO_2)_1$	538.72
15	180	18	16	AISI 316	70% Ar + 30% He	$(CO_2)_2$	380.16
16	180	20	12	AISI 304	He	$(CO_2)_2$	661.40
17	180	20	14	AISI 316	70% Ar + 30% He	Single Layer	527.04
18	180	20	16	Duplex 2205	Ar	$(CO_2)_1$	856.64
19	200	16	12	Duplex 2205	He	$(CO_2)_2$	388.32
20	200	16	14	AISI 304	70% Ar + 30% He	Single Layer	305.76
21	200	16	16	AISI 316	Ar	$(CO_2)_1$	223.20
22	200	18	12	AISI 304	70% Ar + 30% He	$(CO_2)_1$	750.72
23	200	18	14	AISI 316	Ar	$(CO_2)_2$	302.40
24	200	18	16	Duplex 2205	He	Single Layer	453.60
25	200	20	12	AISI 316	Ar	Single Layer	421.44
26	200	20	14	Duplex 2205	He	(CO2)1	656.80
27	200	20	16	AISI 304	70% Ar + 30% He	$(CO_2)_2$	468.64

($(CO_2)_1$: double layer shielding with gas flow rate of 8 L/min, **(**$(CO_2)_2$: double layer shielding with gas flow rate of 12 L/min)

Figure 4.4: Specimen after tensile strength of joints between AISI 316 and Duplex 2205

Analysis of Variance for Tensile Strength

To find out the significance of various factors like current, voltage, filler material, gas flow rate, gas type and single or double layer shielding on tensile strength ANOVA is performed at measured data with 90% confidence level. *F*-test is used to find out the most significant factor correspond to each input parameter. *F*-test is based on the principle that larger the value of *F* calculated, greater the effect on that parameter. Table 4.5 and Table 4.6 shows the results obtained from the ANOVA and response table for tensile strength of AISI 316 and Duplex 2205. From Table 4.5 it is observed that voltage, filler wire, single or double layer shielding and interaction of current × voltage are statistically the most significant parameter that affects the tensile strength.

Table 4.5: ANOVA for tensile strength of joints between AISI 316 and Duplex 2205

Source	Symbol	DF	SS	Variance	*F*-value	Percentage contribution
Current (A)	*A*	2	7874	3937	0.81	1.01
Voltage (V)	*B*	2	248853	124427	25.65	32.18
Flow rate (L/min)	*C*	2	18814	9407	1.94	2.43
Filler wire	*D*	2	188584	94292	19.44	24.38
Gas	*E*	2	818	409	0.08	0.105
Single layer or double layer	*F*	2	111754	55877	11.52	14.45
Current × Voltage	*A* × *B*	4	101254	25314	5.22	13.09
Current × Flow rate	*A* × *C*	4	76386	19097	3.94	9.87
Voltage × Flow rate	*B* × *C*	4	9207	2302	0.47	1.19
Residual Error		2	9702	4851		1.25
Total		26	773247			100

(DF: degree of freedom, SS: sum of squares)

Table 4.6 shows the response table of various input parameters with the rank in term of their relative significance. From the Table 4.6 it is found that voltage is the most significant factor with rank 1 and gas type is least significant factor assigned with rank 6.

Table 4.6: Response Table for tensile strength of joints between AISI 316 and Duplex 2205

Level	Current (A)	Voltage (V)	Flow rate (L/min)	Filler	Gas	Single or double layer
1	427.4	327.5	483.1	499.5	438.3	403.5
2	468.5	447.0	426.3	327.7	447.3	536.6
3	441.2	562.7	427.8	510.0	451.5	397.1
Delta	41.1	235.2	56.7	182.3	13.2	139.6
Rank	5	1	4	2	6	3

Figure 4.5 shows the main effect plot to show the influence of process parameters on joints between AISI 316 and Duplex 2205. In which X-axis show process parameters and Y-axis shows the tensile strength with mean line. Figure 4.5 shows that with increase in voltage, tensile strength increases because with increase in voltage heat input increases. More heat input results in formation of wider bead and more penetration results to high tensile strength. Filler wire of Duplex 2205 shows more tensile strength and decreases by using filler wire of AISI 316 due to fact that solidification of duplex is more resistant to hot cracking and good thermal conductivity and lower thermal expansion than that of AISI304 and AISI316 filler wire. Tensile strength of material also increases by using CO_2 as an outer shielding because by using CO_2 as an outer shielding it would not allow the inner layer of shielding gas to contact with air due to which thermal conductivity of inner shielding gas is maintained and

results in good tensile strength. Figure 4.6 shows the interaction between significant factors such as current and voltage. With increase in current and voltage, tensile strength increases because with increase in these parameters spray transfer of filler metal into the base metal takes place. It is also noted that more heat input results in more diffusion of base material with filler material leads to high tensile strength but too much increase in current results in spatter of arc. Due to which proper fusion of base metal and filler wire would not takes place. Tensile strength is not much influenced by gas type and single or double layer shielding as it lies near the mean line.

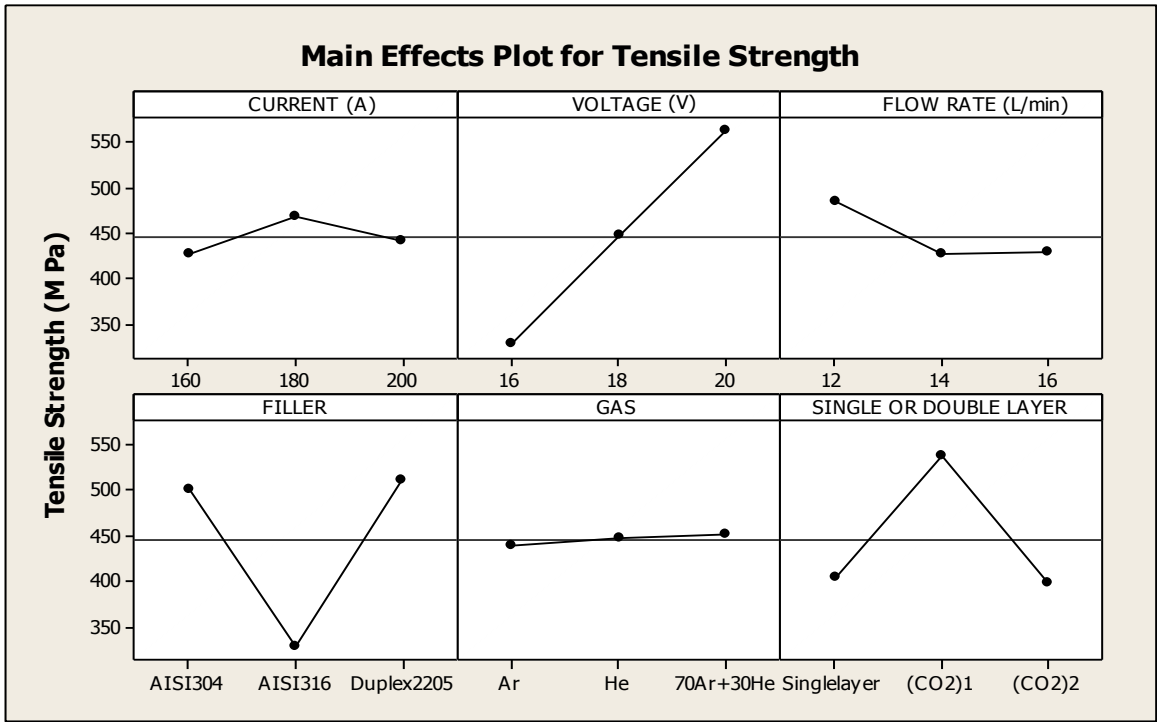

Figure 4.5: Main effect plot to show the influence of process parameters on tensile strength of joints between AISI 316 and Duplex 2205

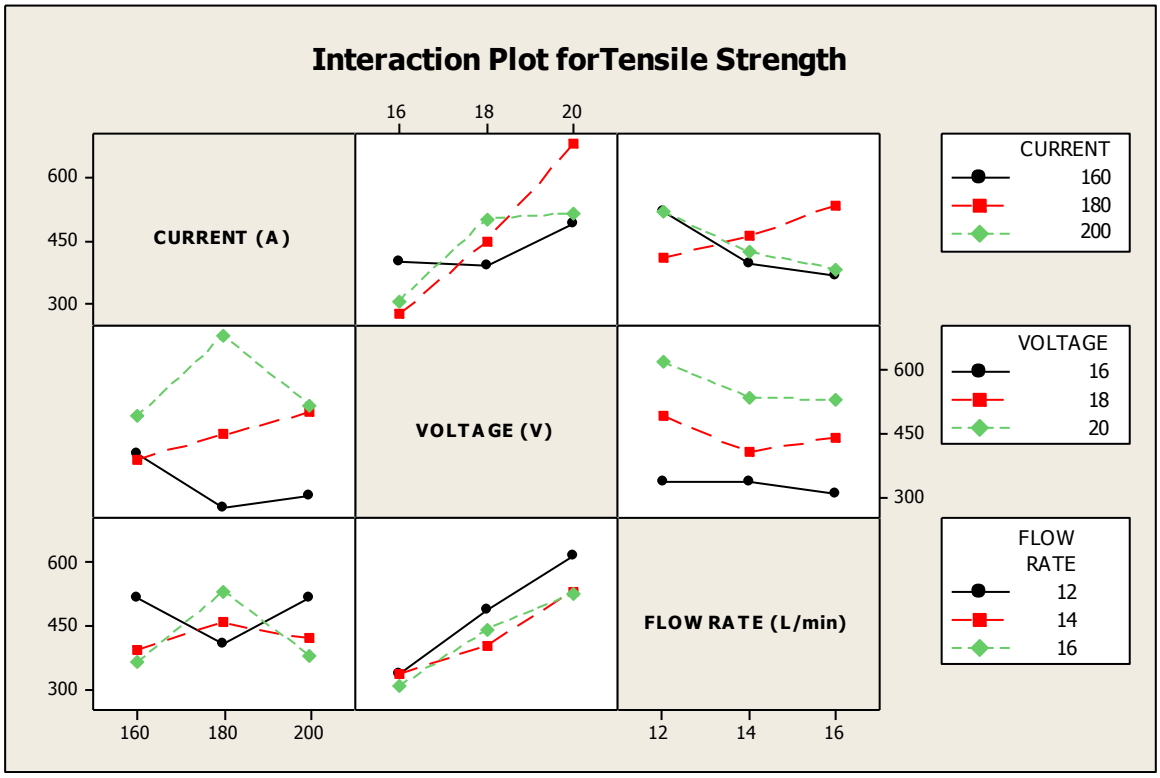

Figure 4.6: Interaction plot for tensile strength of joints between AISI 316 and Duplex 2205

Optimal Design

From the main effect plot and interaction plot in Fig. 4.5 and Fig. 4.6 is used to estimate the maximum tensile strength with optimal design parameters conditions with "higher the better" type response. From Table 4.5 considering higher *F*-value and corresponding percentage contribution voltage, filler wire, single or double layer shielding and interaction between current and voltage are observed significantly influencing the tensile strength. The level of these factors which gives the maximum tensile strength are noted from main effect plot (Fig. 4.5) and the corresponding tensile strength for at these levels of $\overline{B_3}, \overline{D_3}, \overline{F_2}$ are obtained directly from the Table 4.5. For interactions, levels of current × voltage ($A \times B$) are decided from the interaction plot (Fig. 4.6) and maximum tensile strength is observed at $\overline{A_2 \times B_3}$. To obtain the best estimate of a mean when an interaction is present, the trial that include that treatment condition should be averaged. Average tensile strength for these two interactions are obtained by taking the average of three trials (trial 15, 16, 17) for $\overline{A_2 \times B_3}$. Maximum value of current and voltage is selected because tensile strength is 'higher the better' type response. Desired mean value in this case is estimated as:

$$\mu_{B_3,D_3,F_2,A_2\times B_3} = \overline{B_3} + \overline{D_3} + \overline{F_2} + \overline{A_2 \times B_3} - 3\,\overline{T} \qquad (4.3)$$

$$= 562.7 + 510.0 + 536.6 + 681.69 - 1337.19$$

$= 953.8$ MPa

Confidence interval

$$CI = \sqrt{\frac{F_{\alpha,\nu_1,\nu_2} V_e}{n_{eff}}} \quad (4.4)$$

$n_{eff} = \frac{N}{1+DF_{B,D,F,A\times B}} = \frac{27}{1+10} = 2.45$

V_e = Variance of error

$$CI = \sqrt{\frac{2.91 \times 4851}{2.45}} = \pm 75.90 \text{ MPa}$$

Thus the calculated value of tensile strength is (953.8± 75.90) MPa

The value of population μ is 953.8 MPa which is very large than expected value due to influence of some random variable where some parametric combination resulted in very poor joint result in low tensile strength (like experiment no. 4, 9, 10, 21). This leads to poor reduction in trial average ($\overline{T}$). So optimum value selected from trial (trials 7, 18, 22) by taking their mean is 796.10 MPa.

Thus the optimum value of tensile strength is (796.10 ± 75.90) MPa

4.3 Impact Test for Toughness

Impact strength of a material is defined as the capacity of a material to absorb and dissipate energy when load is suddenly applied on the material. Charpy test is used to measure the toughness of welded joints. It is the exact opposite of "brittleness" which carries the implication of sudden failure.

4.3.1 Impact Test for Toughness in Welding of AISI 304 and Duplex 2205

The results of toughness carried out on joints performed as per L_{27} orthogonal array on the welding of materials AISI 304 and Duplex 2205 are given in Table 4.7.

Figure 4.7: Specimens of AISI 304 and Duplex 2205 after toughness test

Table 4.7: Results of toughness for joints between AISI 304 and Duplex 2205

Exp. No	Current (A)	Voltage (V)	Flow rate (L/min)	Filler Wire	Gas Type	Single or Double Layer	Toughness (J)
1	160	16	12	AISI 304	Ar	Single Layer	24.525
2	160	16	14	AISI 316	He	$(CO_2)_1$	23.544
3	160	16	16	Duplex 2205	70% Ar + 30% He	$(CO_2)_2$	4.905
4	160	18	12	AISI 316	He	$(CO_2)_2$	39.240
5	160	18	14	Duplex 2205	70% Ar + 30%He	Single Layer	34.335
6	160	18	16	AISI 304	Ar	$(CO_2)_1$	29.430
7	160	20	12	Duplex 2205	70% Ar + 30%He	$(CO_2)_1$	44.145
8	160	20	14	AISI 304	Ar	$(CO_2)_2$	39.240
9	160	20	16	AISI 316	He	Single Layer	9.810
10	180	16	12	AISI 316	70% Ar + 30% He	$(CO_2)_1$	9.810
11	180	16	14	Duplex 2205	Ar	$(CO_2)_2$	14.715
12	180	16	16	AISI 304	He	Single Layer	44.145
13	180	18	12	Duplex 2205	Ar	Single Layer	27.468
14	180	18	14	AISI 304	He	$(CO_2)_1$	4.905
15	180	18	16	AISI 316	70% Ar + 30% He	$(CO_2)_2$	44.145
16	180	20	12	AISI 304	He	$(CO_2)_2$	63.765
17	180	20	14	AISI 316	70% Ar + 30% He	Single Layer	29.430
18	180	20	16	Duplex 2205	Ar	$(CO_2)_1$	24.525
19	200	16	12	Duplex 2205	He	$(CO_2)_2$	4.905
20	200	16	14	AISI 304	70% Ar + 30% He	Single Layer	34.335
21	200	16	16	AISI 316	Ar	$(CO_2)_1$	14.715
22	200	18	12	AISI 304	70% Ar + 30% He	$(CO_2)_1$	4.901
23	200	18	14	AISI 316	Ar	$(CO_2)_2$	4.901
24	200	18	16	Duplex 2205	He	Single Layer	14.715
25	200	20	12	AISI 316	Ar	Single Layer	29.430
26	200	20	14	Duplex 2205	He	(CO2)1	45.126
27	200	20	16	AISI 304	70% Ar + 30% He	$(CO_2)_2$	37.278

($(CO_2)_1$: double layer shielding with gas flow rate of 8 L/min**,** **(**$(CO_2)_2$: double layer shielding with gas flow rate of 12 L/min)

Analysis of Variance of Tensile Strength

To find out the significance of various factors like current, voltage, filler material, gas flow rate, gas type and single or double layer shielding on toughness ANOVA is performed at measured data with 90% confidence level. *F*-test is used to find out the most significant factor correspond to each input parameter. *F*-test is based on the principle that larger the value of *F* calculated, greater the effect on that parameter. Table 4.8 and Table 4.9 shows the results obtained from the ANOVA and response table for the toughness of AISI 304 and Duplex 2205. From Table 4.8 it is observed that interaction of current × flow rate and interaction of voltage × flow rate are statistically the most significant parameter that affects the tensile strength.

Table 4.8: ANOVA for toughness of joints between AISI 304 and Duplex 2205

Source	Symbol	DF	SS	Variance	*F*-value	Percentage contribution
Current (A)	*A*	2	330.56	165.28	1.76	5.02
Voltage (V)	*B*	2	1353.85	676.92	7.19	20.58
Flow rate (L/min)	*C*	2	35.56	17.78	0.19	0.54
Filler wire	*D*	2	395.69	197.85	2.10	6.01
Gas	*E*	2	108.30	54.15	0.58	1.64
Single layer or double layer	*F*	2	183.15	91.57	0.97	2.78
Current × Voltage	*A* × *B*	4	893.15	223.29	2.37	13.58
Current × Flow rate	*A* × *C*	4	1853.24	463.31	4.92	28.18
Voltage × Flow rate	*B* × *C*	4	1234.17	308.54	3.28	18.76
Residual Error		2	188.24	94.12		2.86
Total		26	6575.90			

(DF: degree of freedom, SS: sum of squares)

Table 4.9 shows the response table of various input parameters with the rank in term of their relative significance. From the Table 4.9 it is found that voltage is the most significant factor with rank 1 and gas flow rate is least significant factor assigned with rank 6.

Table 4.9: Response Table for tensile strength of joints between AISI 316 and Duplex 2205

Level	Current (A)	Voltage (V)	Flow rate (L/min)	Filler	Gas	Single or double layer
1	27.69	19.51	27.58	31.39	23.22	27.58
2	29.21	22.67	25.61	22.78	27.80	22.34
3	21.15	35.86	24.85	23.87	27.03	28.12
Delta	8.07	16.35	2.72	8.61	4.58	5.78
Rank	3	1	6	2	5	4

Figure 4.8 shows the main effect plot to show the influence of process parameters on joints between AISI 304 and Duplex 2205. In which X-axis show process parameters and Y-axis shows the toughness with mean line. Figure 4.8 shows that with increase in current toughness increases up to a suitable heat input but too much increase in current leads to more heat input. Too high heat input may result in a high content of sigma phase. This lowers the toughness in case of Duplex 2205. With increase in voltage toughness increases because increase in voltage heat input increases. More heat input results in more diffusion, flatter and wider bead of base material which leads to more toughness. Toughness of weld material is not much affected by gas type and flow rate of gas. Filler wire of AISI 304 shows more toughness and decreases by using filler wire of Duplex2205 due to large nickel content in AISI304. Toughness of material also increases by using CO_2 as an outer shielding by using flow rate of 12 L/min. Figure 4.9 shows the interaction between significant factors such as current × flow rate and voltage × flow rate. With increase in current and voltage, toughness increases because increase in these parameters heat input increases. More heat input results in more diffusion of base material with filler material which leads to high toughness but too much increase in current results in spatter of arc.

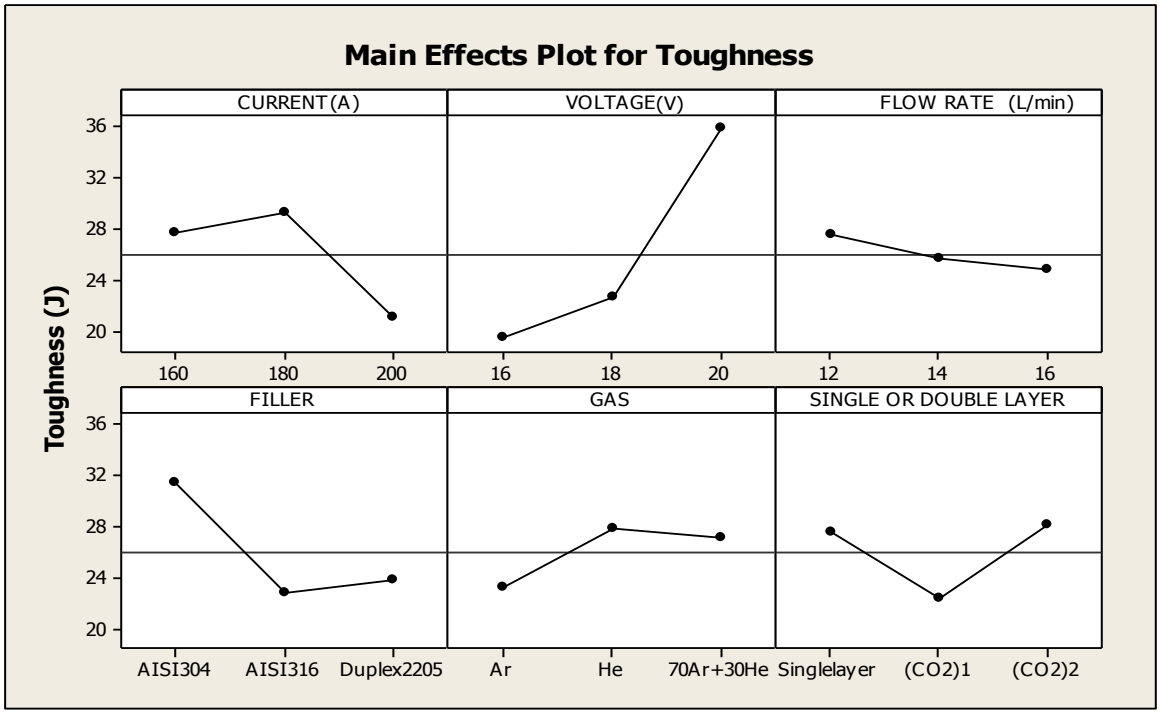

Figure 4.8: Main effect plot to show the influence of process parameters on toughness of joints between AISI 304 and Duplex 2205

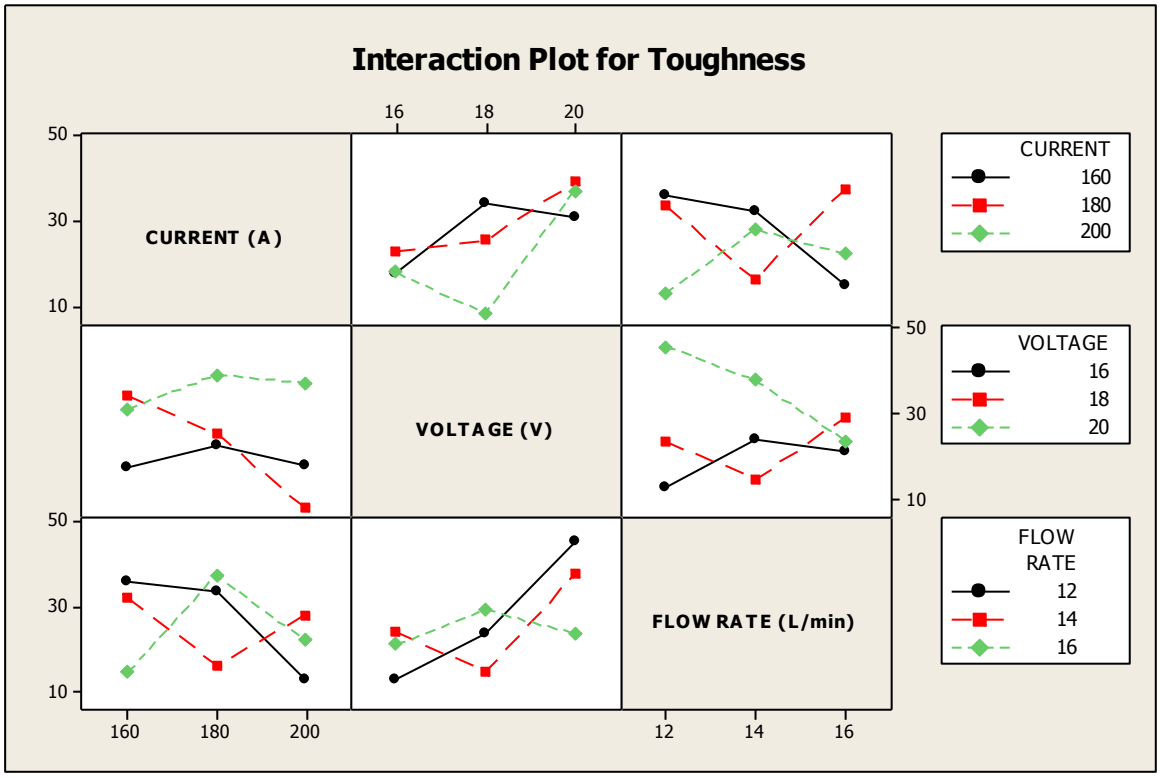

Figure 4.9: Interaction plot for toughness of joints between AISI 304 and Duplex 2205

Optimal design

From the main effect plot and interaction plot in Fig. 4.8 and Fig. 4.9 is used to estimate the maximum toughness with optimal design parameters conditions with "higher the better" type response. From Table 4.8 considering higher *F*-value and corresponding percentage contribution voltage and interaction between current × flow rate and voltage × flow rate are observed significantly influencing the toughness. The levels of these factors which give the maximum toughness are noted from main effect plot (Fig. 4.8) and the corresponding toughness for these levels of $\overline{B_3}$ are obtained directly from the Table 4.6. For interactions, levels of current × flow rate ($A \times C$) and voltage × flow rate ($B \times C$) are decided from the interaction plot (Fig. 4.9) and maximum toughness is observed at $\overline{A_2 \times C_3}$, $\overline{B_3 \times C_1}$. To obtain the best estimate of a mean when an interaction is present, the trial that include that treatment condition should be averaged. Average toughness for these two interactions are obtained by taking the average of three trials (trial 12, 15, 18) for $\overline{A_2 \times C_3}$ and (trial 7, 16, 25) for $\overline{B_3 \times C_1}$. Maximum value of voltage is selected because toughness is 'higher the better' type response. Desired mean value in this case is estimated as:

$$\mu_{B_3, A_2 \times C_3, B_3 \times C_1,} = \overline{B_3} + \overline{A_2 \times C_3} + \overline{B_3 \times C_1} - 2\,\overline{T} \qquad (4.5)$$

$$= 35.86 + 37.60 + 45.78 - 52.02$$

$= 67.21$ J

Confidence interval

$$CI = \sqrt{\frac{F_{\alpha,\nu_1,\nu_2} V_e}{n_{eff}}} \quad (4.6)$$

$$n_{eff} = \frac{N}{1+DF_{B,D,F,A\times B}} = \frac{27}{1+10} = 2.45$$

V_e = Variance (error)

$$CI = \sqrt{\frac{2.91 \times 94.12}{2.45}} = \pm 10.57 \text{ J}$$

Thus the optimum value of toughness is (67.21 ± 10.57) J

4.3.2 Impact Test for Toughness in Welding of AISI 316 and Duplex 2205

The results of toughness carried out on joints performed as per L_{27} orthogonal array on the welding of materials AISI 316 and Duplex 2205 are given in Table 4.10.

Figure 4.10: Specimens of AISI 304 and Duplex 2205 after toughness test

Table 4.10: Results of toughness for joints between AISI 316 and Duplex 2205

Exp. No	Current (A)	Voltage (V)	Flow rate (L/min)	Filler Wire	Gas Type	Single or Double Layer	Toughness (J)
1	160	16	12	AISI 304	Ar	Single Layer	4.905
2	160	16	14	AISI 316	He	$(CO_2)_1$	132.435
3	160	16	16	Duplex 2205	70% Ar + 30% He	$(CO_2)_2$	11.772
4	160	18	12	AISI 316	He	$(CO_2)_2$	14.715
5	160	18	14	Duplex 2205	70% Ar + 30%He	Single Layer	9.810
6	160	18	16	AISI 304	Ar	$(CO_2)_1$	39.240
7	160	20	12	Duplex 2205	70% Ar + 30%He	$(CO_2)_1$	127.530
8	160	20	14	AISI 304	Ar	$(CO_2)_2$	39.240
9	160	20	16	AISI 316	He	Single Layer	4.905
10	180	16	12	AISI 316	70% Ar + 30% He	$(CO_2)_1$	4.905
11	180	16	14	Duplex 2205	Ar	$(CO_2)_2$	4.905
12	180	16	16	AISI 304	He	Single Layer	44.145
13	180	18	12	Duplex 2205	Ar	Single Layer	9.810
14	180	18	14	AISI 304	He	$(CO_2)_1$	14.715
15	180	18	16	AISI 316	70% Ar + 30% He	$(CO_2)_2$	9.810
16	180	20	12	AISI 304	He	$(CO_2)_2$	24.525
17	180	20	14	AISI 316	70% Ar + 30% He	Single Layer	29.430
18	180	20	16	Duplex 2205	Ar	$(CO_2)_1$	107.910
19	200	16	12	Duplex 2205	He	$(CO_2)_2$	44.145
20	200	16	14	AISI 304	70% Ar + 30% He	Single Layer	24.525
21	200	16	16	AISI 316	Ar	$(CO_2)_1$	4.905
22	200	18	12	AISI 304	70% Ar + 30% He	$(CO_2)_1$	44.145
23	200	18	14	AISI 316	Ar	$(CO_2)_2$	4.905
24	200	18	16	Duplex 2205	He	Single Layer	24.525
25	200	20	12	AISI 316	Ar	Single Layer	29.430
26	200	20	14	Duplex 2205	He	(CO2)1	34.335
27	200	20	16	AISI 304	70% Ar + 30% He	$(CO_2)_2$	53.955

($(CO_2)_1$: double layer shielding with gas flow rate of 8 L/min, $(CO_2)_2$: double layer shielding with gas flow rate of 12 L/min)

Analysis of Variance of Toughness

To find out the significance of various factors like current, voltage, filler material, gas flow rate, gas type and single or double layer shielding on tensile strength ANOVA is performed at measured data with 90% confidence level. *F*-test is used to find out the most significant factor correspond to each input parameter. *F*-test is based on the principle that larger the value of *F* calculated, greater the effect on that parameter. Table 4.11 and Table 4.12 shows the results obtained from the ANOVA and response table for the toughness of AISI 316 and Duplex 2205. From Table 4.11 it is observed that voltage, single layer or double layer shielding of gas and interaction of current × flow rate are statistically the most significant parameter that affects the toughness.

Table 4.11: ANOVA for toughness of joints between AISI 316 and Duplex 2205

Source	Symbol	DF	SS	Variance	*F*-value	Percentage contribution
Current (A)	*A*	2	1207.5	603.76	0.18	3.65
Voltage (V)	*B*	2	4432.5	2216.25	0.66	13.41
Flow rate (L/min)	*C*	2	5.6	2.82	0.00	0.01
Filler wire	*D*	2	1096.3	548.15	0.16	3.31
Gas	*E*	2	525.3	262.65	0.08	1.59
Single layer or double layer	*F*	2	7407.3	3703.63	1.11	22.42
Current × Voltage	*A* × *B*	4	1304.0	326.01	0.10	3.94
Current × Flow rate	*A* × *C*	4	6394.9	1598.73	0.48	19.35
Voltage × Flow rate	*B* × *C*	4	3978.3	994.58	0.30	12.04
Residual Error		2	6681.2	3340.60		20.22
Total		26	33033.0			100

Table 4.12 shows the response table of various input parameters with the rank in term of their relative significance. From the Table 4.12 it is found that single or double layer shielding is the most significant factor with rank 1 and gas flow rate is least significant factor assigned with rank 6.

Table 4.12: Response Table for toughness of joints between AISI 316 and Duplex 2205

Level	Current (A)	Voltage (V)	Flow rate (L/min)	Filler	Gas	Single or double layer
1	42.73	30.74	33.79	32.16	27.25	20.17
2	27.80	19.08	32.70	26.16	37.61	56.68
3	29.43	50.14	33.46	41.64	35.10	23.11
Delta	14.93	31.07	1.09	15.48	10.36	36.52
Rank	4	2	6	3	5	1

Figure 4.11 shows the main effect plot to show the influence of process parameters on joints between AISI 304 and Duplex 2205. In which X-axis show process parameters and Y-axis shows the toughness with mean line. Figure 4.11 shows that with increase in voltage toughness increases because increase in voltage heat input increases. More heat input results in flatter and wider bead of base material which leads to more toughness. Toughness of weld material is not much affected by gas type and flow rate of gas. Filler wire of Duplex2205 shows more toughness and decreases by using filler wire of AISI 316 due to more resistance to hot cracking, good thermal conductivity and less thermal expansion coefficient of filler wire. Toughness of material also increases by using CO_2 as an outer shielding by using flow rate of 8 L/min. Figure 4.12 shows the interaction between significant factors such as current × flow rate. With increase in current and flow rate toughness increases because increase in these parameters leads to more heat input. More heat input results in formation of sigma phase due to which toughness may decreases.

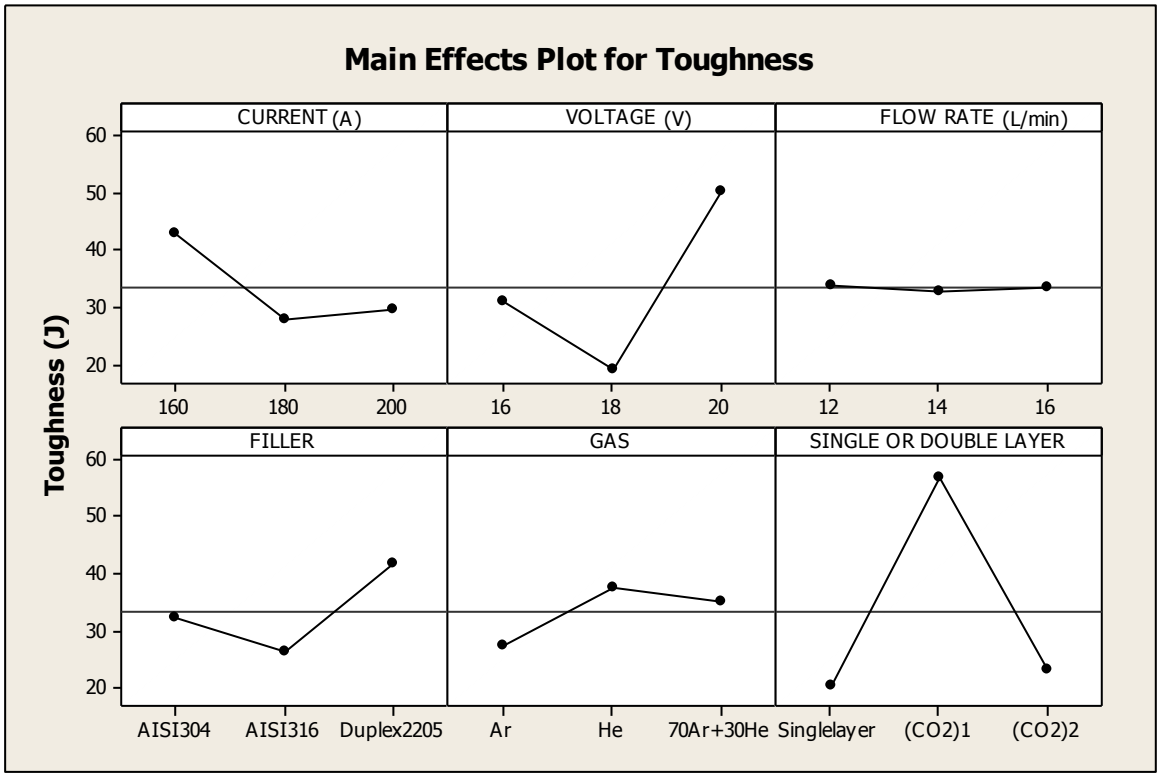

Figure 4.11: Main effect plot to show the influence of process parameters on toughness of joints between AISI 316and Duplex 2205

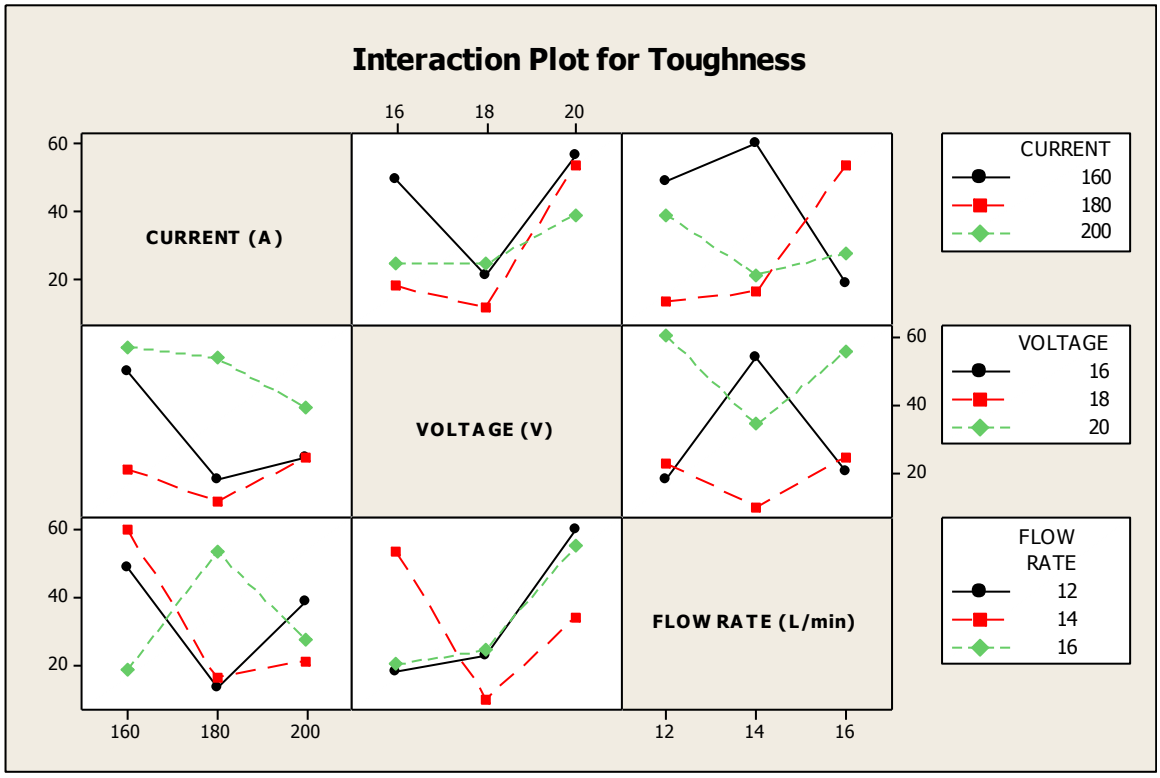

Figure 4.12: Interaction plot for toughness of joints between AISI 316 and Duplex 2205

4.4 Microhardness Test

Microhardness is the surface characteristics that give hardness of a sample at micro level. It is calculated by applying some force on the sample with the help of an indenter. By applying the force with indenter it gives an indent on the sample surface than that indents is used to calculate the microhardness at that particular point. Microhardness is calculated in terms of Vickers's Hardness Number (HVN).

4.4.1 Microhardness of Fusion Zone in Welding of AISI 304 and Duplex 2205

The results of microhardness carried out on joints performed as per L_{27} orthogonal array on the welding of materials AISI 304 and Duplex 2205 are given in Table 4.13.

Table 4.13: Results of microhardness of fusion zone for joints between AISI 304 and DUPLEX 2205

Exp. No	Current (A)	Voltage (V)	Flow rate (L/min)	Filler wire	Gas	Single or Double Layer	Micro hardness (HVN)
1	160	16	12	AISI 304	Ar	Single Layer	285.881
2	160	16	14	AISI 316	He	$(CO_2)_1$	302.725
3	160	16	16	Duplex 2205	70% Ar + 30% He	$(CO_2)_2$	297.873
4	160	18	12	AISI 316	He	$(CO_2)_2$	305.013
5	160	18	14	Duplex 2205	70% Ar + 30%He	Single Layer	304.835
6	160	18	16	AISI 304	Ar	$(CO_2)_1$	306.157
7	160	20	12	Duplex 2205	70% Ar + 30%He	$(CO_2)_1$	307.301
8	160	20	14	AISI 304	Ar	$(CO_2)_2$	306.382
9	160	20	16	AISI 316	He	Single Layer	312.103
10	180	16	12	AISI 316	70% Ar + 30% He	$(CO_2)_1$	316.904
11	180	16	14	Duplex 2205	Ar	$(CO_2)_2$	289.220
12	180	16	16	AISI 304	He	Single Layer	261.535
13	180	18	12	Duplex 2205	Ar	Single Layer	325.171
14	180	18	14	AISI 304	He	$(CO_2)_1$	302.256
15	180	18	16	AISI 316	70% Ar + 30% He	$(CO_2)_2$	328.745
16	180	20	12	AISI 304	He	$(CO_2)_2$	342.976
17	180	20	14	AISI 316	70% Ar + 30% He	Single Layer	337.575
18	180	20	16	Duplex 2205	Ar	$(CO_2)_1$	332.174
19	200	16	12	Duplex 2205	He	$(CO_2)_2$	336.749
20	200	16	14	AISI 304	70% Ar + 30% He	Single Layer	341.323
21	200	16	16	AISI 316	Ar	$(CO_2)_1$	345.898
22	200	18	12	AISI 304	70% Ar + 30% He	$(CO_2)_1$	350.473
23	200	18	14	AISI 316	Ar	$(CO_2)_2$	344.595
24	200	18	16	Duplex 2205	He	Single Layer	338.718
25	200	20	12	AISI 316	Ar	Single Layer	336.644
26	200	20	14	Duplex 2205	He	$(CO2)_1$	332.841
27	200	20	16	AISI 304	70% Ar + 30% He	$(CO_2)_2$	326.964

($(CO_2)_1$: double layer shielding with gas flow rate of 8 L/min, $(CO_2)_2$: double layer shielding with gas flow rate of 12 L/min)

Analysis of Variance of Microhardness at Fusion Zone

To find out the significance of various factors like current, voltage, filler material, gas, flow rate, gas type and single or double layer shielding on microhardness ANOVA is performed at measured data with 90% confidence level. *F*-test is used to find out the most significant factor correspond to each input parameter. *F*-test is based on the principle that larger the value of *F* calculated, greater the effect on that parameter. Table 4.14 and Table 4.15 shows the results obtained from the ANOVA and response table for the microhardness of AISI 304 and Duplex 2205. From Table 4.14 it is observed that current, and interaction of current × voltage are statistically the most significant parameter that affects the microhardness.

Table 4.14: ANOVA for microhardness of joints between AISI 304 and fusion zone

Source	Symbol	DF	SS	Variance	*F*-value	Percentage contribution
Current (A)	*A*	2	6123.3	3061.66	54.88	48.79
Voltage (V)	*B*	2	1547.8	773.88	13.87	12.33
Flow rate (L/min)	*C*	2	201.3	100.64	1.80	1.60
Filler wire	*D*	2	638.2	319.12	5.72	5.08
Gas	*E*	2	330.2	165.09	2.96	2.63
Single layer or double layer	*F*	2	160.8	80.39	1.44	1.28
Current × Voltage	*A* × *B*	4	2545.3	636.32	11.41	20.28
Current × Flow rate	*A* × *C*	4	676.6	169.15	3.03	5.39
Voltage × Flow rate	*B* × *C*	4	214.5	53.62	0.96	1.70
Residual Error		2	111.6	55.78		0.88
Total		26	12549.5			100

Table 4.15 shows the response table of various input parameters with the rank in term of their relative significance. From the Table 4.15 it is found that current is the most significant factor with rank 1 and effect of single layer or double layer is least significant factor assigned with rank 6.

Table 4.15: Response Table for microhardness of joints between AISI 304 and DUPLEX 2205

Level	Current (A)	Voltage (V)	Flow rate (L/min)	Filler	Gas	Single or double layer
1	303.1	308.7	323.0	313.8	319.1	316.0
2	315.2	322.9	318.0	325.6	315.0	321.9
3	339.4	326.1	316.7	318.3	323.6	319.8
Delta	36.2	17.4	6.3	11.8	8.6	5.9
Rank	1	2	5	3	4	6

Figure 4.13 shows the main effect plot to show the influence of process parameters on joints between AISI 304 and Duplex 2205. In which X-axis shows process parameters and Y-axis shows the microhardness with mean line. From Fig. 4.13 and Fig.4.14 it is seen that with increase in current or by the interaction of current × voltage microhardness increases because with increase in current and voltage. In the present study, selected current parameter favour the above condition but if the current and voltage are increased further it may lead to high input energy and coarseness in grain structure and leads to decrease in microhardness. Microhardness of weld material is not much affected by gas type and flow rate of gas. Filler wire of AISI 316 shows more hardness and decreases by using filler wire of AISI 304.

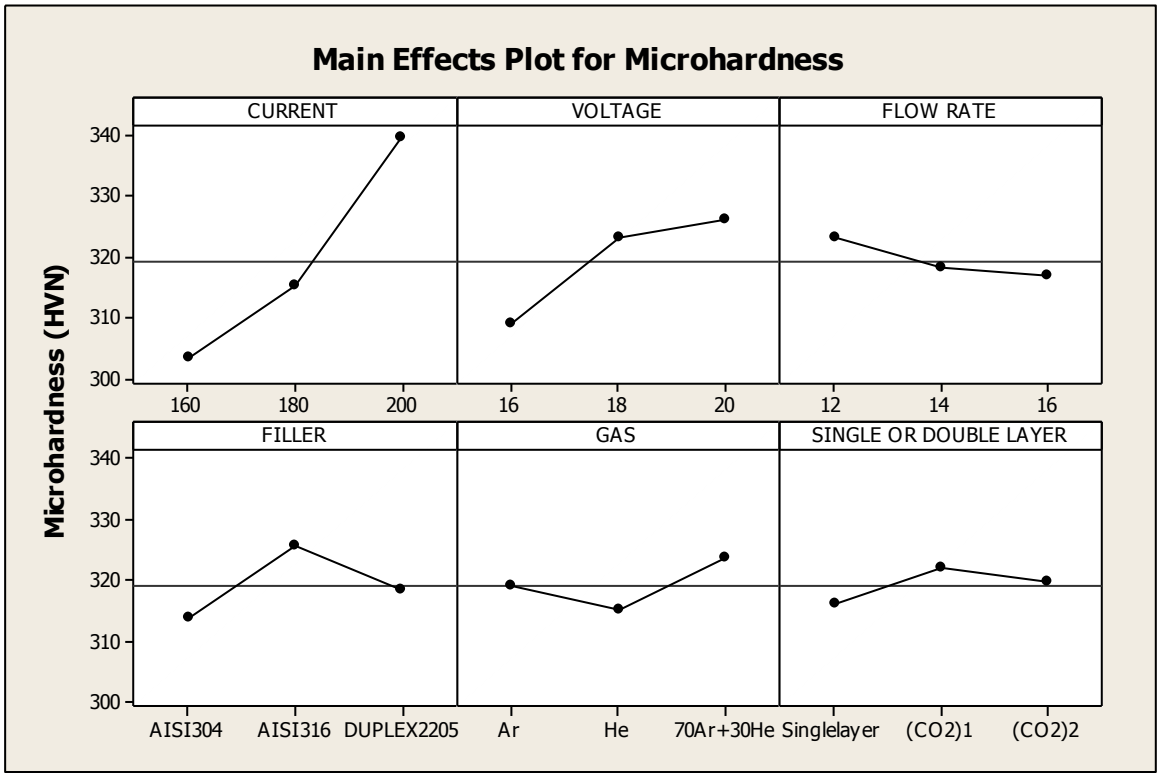

Figure 4.13: Main effect plot to show the influence of process parameters on microhardness of joints between AISI 304 and DULPEX 2205

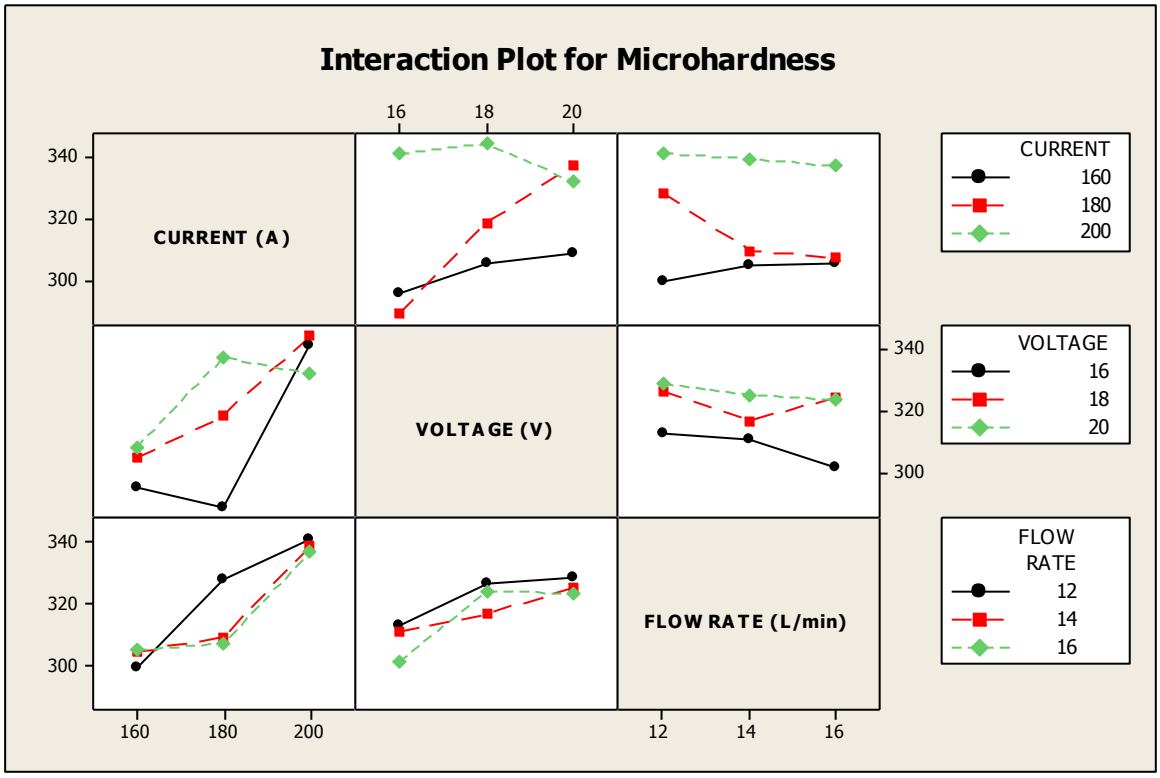

Figure 4.14: Interaction plot for microhardness of joints between AISI 304 and DUPLEX 2205

Optimal design

From the main effect plot and interaction plot in Fig. 4.13 and Fig. 4.14 is used to estimate the maximum microhardness with optimal design parameters conditions with "higher the better" type response. From Table 4.14 considering higher *F*-value and corresponding percentage contribution current and interaction between current × voltage is observed significantly influencing the microhardness. The levels of these factors which give the maximum hardness are noted from main effect plot (Fig. 4.13) and the corresponding hardness for these levels of $\overline{A_3}$ are obtained directly from the Table 4.15. For interactions, levels of current × voltage ($A \times B$) are decided from the interaction plot (Fig. 4.14) and maximum hardness is observed at $\overline{A_3 \times B_2}$. To obtain the best estimate of a mean when an interaction is present, the trial that include that treatment condition should be averaged. Average hardness for this interactions is obtained by taking the average of three trials (trial 22, 23, 34) for $\overline{A_3 \times B_2}$. Maximum value of voltage is selected because hardness is 'higher the better' type response. Desired mean value in this case is estimated as:

$$\mu_{A_3, A_3 \times B_2,} = \overline{A_3} + \overline{A_3 \times B_2} - \overline{T} \qquad (4.7)$$

$$= 339.4 + 344.59 - 319.22$$

$$= 364.77 \text{ HVN}$$

Confidence interval

$$CI = \sqrt{\frac{F_{\alpha,\nu_1,\nu_2} V_e}{n_{eff}}} \quad (4.8)$$

$n_{eff} = \frac{N}{1+DF_{B,D,F,A\times B}} = \frac{27}{1+10} = 2.45$

V_e = Variance of error

$$CI = \sqrt{\frac{2.91 \times 55.78}{2.45}} = \pm 8.13 \text{ HVN}$$

Thus the optimum value of microhardness is (364.77 $\pm$ 8.13) HVN

4.4.2 Microhardness of fusion zone in Welding of AISI 316 and Duplex 2205

The results of microhardness carried out on joints performed as per L_{27} orthogonal array on the welding of materials AISI 316 and Duplex 2205 are given in Table 4.16.

Table 4.16: Results of microhardness of fusion zone for joints between AISI 316 and Duplex 2205

Exp. No	Current (A)	Voltage (V)	Flow rate (L/min)	Filler wire	Gas	Single or Double Layer	Micro hardness (HVN)
1	160	16	12	AISI 304	Ar	Single Layer	291.614
2	160	16	14	AISI 316	He	$(CO_2)_1$	302.663
3	160	16	16	Duplex 2205	70% Ar + 30% He	$(CO_2)_2$	297.138
4	160	18	12	AISI 316	He	$(CO_2)_2$	299.901
5	160	18	14	Duplex 2205	70% Ar + 30%He	Single Layer	305.577
6	160	18	16	AISI 304	Ar	$(CO_2)_1$	280.564
7	160	20	12	Duplex 2205	70% Ar + 30%He	$(CO_2)_1$	304.197
8	160	20	14	AISI 304	Ar	$(CO_2)_2$	279.200
9	160	20	16	AISI 316	He	Single Layer	272.951
10	180	16	12	AISI 316	70% Ar + 30% He	$(CO_2)_1$	274.260
11	180	16	14	Duplex 2205	Ar	$(CO_2)_2$	272.951
12	180	16	16	AISI 304	He	Single Layer	271.642
13	180	18	12	Duplex 2205	Ar	Single Layer	285.630
14	180	18	14	AISI 304	He	$(CO_2)_1$	294.781
15	180	18	16	AISI 316	70% Ar + 30% He	$(CO_2)_2$	317.919
16	180	20	12	AISI 304	He	$(CO_2)_2$	329.488
17	180	20	14	AISI 316	70% Ar + 30% He	Single Layer	341.058
18	180	20	16	Duplex 2205	Ar	$(CO_2)_1$	364.196
19	200	16	12	Duplex 2205	He	$(CO_2)_2$	351.965
20	200	16	14	AISI 304	70% Ar + 30% He	Single Layer	339.734
21	200	16	16	AISI 316	Ar	$(CO_2)_1$	342.792
22	200	18	12	AISI 304	70% Ar + 30% He	$(CO_2)_1$	315.273
23	200	18	14	AISI 316	Ar	$(CO_2)_2$	313.465
24	200	18	16	Duplex 2205	He	Single Layer	311.658
25	200	20	12	AISI 316	Ar	Single Layer	312.863
26	200	20	14	Duplex 2205	He	$(CO2)_1$	311.658
27	200	20	16	AISI 304	70% Ar + 30% He	$(CO_2)_2$	310.453

($(CO_2)_1$: double layer shielding with gas flow rate of 8 L/min, $(CO_2)_2$: double layer shielding with gas flow rate of 12 L/min)

Analysis of Variance of Microhardness at Fusion Zone

To find out the significance of various factors like current, voltage, filler material, gas, flow rate, gas type and single or double layer shielding on microhardness ANOVA is performed at measured data with 90% confidence level. *F*-test is used to find out the most significant factor correspond to each input parameter. *F*-test is based on the principle that larger the value of *F* calculated, greater the effect on that parameter. Table 4.17 and Table 4.18 shows the results obtained from the ANOVA and response table for the microhardness of AISI 316 and Duplex 2205. From Table 4.17 it is observed that current, voltage, filler wire, gas and interaction of current × voltage, current × flow rate of shielding gas are statistically the most significant parameter that affects the microhardness.

Table 4.17: ANOVA for microhardness of joints between AISI 316 and DUPLEX 2205

Source	Symbol	DF	SS	Variance	*F*-value	Percentage contribution
Current (A)	*A*	2	4263.1	2131.54	348.01	25.43
Voltage (V)	*B*	2	639.7	319.84	52.22	3.81
Flow rate (L/min)	*C*	2	3.8	1.88	0.31	0.02
Filler wire	*D*	2	499.3	249.63	40.76	2.97
Gas	*E*	2	272.9	136.43	22.27	1.62
Single layer or double layer	*F*	2	193.5	96.77	15.80	1.15
Current × Voltage	*A* × *B*	4	9633.6	2408.41	393.21	57.47
Current × Flow rate	*A* × *C*	4	1158.3	289.58	47.28	6.91
Voltage × Flow rate	*B* × *C*	4	84.2	21.04	3.44	0.50
Residual Error		2	12.2	6.12		0.07
Total		26	16760.5			

Table 4.18 shows the response table of various input parameters with the rank in term of their relative significance. From the Table 4.18 it is found that current is the most significant factor with rank 1 and flow rate of shielding gas is least significant factor assigned with rank 6.

Table 4.18: Response Table for microhardness of joints between AISI 316 and DUPLEX 2205

Level	Current (A)	Voltage (V)	Flow rate (L/min)	Filler	Gas	Single or double layer
1	292.6	305.0	307.2	301.4	304.8	303.6
2	305.8	302.8	306.8	308.7	305.2	310.0
3	323.3	314.0	307.7	311.7	311.7	308.1
Delta	30.7	11.3	0.9	10.2	6.9	6.4
Rank	1	2	6	3	4	5

Figure 4.15 shows the main effect plot to show the influence of process parameters on joints between AISI 316 and Duplex 2205. In which X-axis show process parameters and Y-axis shows the microhardness with mean line. From Fig. 4.15 and Fig. 4.16 it is seen that with increase in current, voltage and interaction of current × voltage, current × flow rate hardness of weld metal increases because with increase in current and voltage grain nucleation and growth of austenite can lead to reduce the dislocations of grains and work hardening compared to its elementary condition. Among the shielding gas mixture, 70% Argon + 30% Helium will give the better hardness value when compared to other shielding gas mixtures. The sample welded under the 70% Argon + 30% Helium, its microstructure is mainly austenite phase and in small area adjacent to the boundary ferrite structure is formed. As results of the formation of primarily austenitic structure and which presents the nucleation of very fine grain size and low inter granular spacing it will attained the maximum hardness value. And from the results it is clear that increase in current intensity that increases the hardness value for all shielding gases. Filler wire of Duplex2205 shows more hardness and decreases by using filler wire of AISI 304 due to more resistance to hot cracking, good thermal conductivity and less thermal expansion coefficient of filler wire. Microhardness of material also increases by using CO_2 as an outer shielding by using flow rate of 8 L/min.

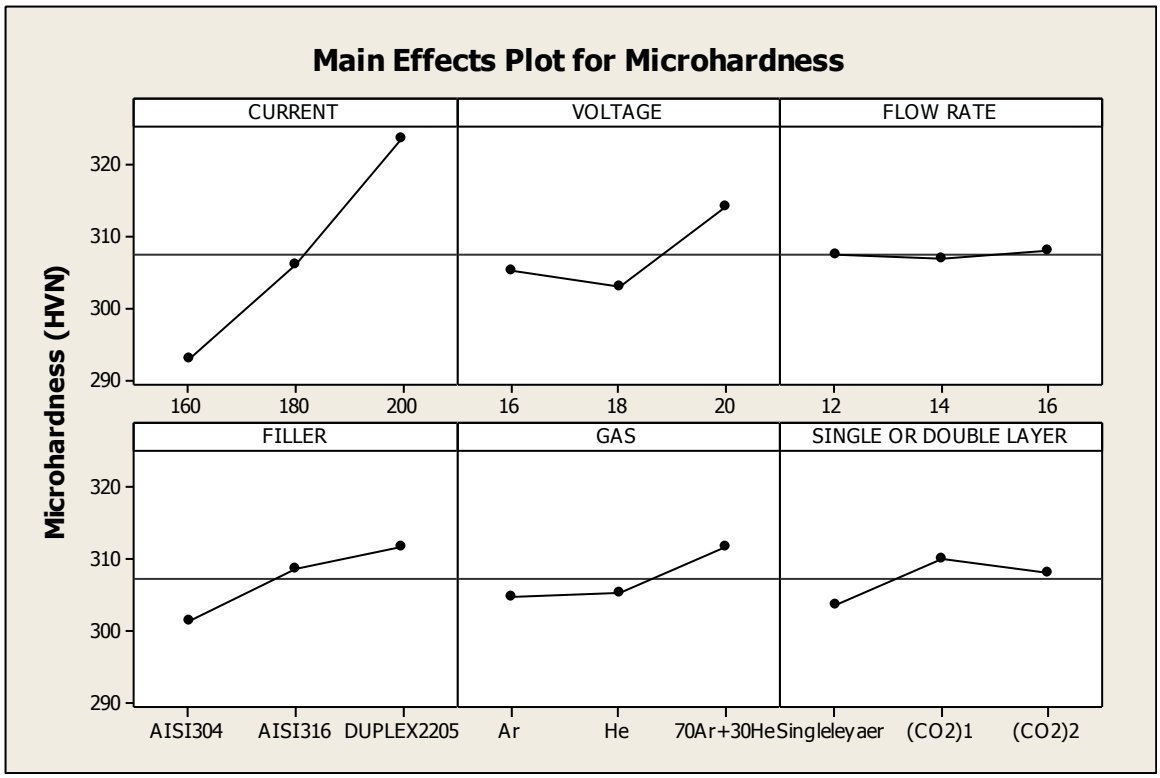

Figure 4.15: Main effect plot to show the influence of process parameters on microhardness of joints between AISI 316 and DULPEX 2205

From the interaction plot between current and flow rate (Fig. 4.16) it is seen that with increase in value of both the process parameters hardness of weld metal increases because with increase in current and flow rate at a particular condition cooling of weld zone is very fast and leads to fine grain structure. This fine grain structure leads to more hardness of weld metal.

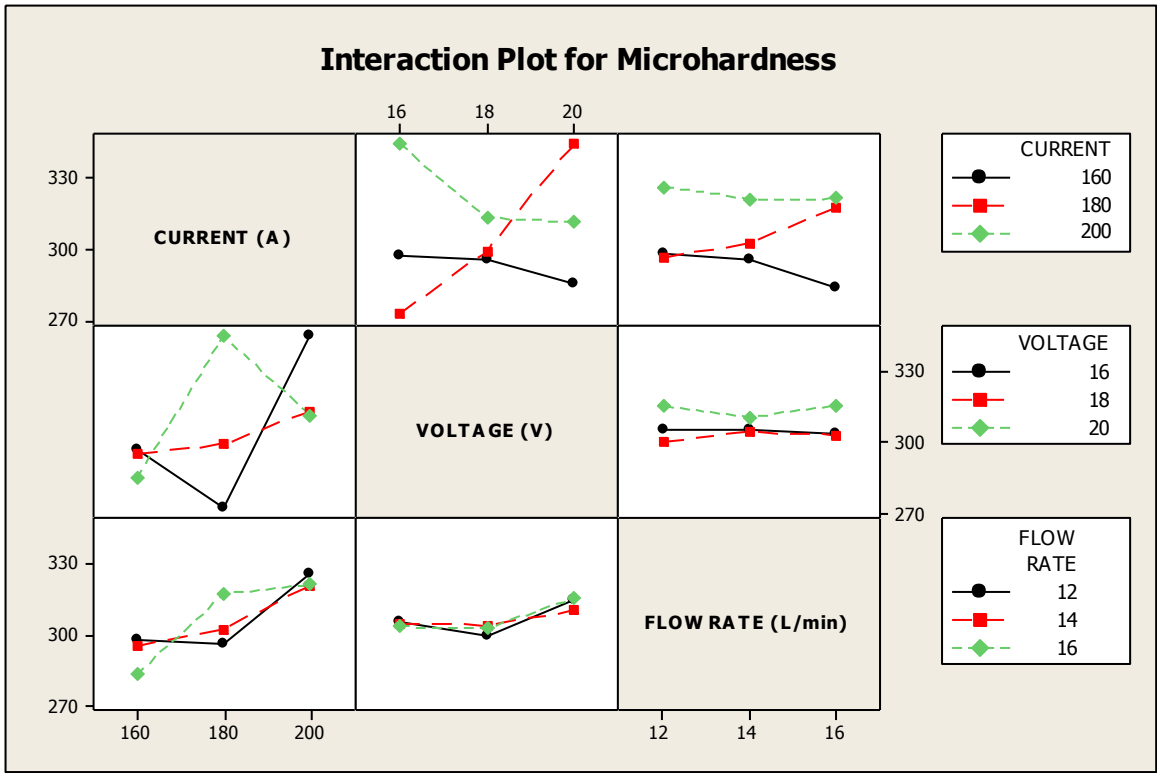

Figure 4.16: Interaction plot for microhardness of joints between AISI 316 and DUPLEX 2205

Optimal design

From the main effect plot and interaction plot in Fig. 4.15 and Fig. 4.16 is used to estimate the maximum microhardness with optimal design parameters conditions with "higher the better" type response. From Table 4.17 considering higher *F*-value and corresponding percentage contribution current, voltage, filler wire and shielding gas are the most significant factors. and from Table 4.18 it is seen that interaction between current × voltage and interaction between voltage × flow rate are observed significantly influencing the microhardness. The levels of these factors which give the maximum hardness are noted from main effect plot (Fig. 4.15) and the corresponding hardness for these levels of $\overline{A_3}$, $\overline{B_3}$, $\overline{D_3}$, $\overline{E_3}$ are obtained directly from the Table 4.18. For interactions, levels of current × voltage ($A \times B$)

and current × flow rate are decided from the interaction plot (Fig. 4.16) and maximum hardness is observed at $\overline{A_2 \times B_3}$, $\overline{A_3 \times C_1}$. To obtain the best estimate of a mean when an interaction is present, the trial that include that treatment condition should be averaged. Average hardness for these interactions is obtained by taking the average of three trials (trial 16, 17, 18) for $\overline{A_2 \times B_3}$ and by taking the average of three trials (trial 19, 22, 25) for$\overline{A_3 \times C_1}$. Maximum value of significant parameters are selected because hardness is 'higher the better' type response. Desired mean value in this case is estimated as:

$$\mu_{A_3,B_3,D_3,E_3,A_2\times B_3,A_3\times C_1,} = \overline{A_3} + \overline{B_3} + \overline{D_3} + \overline{E_3} + \overline{A_2 \times B_3} + \overline{A_3 \times C_1} - 5\,\overline{T} \quad (4.9)$$

$$= 323.3 + 314.0 + 311.7 + 311.7 + 344.9 + 326.7 - 1536.22$$

$$= 396.08 \text{ HVN}$$

Confidence interval

$$CI = \sqrt{\frac{F_{\alpha,\nu_1,\nu_2} V_e}{n_{eff}}} \quad (4.10)$$

$$n_{eff} = \frac{N}{1+DF_{B,D,F,A\times B}} = \frac{27}{1+10} = 2.45$$

V_e = Variance of error

$$CI = \sqrt{\frac{2.91 \times 6.12}{2.45}} = \pm 2.69 \text{ HVN}$$

Thus the optimum value of microhardness is (396.08 $\pm$ 2.69) HVN

4.5 Weld Distortion

Distortion in a welded structure is due to the non-uniform contraction and expansion of the weld material and surrounding base material, caused by the heating and cooling of material during welding process. After welding of the plates, disortion is measured from the centre of the two plates to the outer edge of the plate. For this height is measured from the centre of the butt joint and moved the dial indicator in axial direction (ΔX) and height is measured in vertical direction at the free end and is denoted by (ΔZ). After getting the value of (ΔX) and (ΔZ) angular deformation is measured from the relation given in Eq. (4.11).

$$tan\theta = \frac{\Delta X}{\Delta Z} \quad (4.11)$$

Where θ = angular distortion

ΔX = horizontal distance (mm)

ΔZ = vertical distance (mm)

4.5.1 Distortion in Welding of AISI 304 and Duplex 2205

The results of weld distortion carried out on joints performed as per L_{27} orthogonal array on the welding of materials AISI 304 and Duplex 2205 are given in Table 4.19.

Table 4.19: Results of weld distortion of joints between AISI 304 and Duplex 2205

Exp. No.	Current (A)	Voltage (V)	Flow rate (L/min)	Filler wire	Gas type	Single or double layer	Distortion (°)
1	160	16	12	AISI 304	Ar	Single Layer	0.057
2	160	16	14	AISI 316	He	$(CO_2)_1$	0.515
3	160	16	16	Duplex 2205	70% Ar + 30% He	$(CO_2)_2$	0.487
4	160	18	12	AISI 316	He	$(CO_2)_2$	0.200
5	160	18	14	Duplex 2205	70% Ar + 30% He	Single Layer	2.233
6	160	18	16	AISI 304	Ar	$(CO_2)_1$	0.973
7	160	20	12	Duplex 2205	70% Ar + 30% He	$(CO_2)_1$	3.205
8	160	20	14	AISI 304	Ar	$(CO_2)_2$	1.918
9	160	20	16	AISI 316	He	Single Layer	1.145
10	180	16	12	AISI 316	70% Ar + 30% He	$(CO_2)_1$	1.231
11	180	16	14	Duplex 2205	Ar	$(CO_2)_2$	0.744
12	180	16	16	AISI 304	He	Single Layer	1.059
13	180	18	12	Duplex 2205	Ar	Single Layer	0.515
14	180	18	14	AISI 304	He	$(CO_2)_1$	0.515
15	180	18	16	AISI 316	70% Ar + 30% He	$(CO_2)_2$	0.200
16	180	20	12	AISI 304	He	$(CO_2)_2$	1.460
17	180	20	14	AISI 316	70% Ar + 30% He	Single Layer	1.403
18	180	20	16	Duplex 2205	Ar	$(CO_2)_1$	2.405
19	200	16	12	Duplex 2205	He	$(CO_2)_2$	1.231
20	200	16	14	AISI 304	70% Ar + 30% He	Single Layer	0.401
21	200	16	16	AISI 316	Ar	$(CO_2)_1$	0.802
22	200	18	12	AISI 304	70% Ar + 30% He	$(CO_2)_1$	1.632
23	200	18	14	AISI 316	Ar	$(CO_2)_2$	0.171
24	200	18	16	Duplex 2205	He	Single Layer	0.687
25	200	20	12	AISI 316	Ar	Single Layer	0.315
26	200	20	14	Duplex 2205	He	(CO2)1	0.114
27	200	20	16	AISI 304	70% Ar + 30% He	$(CO_2)_2$	0.744

($(CO_2)_1$: double layer shielding with gas flow rate of 8 L/min, $(CO_2)_2$: double layer shielding with gas flow rate of 12 L/min)

Analysis of Variance of Weld Distortion

To find out the significance of various factors like current, voltage, filler material, gas flow rate, gas type and single or double layer shielding on weld distortion ANOVA is performed at measured data with 90% confidence level. *F*-test is used to find out the most significant factor correspond to each input parameter. *F*-test is based on the principle that larger the value of *F* calculated, greater the effect on that parameter. Table 4.20 and Table 4.21 shows the results obtained from the ANOVA and response table for the weld distortion of AISI 304 and Duplex 2205. From Table 4.20 it is observed that voltage is statistically the most significant parameter that affects the weld distortion.

Table 4.20: ANOVA for weld distortion of joints between AISI 304 and Duplex 2205

Source	Symbol	DF	SS	Variance	*F*-value	Percentage contribution
Current (A)	*A*	2	1.2864	0.6432	7.18	8.143
Voltage (V)	*B*	2	2.5832	1.2915	14.41	16.353
Flow rate (L/min)	*C*	2	0.2000	0.1000	1.12	1.266
Filler wire	*D*	2	1.7667	0.8833	9.86	11.184
Gas	*E*	2	1.3119	0.6559	7.32	8.305
Single layer or double layer	*F*	2	1.1549	0.5774	6.44	7.311
Current × Voltage	*A* × *B*	4	5.0514	1.2628	14.09	31.978
Current × Flow rate	*A* × *C*	4	1.7375	0.4343	4.85	10.999
Voltage × Flow rate	*B* × *C*	4	0.5246	0.1311	1.46	3.321
Residual Error		2	0.1792	0.0896		1.134
Total		26	15.7960			100

(DF: degree of freedom, SS: sum of squares)

Table 4.21 shows the response table of various input parameters with the rank in term of their relative significance. From the Table 4.21 it is found that voltage is the most significant factor with rank 1 and flow rate of shielding gas is least significant factor.

Table 4.21: Response Table for Weld Distortion of joints between AISI 304 and Duplex 2205

Level	Current (A)	Voltage (V)	Flow rate (L/min)	Filler	Gas	Single or double layer
1	1.1926	0.7252	1.0940	0.9732	0.8778	0.8683
2	1.0591	0.7918	0.8904	0.6647	0.7696	1.2658
3	0.6774	1.4121	0.9447	1.2912	1.2818	0.7950
Delta	0.5151	0.6869	0.2036	0.6266	0.5122	0.4708
Rank	3	1	6	2	4	5

Figure 4.17 shows the main effect plot to show the influence of process parameters on joints between AISI 304 and Duplex 2205. In which X-axis show process parameters taken and Y-axis shows the weld distortion with mean line. Figure 4.17 shows that with increase in voltage weld distortion increases because with increase in voltage heat input increases and more heat input results increase in temperature leads to weld distortion. Taking other process parameters in account, it is seen that with increase in current weld distortion decreases. Weld distortion is not much influenced by flow rate of gas as it is deviated near the mean line. By using filler material of AISI 316 minimum weld distortion is obtained. It is also seen that when CO_2 is used as outer shielding gas with flow rate of 12 L/min and helium as inner shielding gas distortion is minimum and maximum with flow rate of 8 L/min.

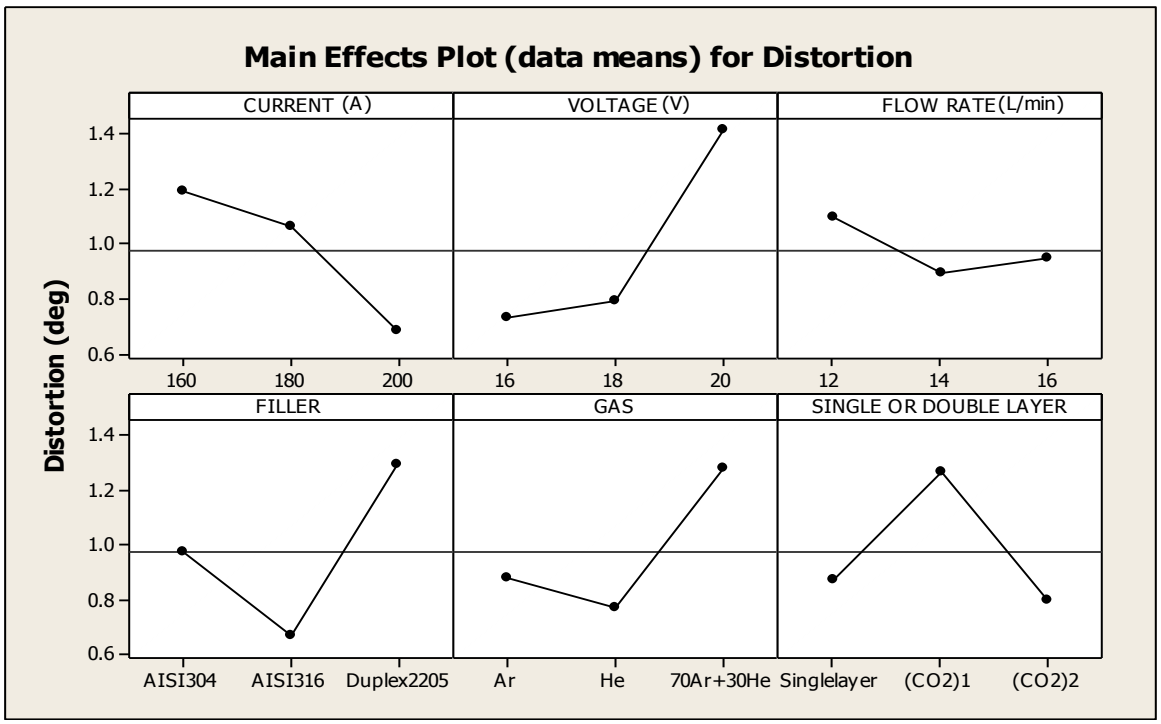

Figure 4.17: Main effect plot to show the influence of process parameters on weld distortion of joints between AISI 304 and Duplex 2205

Figure 4.18 shows the Interaction between current and voltage is observed statistically significant. With increase in current and voltage together heat input increases and leads to more temperature of arc and resulting in welding distortion.

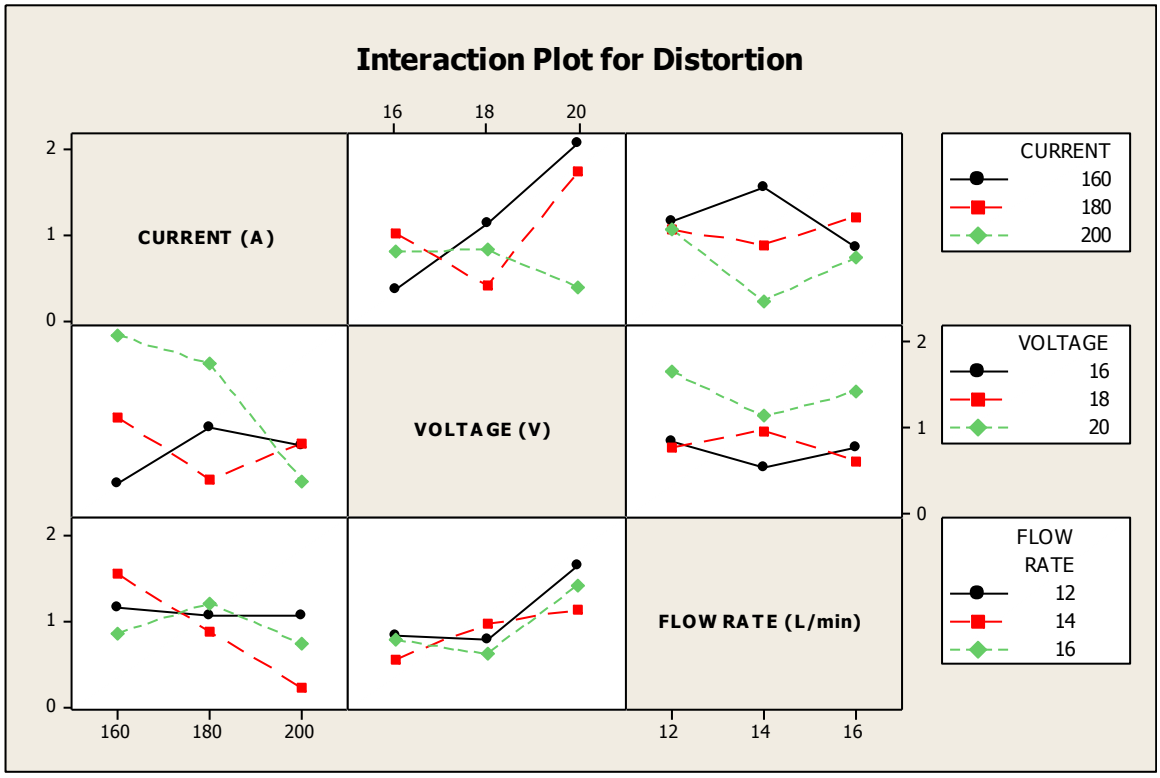

Figure 4.18: Interaction plot for weld distortion of joints between AISI 304 and Duplex 2205

Optimal Design

From the main effect plot and interaction plot in Fig. 4.17 and Fig. 4.18 is used to estimate the maximum weld distortion with optimal design parameters conditions. From Table 4.20 considering higher *F*-value and corresponding percentage contribution voltage and interaction between current and voltage are observed significantly influencing the weld distortion. The level of these factors which gives the minimum weld distortion are noted from main effect plot (Fig. 4.17) and the corresponding weld distortion for at these levels of $\overline{B_1}$ is obtained directly from the Table 4.21. For interactions, levels of current × voltage (*A*×*B*) are decided from the interaction plot (Fig. 4.18) and minimum weld distortion is observed at$\overline{A_1 \times B_1}$. To obtain the best estimate of a mean when an interaction is present, the trial that include that treatment condition should be averaged. Average weld distortion for these two interactions are obtained by taking the average of three trials (trial 1, 2, 3) for$\overline{A_1 \times B_1}$. Minimum value of current and voltage is selected because weld distortion is 'lower the better' type response. Desired mean value in this case is estimated as:

$$\mu_{B_1,A_1\times B_1} = \overline{B_1} + \overline{A_1 \times B_1} - \overline{T} \qquad (4.12)$$

$$= 0.7252 + 0.353 - 1.952$$

$$= 0.101°$$

Confidence interval

$$CI = \sqrt{\frac{F_{\alpha,\nu_1,\nu_2} V_e}{n_{eff}}} \quad (4.13)$$

Where Fα, ν_1, ν_2 = *F* ratio

α = 0.1 (risk)

Confidence = 1 – α

ν_1 = DF for mean (always 1)

ν_2 = DF for total (= 26)

$\overline{T}$ = Average of all experimental trial

n_{eff} = Number of tests under that condition using the participating factors

$$n_{eff} = \frac{N}{1+DF_{B_1,A_1\times B_1}} = \frac{27}{1+6} = 3.85$$

N is the number of trial in the experiment

V_e = Variance of error

$$CI = \sqrt{\frac{2.91 \times 0.0896}{3.85}} = \pm 0.260°$$

Thus the optimum value of weld distortion is (0.1019° $\pm$ 0.260°)

4.5.2 Distortion in Welding of AISI 316 and Duplex 2205

The results of weld distortion carried out on joints performed as per L_{27} orthogonal array on the welding of materials AISI 316 and Duplex 2205 are given in Table 4.22.

Table 4.22: Results of weld distortion of joints between AISI 316 and Duplex 2205

Exp. No.	Current (A)	Voltage (V)	Flow rate (L/min)	Filler	Gas	Single or Double Layer	Distortion (°)
1	160	16	12	AISI 304	Ar	Single Layer	2.633
2	160	16	14	AISI 316	He	$(CO_2)_1$	0.068
3	160	16	16	Duplex 2205	70% Ar + 30% He	$(CO_2)_2$	2.405
4	160	18	12	AISI 316	He	$(CO_2)_2$	0.085
5	160	18	14	Duplex 2205	70% Ar + 30% He	Single Layer	2.405
6	160	18	16	AISI 304	Ar	$(CO_2)_1$	0.401
7	160	20	12	Duplex 2205	70% Ar + 30% He	$(CO_2)_1$	1.031
8	160	20	14	AISI 304	Ar	$(CO_2)_2$	1.432
9	160	20	16	AISI 316	He	Single Layer	3.233
10	180	16	12	AISI 316	70% Ar + 30% He	$(CO_2)_1$	0.630
11	180	16	14	Duplex 2205	Ar	$(CO_2)_2$	0.601
12	180	16	16	AISI 304	He	Single Layer	2.433
13	180	18	12	Duplex 2205	Ar	Single Layer	0.716
14	180	18	14	AISI 304	He	$(CO_2)_1$	2.233
15	180	18	16	AISI 316	70% Ar + 30% He	$(CO_2)_2$	1.002
16	180	20	12	AISI 304	He	$(CO_2)_2$	2.359
17	180	20	14	AISI 316	70% Ar + 30% He	Single Layer	0.572
18	180	20	16	Duplex 2205	Ar	$(CO_2)_1$	2.405
19	200	16	12	Duplex 2205	He	$(CO_2)_2$	1.231
20	200	16	14	AISI 304	70% Ar + 30% He	Single Layer	1.517
21	200	16	16	AISI 316	Ar	$(CO_2)_1$	0.372
22	200	18	12	AISI 304	70% Ar + 30% He	$(CO_2)_1$	2.262
23	200	18	14	AISI 316	Ar	$(CO_2)_2$	1.059
24	200	18	16	Duplex 2205	He	Single Layer	1.145
25	200	20	12	AISI 316	Ar	Single Layer	2.719
26	200	20	14	Duplex 2205	He	(CO2)1	0.687
27	200	20	16	AISI 304	70% Ar + 30% He	$(CO_2)_2$	1.775

($(CO_2)_1$: double layer shielding with gas flow rate of 8 L/min, $(CO_2)_2$: double layer shielding with gas flow rate of 12 L/min)

Analysis of variance of weld distortion

To find out the significance of various factors like current, voltage, filler material, gas, flow rate, gas type and single or double layer shielding on weld distortion ANOVA is performed at measured data with 90% confidence level. *F*-test is used to find out the most significant factor correspond to each input parameter. *F*-test is based on the principle that larger the value of *F* calculated, greater the effect on that parameter. Table 4.23 and Table 4.24 shows the results obtained from the ANOVA and response table for the weld distortion of AISI 316 and Duplex 2205. From Table 4.23 it is observed that filler wire, single layer or double layer shielding, interactions of current and flow rate, voltage and flow rate are the most significant parameters that affect the weld distortion.

Table 4.23: ANOVA for weld distortion of joints between AISI 304 and Duplex 2205

Source	Symbol	DF	SS	Variance	*F*-value	Percentage contribution
Current (A)	*A*	2	0.0534	0.02670	0.02	0.24
Voltage (V)	*B*	2	1.5958	0.79789	0.63	7.22
Flow rate (L/min)	*C*	2	1.2207	0.61033	0.48	5.52
Filler wire	*D*	2	3.0081	1.50407	1.19	13.61
Gas	*E*	2	0.1073	0.05363	0.04	0.48
Single layer or double layer	*F*	2	3.1828	1.59141	1.26	14.40
Current × Voltage	*A* × *B*	4	1.1252	0.28131	0.22	5.09
Current × Flow rate	*A* × *C*	4	2.9591	0.73978	0.59	13.39
Voltage × Flow rate	*B* × *C*	4	6.3109	1.57772	1.25	28.57
Residual Error		2	2.5254	1.26269		11.43
Total		26	22.0887			100

(DF: degree of freedom, SS: sum of squares)

Table 4.24 shows the response table of various input parameters with the rank in term of their variation with weld distortion. From the Table 4.24 it is observed that filler wire shows more variation and assigned rank 1 and current show less variation so assigned with rank 6.

Table 4.24: Response Table for Weld Distortion of joints between AISI 316 and Duplex 2205

Level	Current (A)	Voltage (V)	Flow rate (L/min)	Filler	Gas	Single or double layer
1	1.521	1.321	1.518	1.894	1.371	1.930
2	1.439	1.256	1.175	1.082	1.497	1.121
3	1.419	1.801	1.686	1.403	1.511	1.328
Delta	0.103	0.545	0.511	0.812	0.140	0.809
Rank	6	3	4	1	5	2

Figure 4.19 shows the main effect plot to show the influence of process parameters on joints between AISI 316 and Duplex 2205. In which X-axis shows the process parameters and Y-axis shows the weld distortion with mean line. Figure 4.20 shows that welds distortion is not much influenced by current and gas type as they are shown nears the mean line of weld distortion. With increase in voltage and gas flow rate weld distortion first decreases and then increases. Effect of filler wire is that if filler wire of AISI 304 is used than weld distortion is more and by using filler wire AISI 316 weld distortion is less. It is also seen that minimum distortion is obtained by using CO_2 as an outer shielding gas with flow rate of 8 L/min.

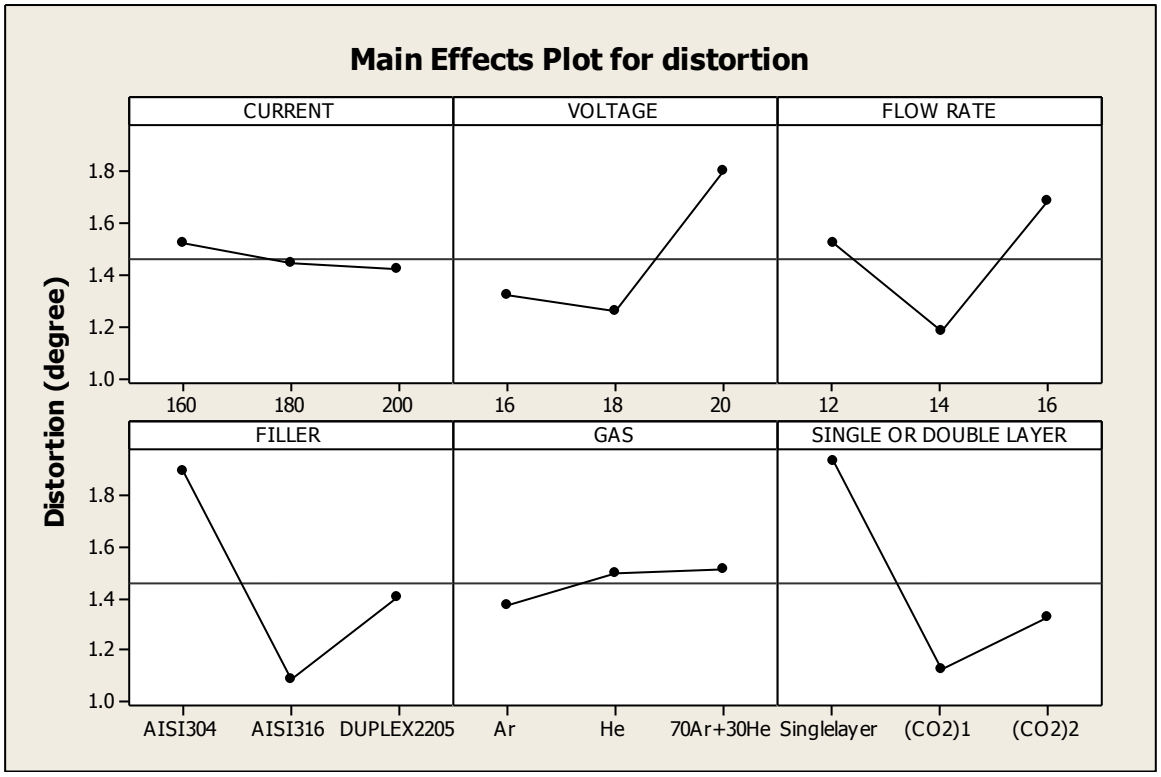

Figure 4.19: Main effect plot to show the influence of process parameters on weld distortion of joints between AISI 316 and Duplex 2205

Figure 4.20 shows the interactions plot between current, voltage and flow rate. Out of which interactions of current and flow rate, voltage and flow rate shows higher percentage contribution as observed in Table 4.24. With increase in current and flow rate of gas together heat input increases with current and weld metal tries to expand and with increase in flow rate weld metal tries to contract and results in weld distortion. Interaction of voltage and flow rate also has same effect as that of current and flow rate of gas.

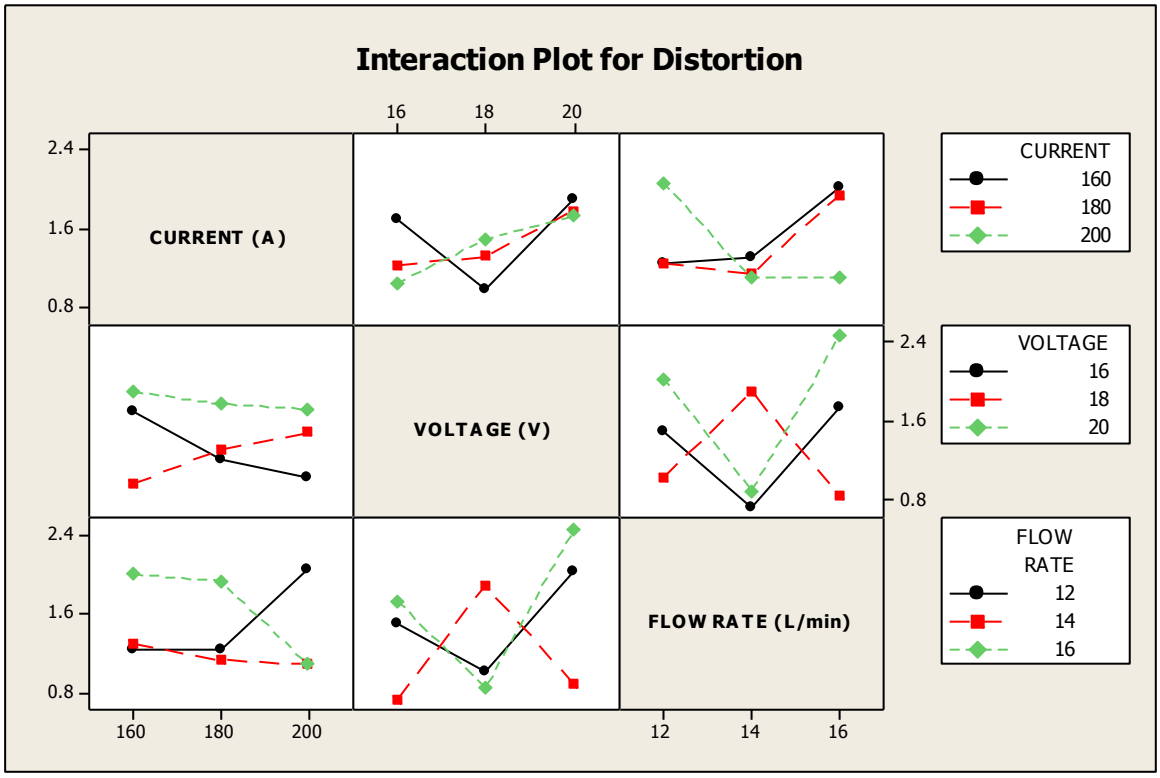

Figure 4.20: Interaction plot for weld distortion of joints between AISI 316 and Duplex 2205

Optimal Design

From the main effect plot and interaction plot in Fig. 4.19 and Fig. 4.20 is used to estimate the minimum weld distortion with optimal design parameters conditions. From Table 4.19 considering higher percentage contribution of filler wire, single or double layer shielding gas and interaction of current and flow rate, voltage and flow rate are observed significantly influencing. $\overline{D_1}$ and $\overline{F_2}$ is obtained directly from the Table 4.20 by selecting the minimum value of filler wire, and single or double layer shielding, $\overline{A_{3\times}C_2}$ and $\overline{B_{1\times}C_2}$ is obtained by first selecting the current, voltage and flow rate at minimum distortion from Fig. 4.19 and then taking average of that process parameter conditions. Minimum value of current, voltage and flow rate is selected because weld distortion is 'lower the better' type response. Desired mean value in this case is estimated as:

$$\mu_{D_2,F_2,A_3\times C_2,B_1\times C_2} = \overline{D_2} + \overline{F_2} + \overline{A_3 \times C_2} + \overline{B_3 \times C_2} - 3\overline{T}$$

$$= 1.403 + 1.121 + 1.087 + 1.135 - 4.379$$

$$= 0.367°$$

Confidence interval

$$CI = \sqrt{\frac{F_{\alpha,\nu_1,\nu_2} V_e}{n_{eff}}} \qquad (4.14)$$

Where Fα, v_1, v_2 = *F* ratio

α = 0.1 (risk)

Confidence = 1 – α

ν_1 = DF for mean (always 1)

ν_2 = DF for total (26)

$\overline{T}$ = Average of an experimental trial

n_{eff} = Number of tests under that condition using the participating factors

$n_{eff} = \frac{N}{1+DF_{D_1,F_2,A_3\times C_2,B_1\times C_2}} = \frac{27}{1+12} = 2.07$

N is the number of trial in the experiment

V_e = Variance of error

$CI = \sqrt{\frac{2.91 \times 1.2626}{2.076}} = \pm 1.33°$

Thus the optimum value of weld distortion is (0.1019 $\pm$ 1.33) °

4.6 Dye Penetration Test

Dye penetration method is used for inspecting weld bead when attempting to locate flaws open to the surface of non-porous materials. Basic steps that are performed on the material during inspection, based on the particular technique being used.

4.6.1 Dye Penetration Test for welding of AISI 304 and Duplex 2205

The visual inspection of dye penetration carried out on joints performed as per L_{27} orthogonal array on the welding of materials AISI 304 and Duplex 2205 are given in Table 4.25.

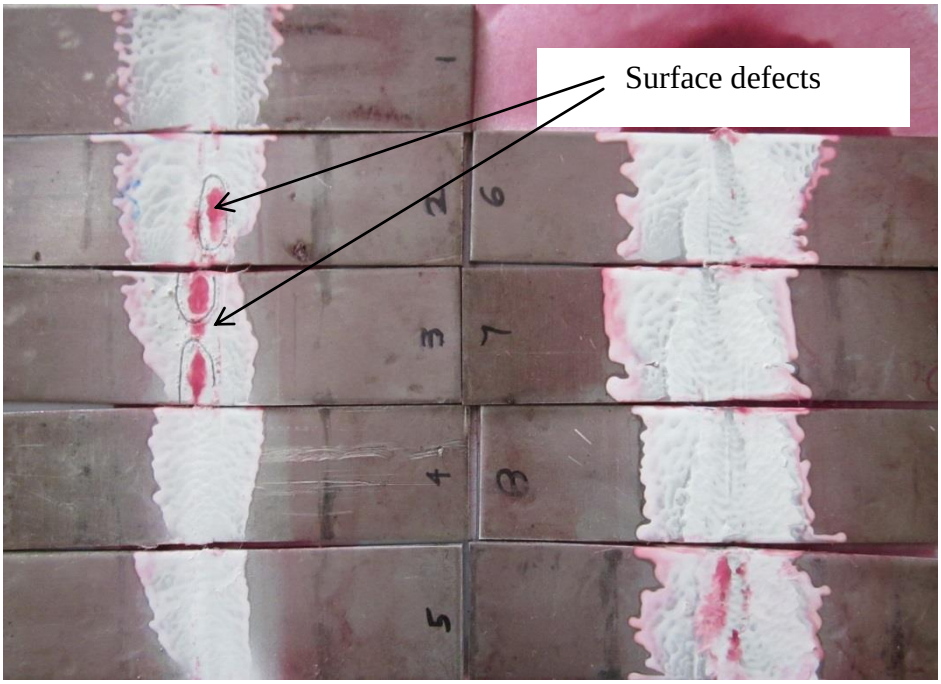

(a)

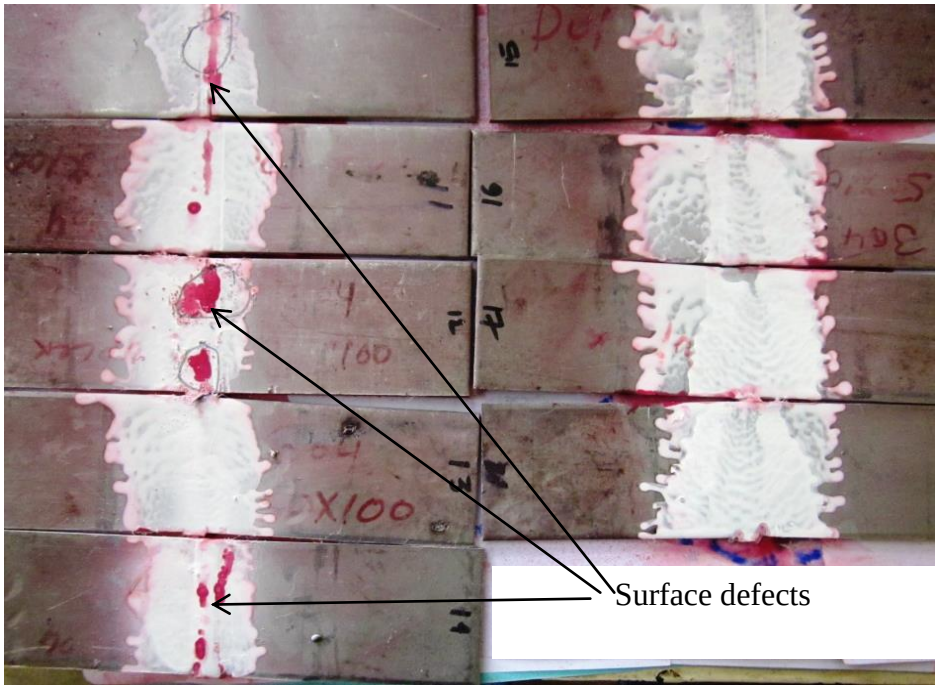

(b)

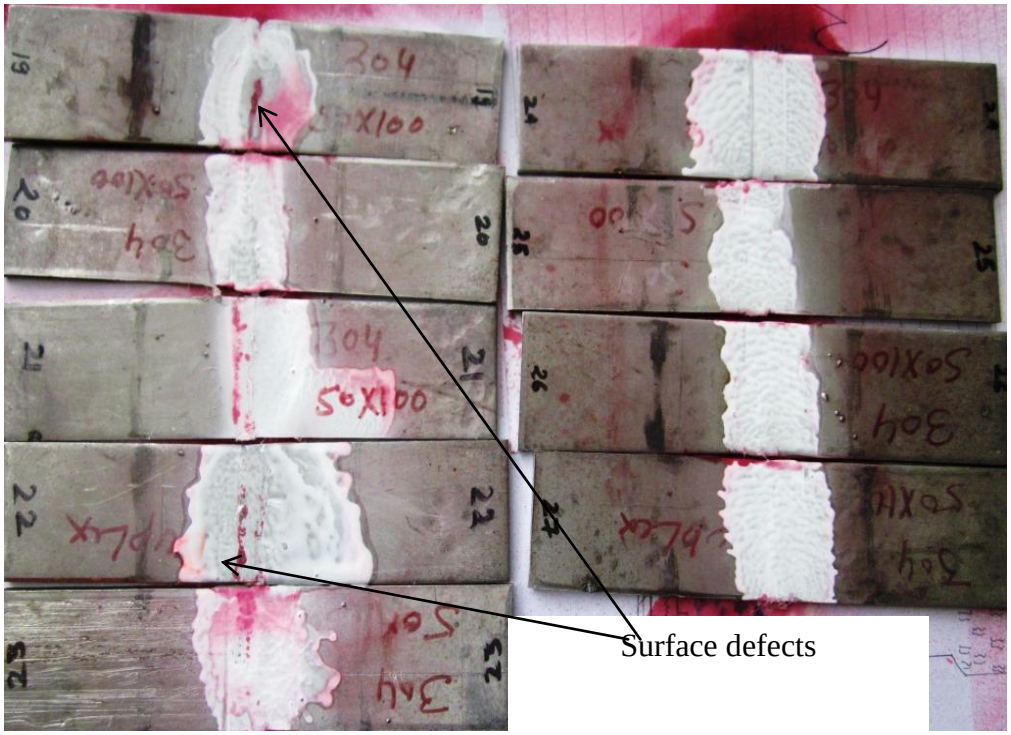

(c)

Figure 4.21: Results of dye penetrant test (a), (b), (c) carried on AISI 304 and Duplex 2205

Figure 4.21 shows that welded joints have surface defects in trial (trial no. 2, 3, 10, 12, 14, 19, 22). These surface defects are due to the use of helium as a shielding gas. Helium is lighter than argon because of it tends to rise around the nozzle and results in porous bead.

After the visual inspection of cracks using dye penetration, optical microscope is used to find out the surface cracks on weld surface. By using optical microscope, weld surface is examined for cracks measurements.

Table 4.25: Results of surface cracks for joints between AISI 304 and Duplex 2205

Exp. No.	Current (A)	Voltage (V)	Flow rate (L/min)	Filler wire	Gas type	Single or double layer	Average crack length (mm)
1	160	16	12	AISI 304	Ar	Single Layer	1.215
2	160	16	14	AISI 316	He	$(CO_2)_1$	2.334
3	160	16	16	Duplex 2205	70% Ar + 30% He	$(CO_2)_2$	1.529
4	160	18	12	AISI 316	He	$(CO_2)_2$	0.813
5	160	18	14	Duplex 2205	70% Ar + 30% He	Single Layer	1.350
6	160	18	16	AISI 304	Ar	$(CO_2)_1$	2.348
7	160	20	12	Duplex 2205	70% Ar + 30% He	$(CO_2)_1$	No cracks
8	160	20	14	AISI 304	Ar	$(CO_2)_2$	No cracks
9	160	20	16	AISI 316	He	Single Layer	0.317
10	180	16	12	AISI 316	70% Ar + 30% He	$(CO_2)_1$	0.395
11	180	16	14	Duplex 2205	Ar	$(CO_2)_2$	No crack
12	180	16	16	AISI 304	He	Single Layer	0.808
13	180	18	12	Duplex 2205	Ar	Single Layer	1.108
14	180	18	14	AISI 304	He	$(CO_2)_1$	0.279
15	180	18	16	AISI 316	70% Ar + 30% He	$(CO_2)_2$	No crack
16	180	20	12	AISI 304	He	$(CO_2)_2$	0.768
17	180	20	14	AISI 316	70% Ar + 30% He	Single Layer	0.972
18	180	20	16	Duplex 2205	Ar	$(CO_2)_1$	No crack
19	200	16	12	Duplex 2205	He	$(CO_2)_2$	2.972
20	200	16	14	AISI 304	70% Ar + 30% He	Single Layer	No crack
21	200	16	16	AISI 316	Ar	$(CO_2)_1$	0.526
22	200	18	12	AISI 304	70% Ar + 30% He	$(CO_2)_1$	1.155
23	200	18	14	AISI 316	Ar	$(CO_2)_2$	1.243
24	200	18	16	Duplex 2205	He	Single Layer	No crack
25	200	20	12	AISI 316	Ar	Single Layer	2.059
26	200	20	14	Duplex 2205	He	(CO2)1	No cracks
27	200	20	16	AISI 304	70% Ar + 30% He	$(CO_2)_2$	1.354

Table 4.26: Response of cracks at different process parameters for AISI 304 and DUPLEX 2205

Average crack length (mm)	Trial no.	Total number of experiments
≤ 1	4, 7, 8, 9, 10, 11, 12, 14, 15, 16, 17, 18, 20, 21, 24, 26	16
1 ≤ 2	1, 3, 5, 13, 22, 23, 27	7
2 ≤ 3	2, 6, 19, 25	4

4.6.2 Dye Penetration Test for welding of AISI 316 and Duplex 2205

The visual inspection of dye penetration carried out on joints performed as per L_{27} orthogonal array on the welding of materials AISI 316 and Duplex 2205 are given in Table 4.28.

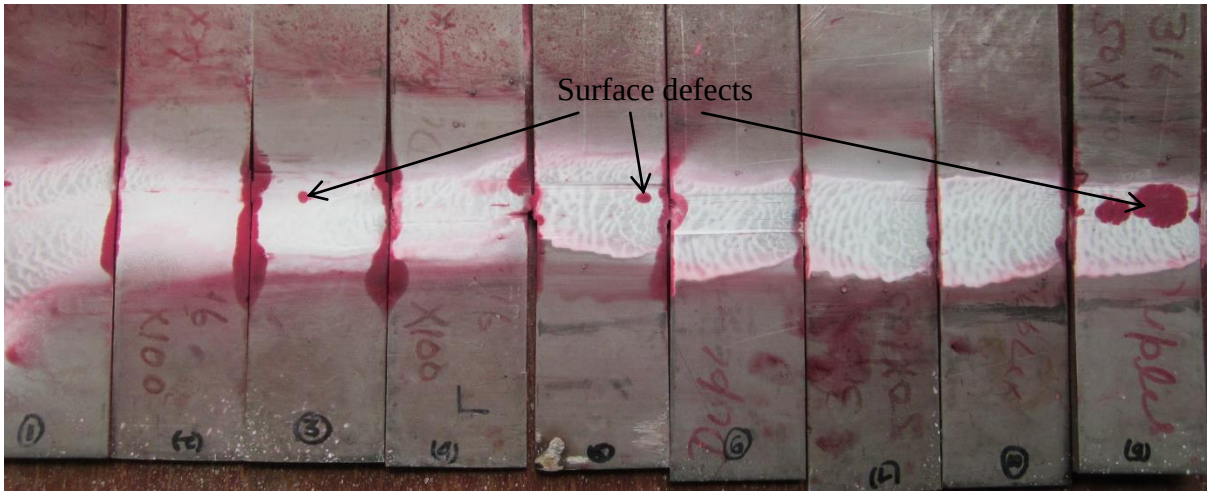

(a)

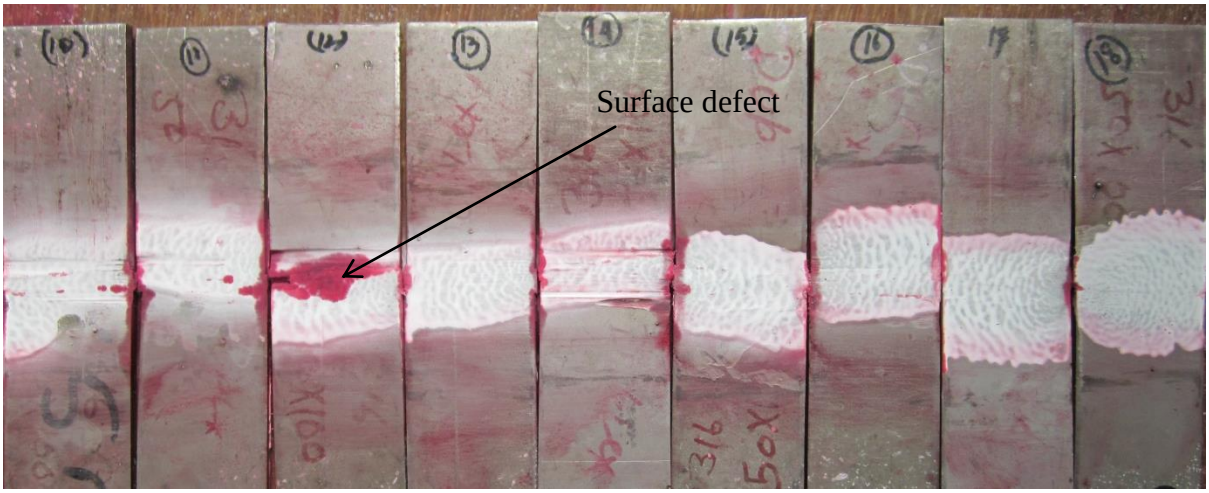

(b)

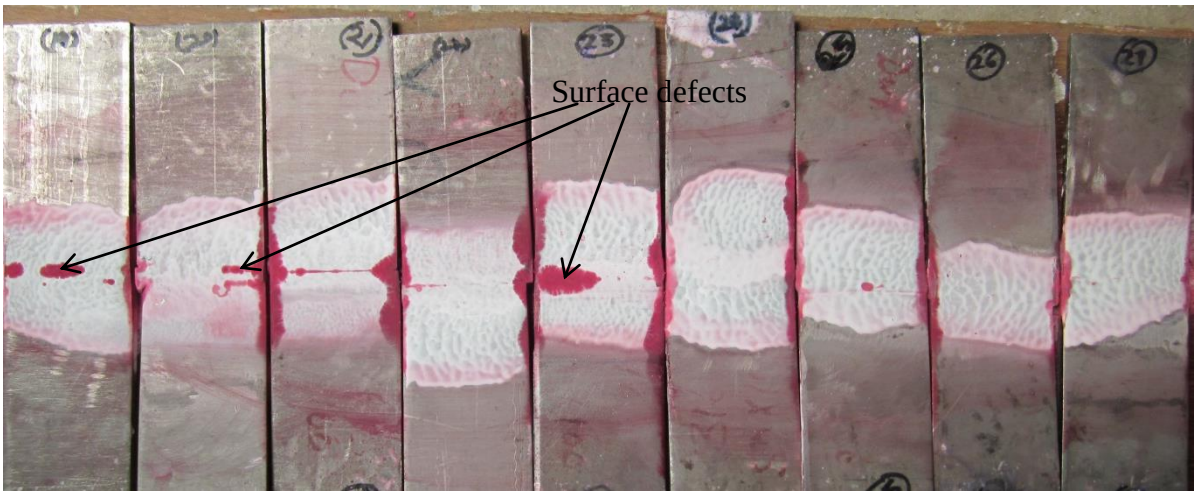

(c)

Figure 4.22: Results of dye penetrant test (a), (b), (c) carried on AISI 316 and Duplex2205

Figure 4.22 Shows that welded joints have surface defect in trial (trial no. 3, 5, 9, 12, 19, 20, 23). These surface defects are due to the use of helium as a shielding gas. Helium is lighter than argon because of it tends to rise around the nozzle and results in porous bead.

After the visual inspection of cracks using dye penetration, optical microscope is used to find out the surface cracks on weld surface. By using optical microscope, weld surface is examined for cracks measurements. After taking all the measured values, average length of crack is calculated for each trial by dividing the total cracks length to the number of cracks. Based on the average value cracks are assigned with different rank. The crack with minimum average length is assigned with rank 1 and crack with higher average length are assigned with rank last. Table 4.28 shows the average value of surface crack at each trial.

Table 4.27: Response of cracks at different process parameters for AISI 316 and DUPLEX 2205

Average crack length (mm)	Trial no.	Total number of experiments
≤ 1	4, 7, 8, 9, 10, 11, 12, 14, 15, 16, 17, 18, 20, 21, 24, 26	16
$1 \leq 2$	1, 3, 5, 13, 22, 23, 27	7
$2 \leq 3$	2, 6, 19, 25	4

Table 4.28: Results of surface cracks for joints between AISI 316 and Duplex 2205

Exp. No.	Current (A)	Voltage (V)	Flow rate (L/min)	Filler wire	Gas type	Single or double layer	Average crack length (mm)
1	160	16	12	AISI 304	Ar	Single Layer	1.198
2	160	16	14	AISI 316	He	$(CO_2)_1$	1.159
3	160	16	16	Duplex 2205	70% Ar + 30% He	$(CO_2)_2$	0.630
4	160	18	12	AISI 316	He	$(CO_2)_2$	0.685
5	160	18	14	Duplex 2205	70% Ar + 30% He	Single Layer	0
6	160	18	16	AISI 304	Ar	$(CO_2)_1$	0.339
7	160	20	12	Duplex 2205	70% Ar + 30% He	$(CO_2)_1$	0
8	160	20	14	AISI 304	Ar	$(CO_2)_2$	1.061
9	160	20	16	AISI 316	He	Single Layer	2.907
10	180	16	12	AISI 316	70% Ar + 30% He	$(CO_2)_1$	1.422
11	180	16	14	Duplex 2205	Ar	$(CO_2)_2$	0.819
12	180	16	16	AISI 304	He	Single Layer	0
13	180	18	12	Duplex 2205	Ar	Single Layer	1.880
14	180	18	14	AISI 304	He	$(CO_2)_1$	1.299
15	180	18	16	AISI 316	70% Ar + 30% He	$(CO_2)_2$	2.131
16	180	20	12	AISI 304	He	$(CO_2)_2$	1.182
17	180	20	14	AISI 316	70% Ar + 30% He	Single Layer	0
18	180	20	16	Duplex 2205	Ar	$(CO_2)_1$	0.198
19	200	16	12	Duplex 2205	He	$(CO_2)_2$	0
20	200	16	14	AISI 304	70% Ar + 30% He	Single Layer	0
21	200	16	16	AISI 316	Ar	$(CO_2)_1$	1.222
22	200	18	12	AISI 304	70% Ar + 30% He	$(CO_2)_1$	0.438
23	200	18	14	AISI 316	Ar	$(CO_2)_2$	0.521
24	200	18	16	Duplex 2205	He	Single Layer	0.272
25	200	20	12	AISI 316	Ar	Single Layer	0.478
26	200	20	14	Duplex 2205	He	(CO2)1	0.925
27	200	20	16	AISI 304	70% Ar + 30% He	$(CO_2)_2$	0

4.7 Metallurgical Analysis Using Scanning Electron Microscope

Microstructure analysis was carried out on some selected samples using scanning electron microscope (SEM) machine (Model-JEOL JSM-6480LV) to study change in microstructure after welding with GMAW. SEM is mainly used for imaging the surface and detecting small surface features. Sample preparation was done as per standard requirement. SEM micrographs are taken at 500× and 1500×. Sample preparation mainly involves cutting the machined samples group in smaller size, so that 4 samples can be accommodated on a slit in a manner to properly accommodate the samples on SEM machine, cleaning of samples by acetone to properly clean the machined surface. SEM micrographs are arranged as per workpiece material.

4.7.1 Metallurgical Analysis of Joints between AISI 304 and Duplex 2205

Base metal of AISI 304	Base metal of Duplex 2205
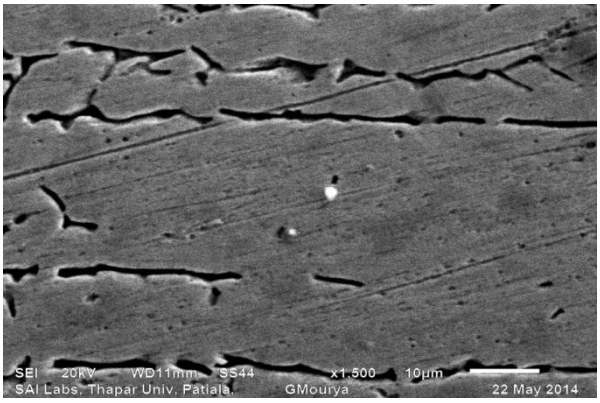	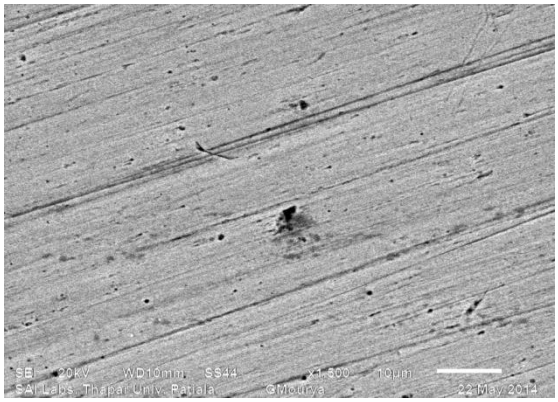

Figure 4.23: SEM of base metal AISI 304 and Duplex 2205

Table 4.29: Scanned electron microscopy of AISI 304 and Duplex 2205 at different trial conditions

Trial. No	Parameters Current(A), voltage(V), flow rate(L/min), filler wire, gas, single or double layer shielding	Interface between AISI 304 and fusion zone at 500x (a)	Interface between duplex and fusion zone at 500x (b)	Fusion zone of weld metal at 1500x (c)
7.	160, 20, 12, Duplex2205, 70Ar+30He, double layer shielding with CO2 of flow rate 8 L/min	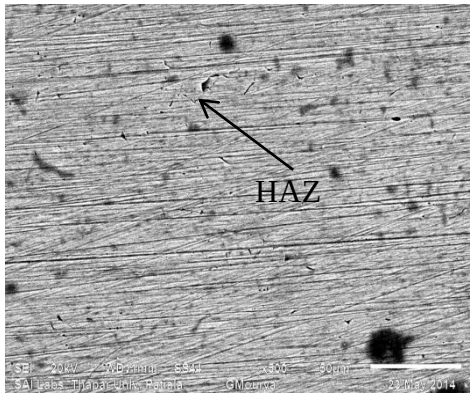	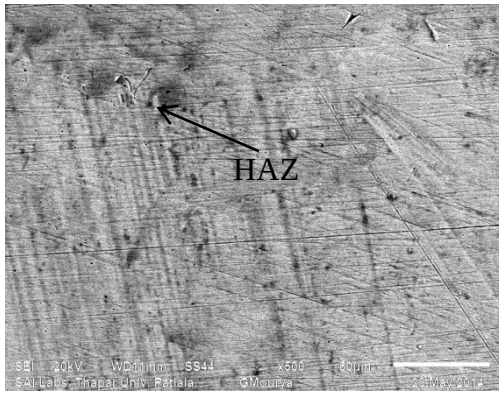	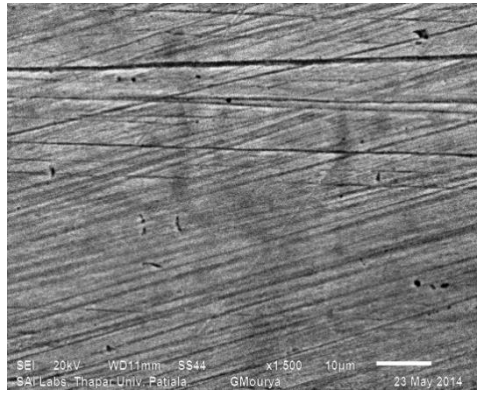

10.	180, 16, 12, AISI 316, 70Ar+30He, double layer shielding with CO2 of flow rate 8 L/min	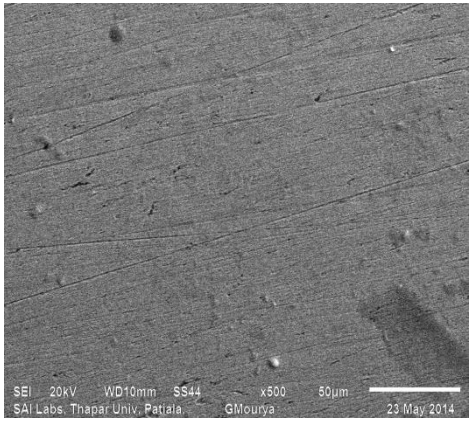	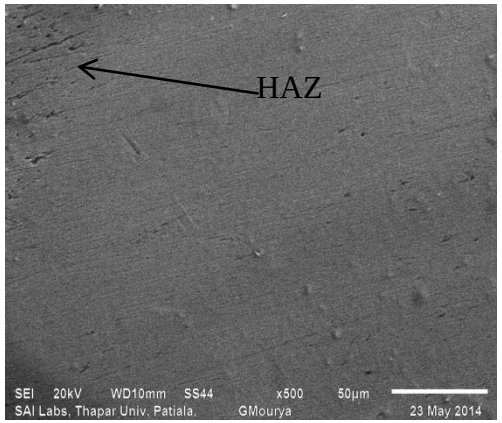	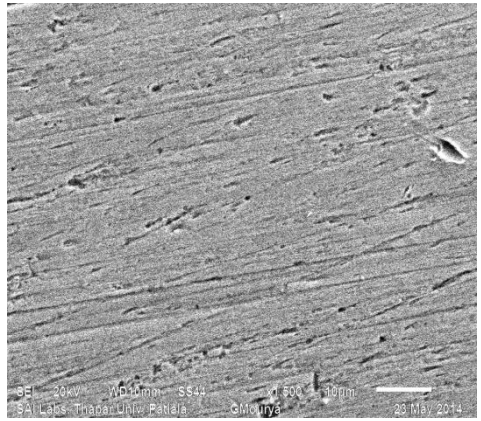
12.	180, 16, 16, AISI 304, He, single layer shielding		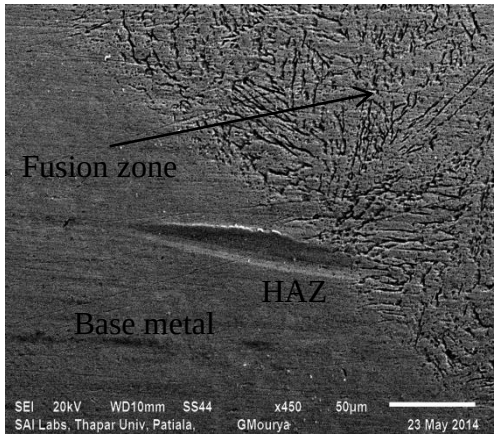	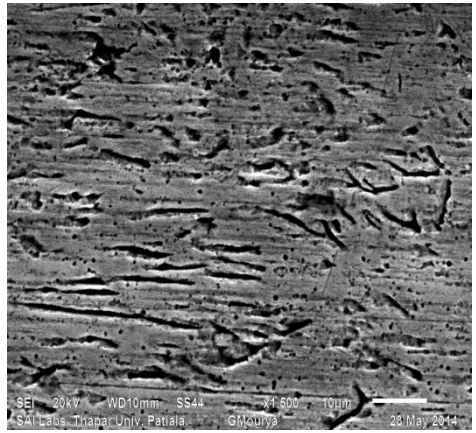

16.	180, 20, 12, AISI 304, He, double layer shielding with CO2 of flow rate 12 L/min	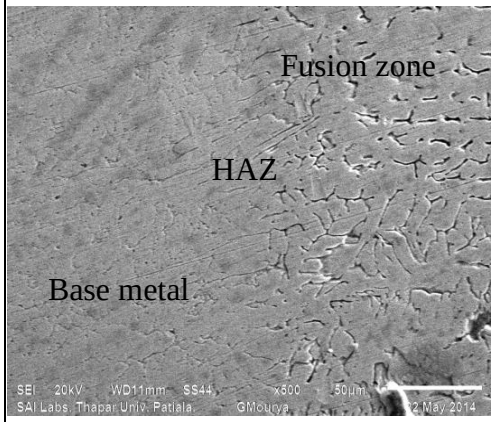	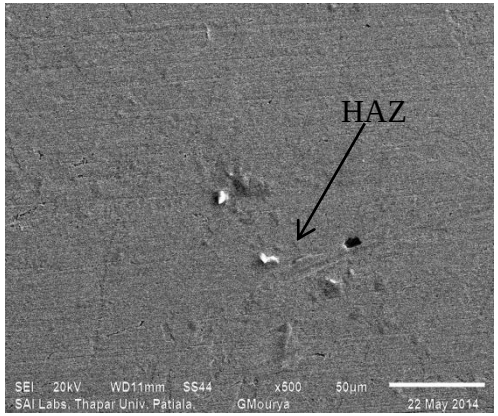	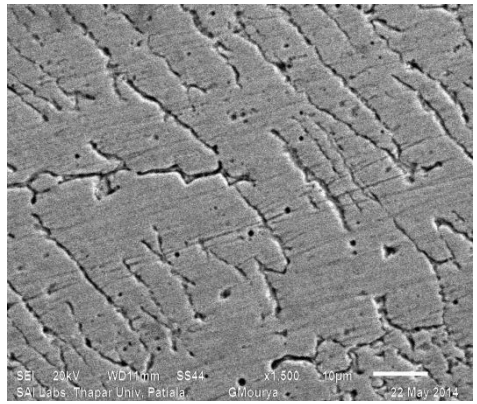
18.	180, 20, 16, Duplex2205, Ar, double layer shielding with CO2 of flow rate 8 L/min	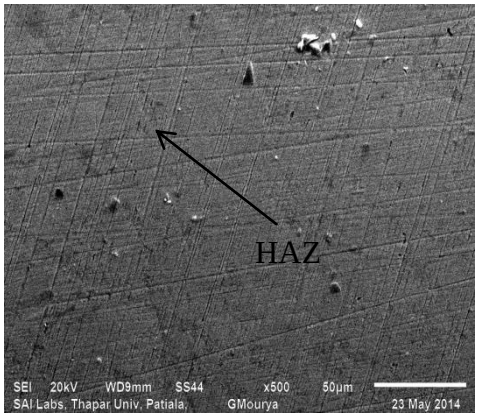	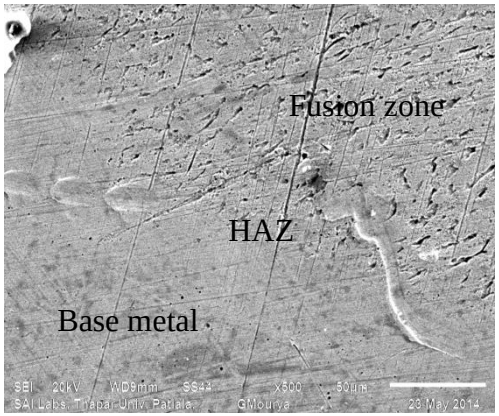	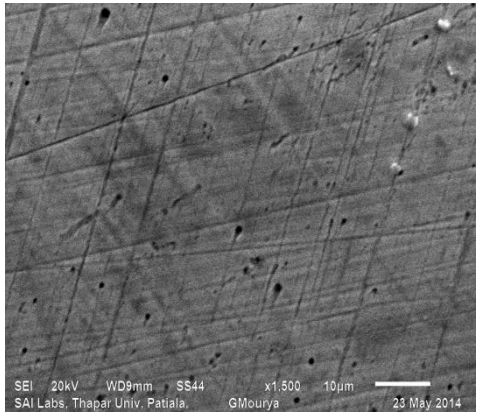

22.	200, 18, 12, AISI 304, 70Ar+30He, double layer shielding with CO2 of flow rate 8 L/min	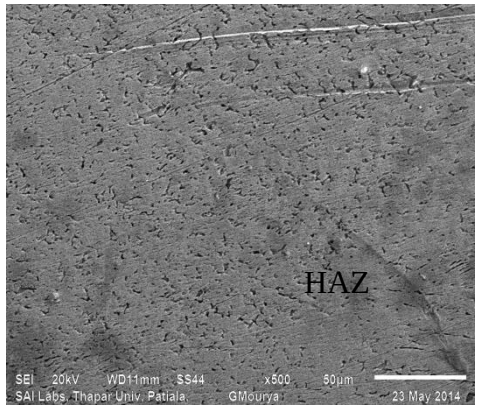	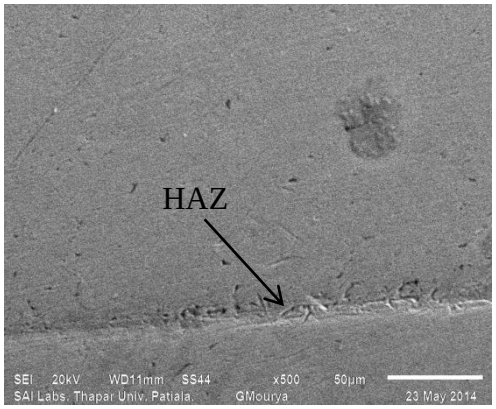	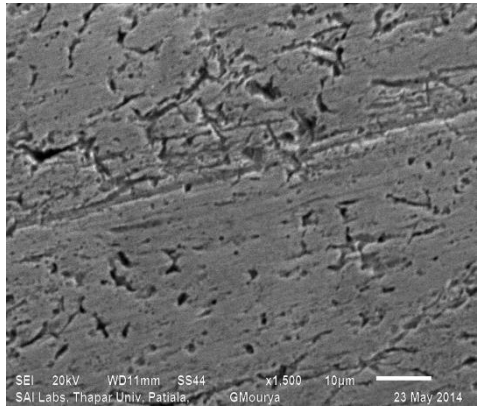
27.	200, 20, 16, AISI 304, 70Ar+30He, double layer shielding with CO_2 of flow rate 12 L/min	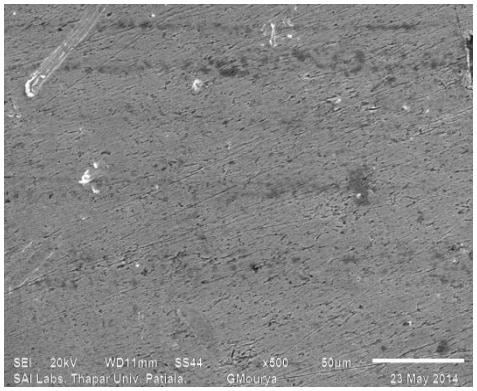	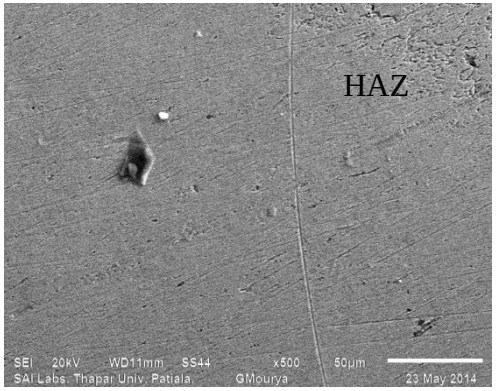	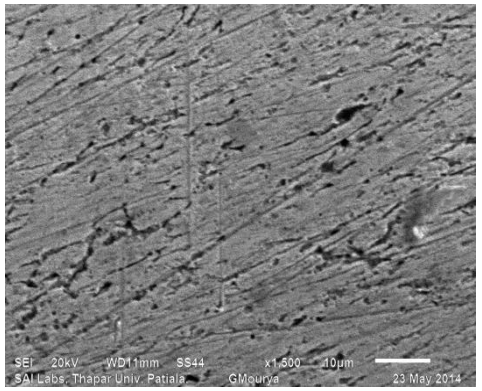

Microstructural observations of the weld fusion zone and HAZ of dissimilar joints between AISI 304 and DUPLEX 2205 for some of the samples are carried out by SEM is shown in Table 4.29. In welding metallurgy of AISI 304, α ferrite describes the low temperature ferrite and δ ferrite refers to high temperature ferrite. Sigma phase denotes low temperature equilibrium phase is present in Duplex 2205. When Cr > 24 % and heat input rate is more than 2.6 KJ than sigma phase is formed. Sigma is hard and brittle phase is usually undesirable in Duplex 2205. In present study the duplex stainless steel and austenitic stainless steel base metal and weld metal are subjected to a series of thermal cycles. As a result, complex microstructural transformations occur, affecting the δ/γ phase balance in the steel. The difference in cooling rate between the central region of the weld and the regions near the fusion boundaries affects the δ/γ equilibrium in the weldmetal. During heating, near the high temperature peak, the structure transformed to ferrite almost entirely. Then the ferrite partially transformed to austenite. Also lower Cr/Ni ratio promotes austenite formation and higher Cr/Ni ratio promotes ferrite formation. From the composition of the present workpiece material, values of Cr_{eq} (= Cr + 1.5Si + Mo + 0.5Cb) and Ni_{eq} (= Ni + 0.5Mn + 30C + 30N) are obtained as 19.607 and 16.329, respectively. Subsequently observed that there is zero content of the amount of δ ferrite ($\delta = 3(Cr_{eq} - 0.93Ni_{eq} - 6.7)$). Also, the ratio of Cr and Ni percentage is calculated as 1.20 and lower Cr/Ni ratio promotes austenite formation whereas a high value of Cr/Ni ratio promotes ferrite formation. High cooling rate supresses the formation of austenite and some ferrite will remain in the microstructure.

There are four solidification and solid-state transformation possibilities for austenitic stainless steel weld metals. These reactions are and related to the Fe-Cr-Ni phase diagram. AF solidification modes are associated with primary austenite solidification, whereby austenite is the first phase to form upon solidification. The solidification if some ferrite forms at the end of the primary austenite solidification process via a eutectic reaction, solidification is termed Type AF. This occurs if sufficient ferrite-promoting elements (primarily Cr and Mo) partition to the solidification sub grain boundaries during solidification to promote the formation of ferrite as a terminal solidification product. This is thought to occur by a eutectic reaction and is represented by the three-phase triangular region of the phase. The ferrite that forms along the boundary is relatively stable and resists transformation to austenite during weld cooling since it is already enriched in ferrite-promoting elements.

Table 4.29 shows the SEM of weld fusion zone and heat affected zone for 12 L/min, 14 L/min and 16 L/min flow rate of shielding gas of Ar, He and mixture of Ar and He with double layer shielding of CO_2. SEM of some experimental trails with different value of

process parameters such as current and voltage with constant speed are converted to heat input rate. This heat input rate at each of three gas flow rate with effect of double layer shielding is observed and analysed. High heat input rate (1.6 kJ) in trial no.7 results in fast cooling rate. Due to faster cooling rate fine grains are formed. In this solidification cells and dendritic structure can be observed and results in good toughness and tensile strength is achieved. In trial no. 10 rate of heat input (1.44 kJ) is less than trial 7 (1.6 kJ) due to which proper fusion is not takes place and results in poor toughness. In fusion zone of trial no. 12, 16 with heat input rate of 1.44 kJ and 1.8 kJ the solidification temperature range of austenite, ferrite and liquid coexist. Ferrite that formed is the residual of high temperature ferrite (δ ferrite). Improper fusion is seen at interference of Duplex 2205 and fusion zone because large heat input is required for proper fusion in case of Duplex 2205. Nickel and Nitrogen is austenite stabilizer by adding these elements in base metal austenitic structure will form and results in good toughness and tensile strength. In trial no. 18 filler wire used of Duplex 2205 contains 0.15% nitrogen and leads to formation of Type A or Type AF structure. By applying more heat input and gas flow rate with addition of nitrogen in base metal results in high tensile strength and good toughness. If high heat input of 1.8 kJ and 2.0 kJ is applied in (trial no. 22, 27) with lesser gas flow rate grain size is increasing. At higher heat input, grain boundary migration and increases mean grain diameter. Due to which coarse grain structure is formed and leads to ductility in material. Due to ductility in material good tensile strength is obtained but toughness is not obtained so much.

4.7.2 Metallurgical Analysis of Joints between AISI 316 and Duplex 2205

Base metal of AISI 316	Base metal of Duplex 2205
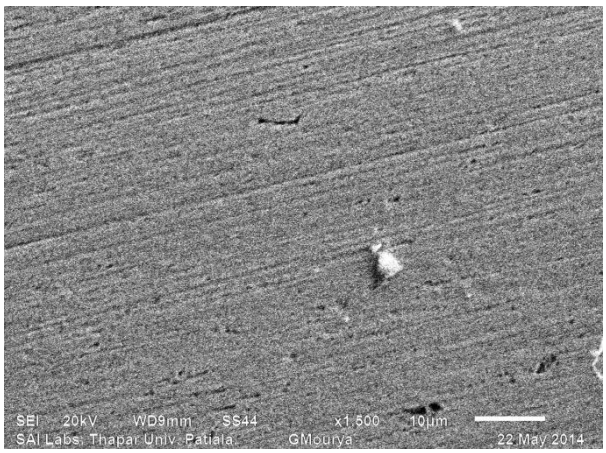	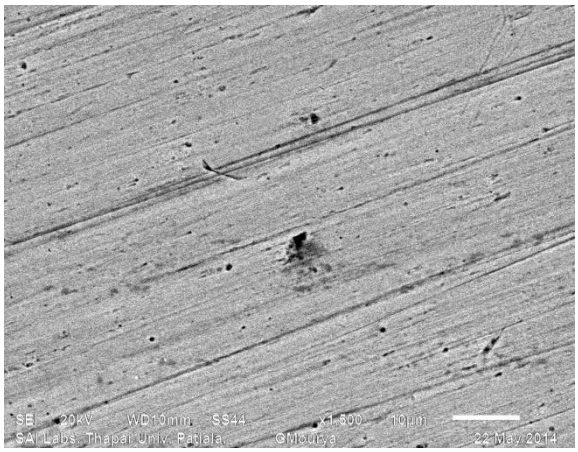

Figure 4.24: SEM of base metal AISI 316 and Duplex 2205

Microstructural observations of the weld fusion zone and HAZ of dissimilar joints for some of the samples are carried out by SEM is shown in Table 4.30. In the present study, workpiece material used is AISI 316 and Duplex 2205. In welding metallurgy of AISI 316, α ferrite describes the low temperature ferrite and δ ferrite refers to high temperature ferrite. Sigma phase denotes low temperature equilibrium phase is present in Duplex 2205. When Cr > 24 % and heat input rate is more than 2.6 KJ than sigma phase is formed. Sigma is hard and brittle phase is usually undesirable in Duplex 2205. Also lower Cr/Ni ratio promotes austenite formation and higher Cr/Ni ratio promotes ferrite formation. Also lower Cr/Ni ratio promotes austenite formation and higher Cr/Ni ratio promotes ferrite formation. From the composition of the present workpiece material, values of Cr_{eq} (= Cr + 1.5Si + Mo + 0.5Cb) and Ni_{eq} (= Ni + 0.5Mn + 30C + 30N) are obtained as 19.307 and 16.596, respectively. Subsequently observed that there is zero content of the amount of δ ferrite ($\delta = 3(Cr_{eq} - 0.93Ni_{eq} - 6.7)$). Also, the ratio of Cr and Ni percentage is calculated as 1.16 and lower Cr/Ni ratio promotes austenite formation whereas a high value of Cr/Ni ratio promotes ferrite formation.

Table 4.30 Scanned electron microscopy in welding of AISI 316 and Duplex 2205

Trial No.	Parameters Current(A), voltage(V), flow rate(L/min), filler wire, gas, single or double layer shielding	Interface between AISI 316 and fusion zone at 500x (a)	Interface between duplex and fusion zone at 500x (b)	Fusion zone of weld metal at 1500x (c)
2.	160, 16, 14, AISI 316, He, double layer shielding with CO_2 of flow rate 8 L/min	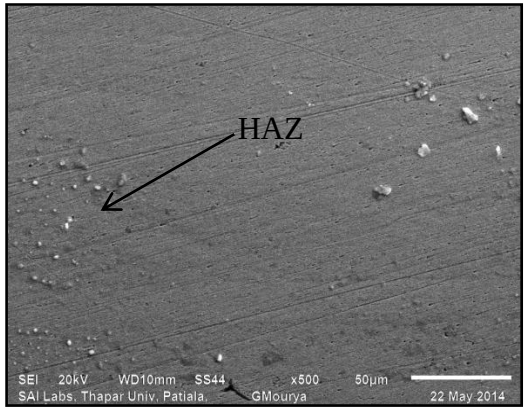	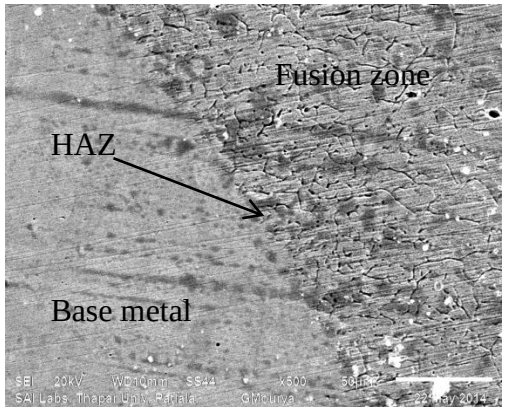	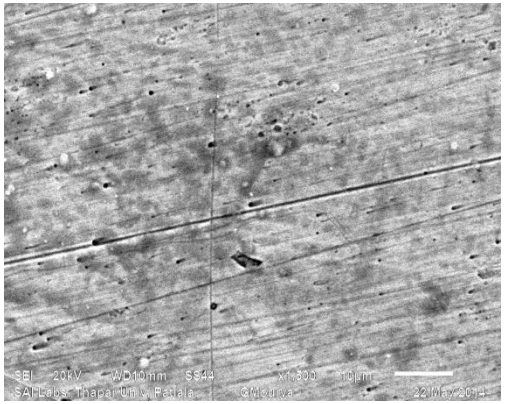

7.	160, 20, 12, Duplex2205, 70Ar+30He, double layer shielding with CO_2 of flow rate 8 L/min	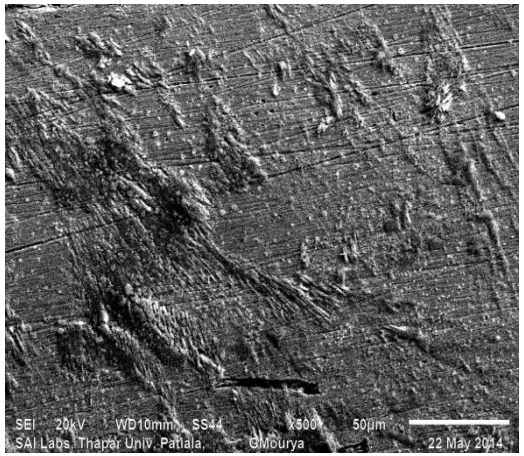	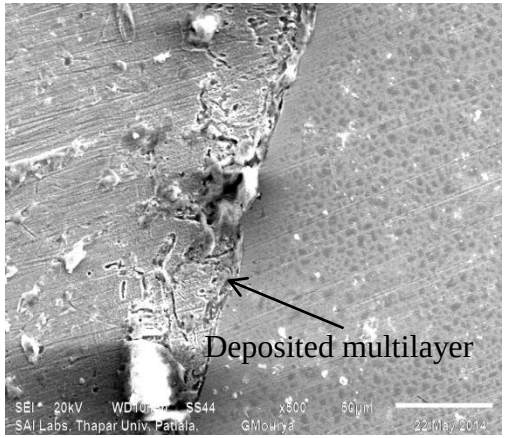	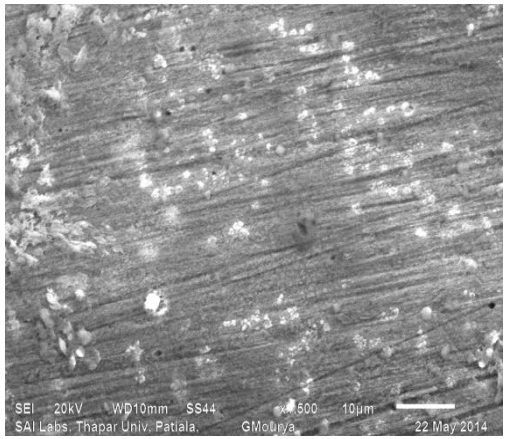
10.	180, 16, 12, AISI 316, 70Ar+30He, double layer shielding with CO_2 of flow rate 8 L/min	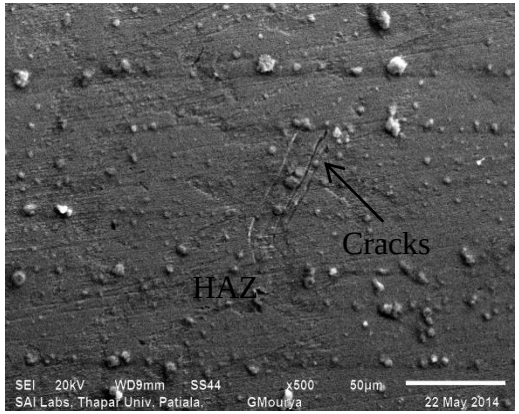	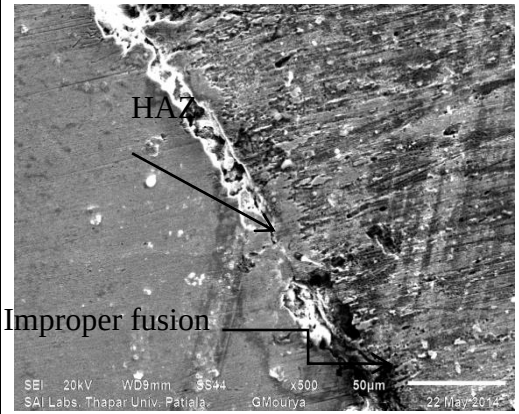	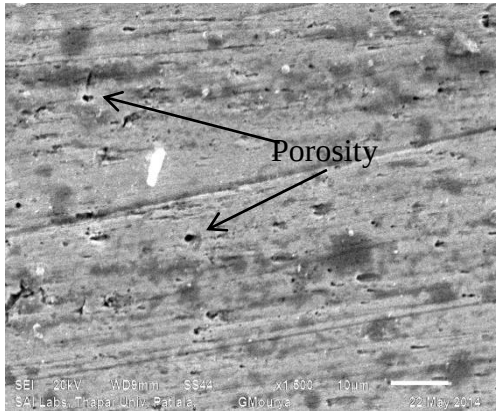

12.	180, 16, 16, AISI 304, He, single layer shielding	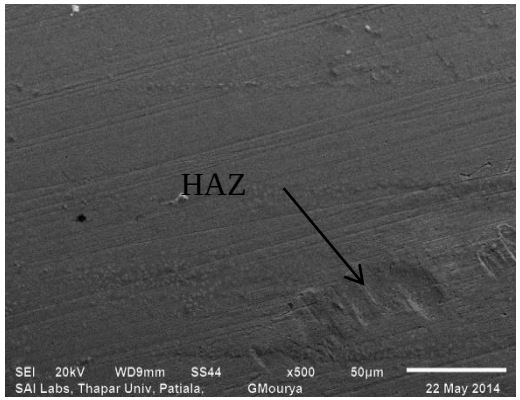	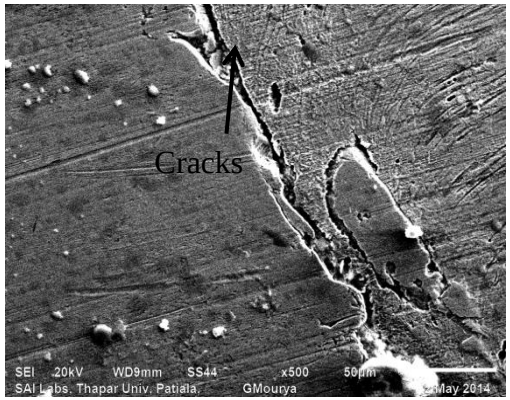	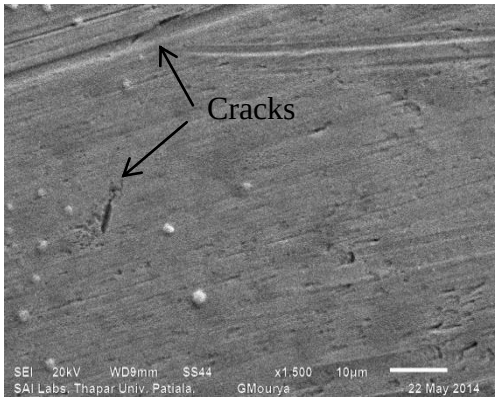
18.	180, 20, 16, Duplex2205, Ar, double layer shielding with CO_2 of flow rate 8 L/min	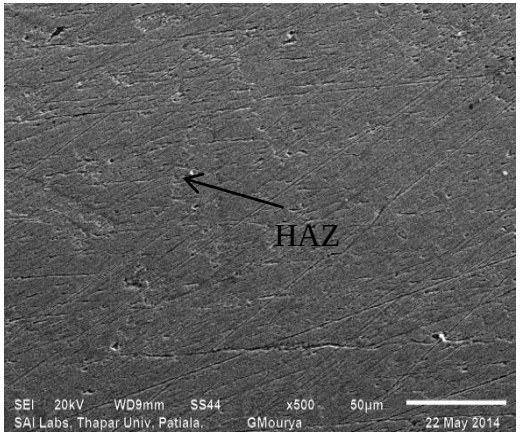	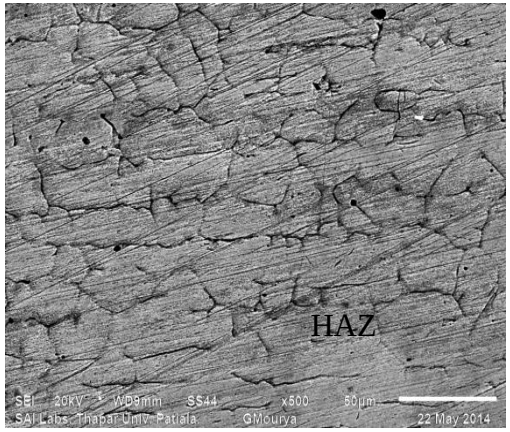	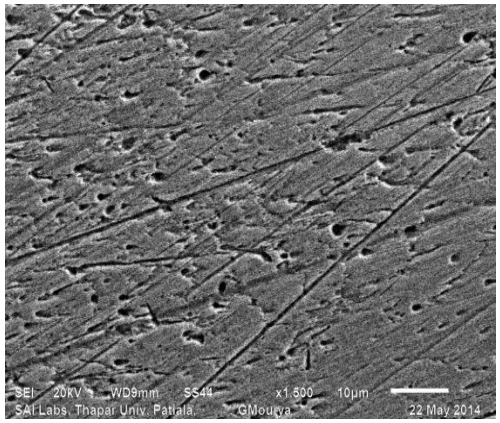

22.	200, 18, 12, AISI 304, 70Ar+30He, double layer shielding with CO_2 of flow rate 8 L/min	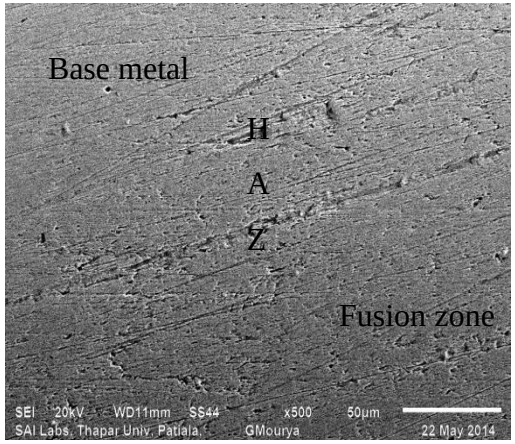	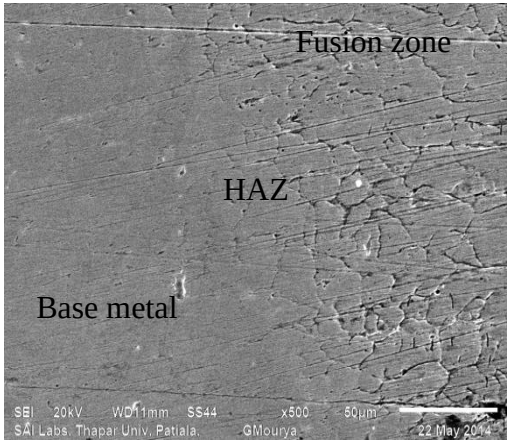	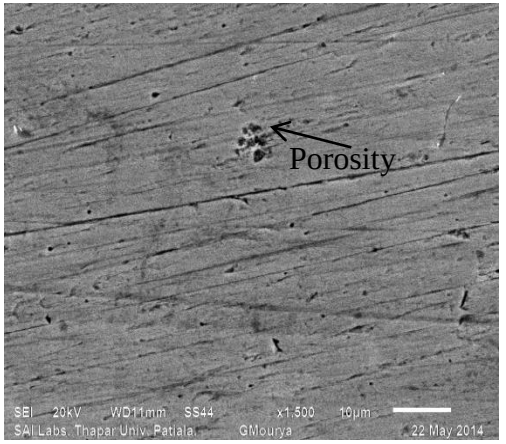
27.	200, 20, 16, AISI 304, 70Ar+30He, double layer shielding with CO_2 of flow rate 12 L/min	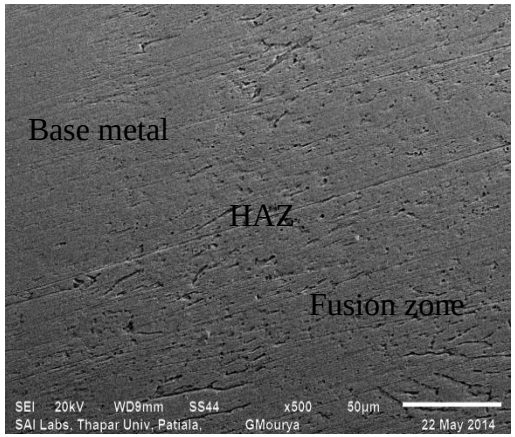	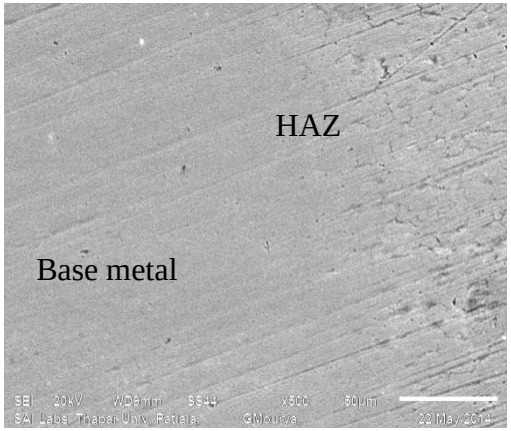	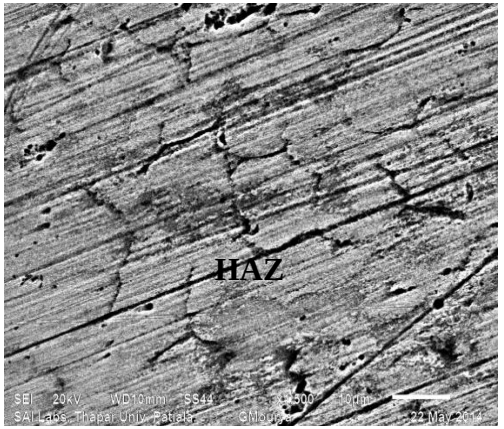

There are four solidification and solid-state transformation possibilities for austenitic stainless steel weld metals. These reactions are and related to the Fe-Cr-Ni phase diagram. In our study, Type A and Type AF solidification was obtained as shown in Table 4.30. AF solidification modes are associated with primary austenite solidification, whereby austenite is the first phase to form upon solidification. The solidification if some ferrite forms at the end of the primary austenite solidification process via a eutectic reaction, solidification is termed Type AF. This occurs if sufficient ferrite-promoting elements (primarily Cr and Mo) partition to the solidification sub grain boundaries during solidification to promote the formation of ferrite as a terminal solidification product. This is thought to occur by a eutectic reaction and is represented by the three-phase triangular region of the phase. The ferrite that forms along the boundary is relatively stable and resists transformation to austenite during weld cooling since it is already enriched in ferrite-promoting elements.

With regards to the weld zone in Table 4.30 the dependence of the dendritic microstructure on welding heat input used is clearly observed i.e. dendrite size and inter dendritic spacing is relatively fine at lower heat input of 1.28 KJ, 1.6 KJ and 1.8 KJ in (trial no. 2, 7, 18) due to faster cooling rates with flow rate of 14 L/min and 16 L/min, consequently allowing lesser solidification time for the resultant dendritic growth leads to Type A and Type AF solidification and results in high toughness and tensile strength. In (trial 10) heat input of 1.44 KJ is applied but results in poor toughness. It may be due to porosity in the fusion zone and improper fusion at HAZ with lower gas flow rate of shielding gas i.e. 12 L/min. In trial no. 12 with heat input of 1.44 KJ good toughness is not achieved because from the SEM of trial no. 12 in Table 4.30 it is seen that there is lot of cracks at the HAZ, these cracks may be due to use of single layer shielding gas because in other trial condition of same heat input double layer shielding gas is used with outer gas flow rate of 8 L/min. Conversely, coarse dendritic microstructure is possessed as shown in Table 4.30 (trial no. 22, 27) by the weld zone corresponding to higher welding heat input, as relatively slower cooling rate provides these dendrites with sufficient time to grow, as per the solidification kinetics existing locally. In trial no.22 rate of heat input is low (1.8 KJ) but shielding gas flow rate is 12 L/min leads to formation of ferrite structure. Whereas in trial no. 27 rate of heat input is more i.e. 2 KJ leads to formation of coarse grain size in fusion zone and results in poor toughness as shown in (trial no. 27) of Table 4.30. This observation is based upon the theory of solidification which states that high welding heat input into the joint would result into high heat accumulation, thus resulting into low temperature gradient and slow growth rate, consequently leading to a significant increase in the dendrite arm spacing. Conversely low

heat input combination into the joint would tend to make steep temperature gradient in combination with rapid growth rate thus resulting in small dendrite arm spacing. As observed from the photomicrographs of the heat affected zones (HAZs) of these weldments shown in (trial no. 22, 27) from Table 4.30, grain coarsening effect is induced which tends to weaken this part of the joint and, thus could affect the functional performance of the weld joint in actual service.

Chapter 5

Conclusions and Scope for Future Work

5.1 Conclusion

This study was mainly aimed at finding the most significant process parameters and optimal solution for joining of dissimilar materials between (AISI 316 and DUPLEX 2205) and (AISI 304 and DUPLEX 2205). Different process parameters like current (160A, 180A, 200A), voltage (16V, 18V, 20V), gas flow rate (12 to 16 L/min.), filler wire (AISI 304, AISI 316 and DULEX 2205), shielding gas type (Ar, He and mixture of Ar and He) and effect of single layer or double layer shielding gas varied at three levels of each parameter. Different response characteristics considered are tensile strength, toughness, microhardness, weld distortion, visual inspection of cracks and metallurgical analysis of some selected machined samples. Some important conclusions that are drawn on the basis of analysis of results (using ANOVA) and metallurgical study are:

- Tensile strength results for joining AISI 304 and DUPLEX 2205 mainly depends on voltage, filler wire and gas flow rate. Because with increase in voltage and shielding gas flow rate tensile strength increases. By using filler wire of DUPLEX 2205 more tensile strength is obtained.
- In case of AISI 316 and DUPLEX 2205 more tensile strength is obtained as voltage is increased. More tensile strength is achieved with filler wire of DUPLEX 2205 as in previous case. By using double layer shielding with a gas flow rate of 8 L/min more tensile strength is achieved.
- Charpy impact test results for AISI 304 and DUPLEX 2205 shows that toughness at room temperature mainly depends on the value of voltage, filler wire and current used. Toughness value is higher at lower welding current as current is increased above 180A toughness value decreases. With increase in voltage toughness increases. By using filler wire of AISI 304 toughness increases.
- Charpy impact test results for AISI 316 and DUPLEX 2205 shows that toughness at room temperature mainly depends on the value of voltage, single or double layer shielding and filler wire. Toughness value is firstly decreases with increase in voltage

but when voltage is increased above 18V toughness increases. If filler wire of DUPLEX 2205 is used than toughness increases.

- Microhardness results for joining of both (AISI 304 and DUPLEX 2205) and (AISI 316 and DUPLEX 2205) show that with increase in current and voltage hardness increases. Filler wire of AISI 316 show more microhardness as compared to AISI 304 and DUPLEX 2205.
- Weld distortion for joining of AISI 304 and DUPLEX 2205 shows that with increase in rate of heat input weld distortion increases which is obtained by the product of current and voltage. By using a mixture of Ar and He as a shielding gas welding distortion increases because it leads to increase in heat input.
- Weld distortion for joining of AISI 316 and DUPLEX 2205 shows that with increase in voltage weld distortion increases. Effect of flow rate of shielding gas i.e. with increase in flow rate weld distortion increases. AISI 304 shows more weld distortion as compared to AISI 316 and DUPLEX 2205. By using double layer shielding gas with flow rate of 8 L/min less weld distortion is obtained.
- Dye penetrant test (DPT) results for joining of dissimilar material (AISI 304 with DUPLEX 2205 and AISI 316 with DUPLEX 2205) material shows that there is no surface crack in the welded region except when pure helium is used as a shielding gas. In case of pure helium as a shielding gas there is a problem of porosity in weld region. In general the results show that quality of welding was very good.
- Scanned electron microscopy of (AISI 304 and DUPLEX 2205) and (AISI 316 and DUPLEX 2205) shows that with increase in rate of heat input ferrite structure is obtained and there is a tendency of formation of sigma phase in DUPLEX 2205 which will reduce the toughness and tensile strength. If the rate of heat input is less than desired value then proper fusion of weld metal is not taken place and results in cracks at the interference. Effect of shielding gas flow rate is that if flow rate is more than faster cooling of weld metal takes place and leads to austenitic and (austenitic + ferrite) solidification.

5.2 Future Scope

Following are the some of the future recommendations:

- Effect of hydrogen has been studied by many researchers on various grades of steels. Same may also be carried out for dissimilar material joining of AISI 304 and AISI 316 with DUPLEX 2205.
- Effect of post weld heat treatment (PWHT) has been studied by many researchers for various grades of steels. Same may also be carried for these materials.
- Bending and reverse bending test etc. may also be carried along with other non-destructive tests like radiography, ultrasonic testing etc.
- Welding speed may be an important parameter in GMAW process and may be studied in fully/semi-automatic GMAW welding machines.
- Microstructure analysis may be carried on the welded joints by using XRD to study the various grains.
- Effect of flux material may be carried out in GMAW process.

References

Abbasi, K.; Alam, S.; Khan, M.I. (2011) An experimental study on the effect of increased pressure on GMAW welding arc. *International Journal of Applied Engineering Research*, 2: 22–27.

Durgutlu, A. (2004) Experimental investigation of the effect of hydrogen in argon as a shielding gas on GTAW welding of austenitic stainless steel. *Materials and Design*, 25: 19–23.

Ebrahimnia, M.; Goodarzi, M.; Nouri, M.; Sheikhi M. (2009) Study of the effect of shielding gas composition on the mechanical weld properties of steel ST 37-2 in gas metal arc welding. *Materials and Design*, 30: 3891–3895.

Elsawy, A.H. (2001) Characterization of the GTAW fusion line phase for super ferritic stainless steel weldments. *Journal of Materials Processing Technology*, 118: 128–132.

Gulnec, B.; Develi, K.; Kahraman, N.; Durgutlu, A. (2005), Experimental study of the effect of hydrogen in argon as a shielding gas in GMAW welding of austenitic stainless steel. *International Journal of Hydrogen Energy*, 30: 1475–1481.

Ibrahim, I.A.; Mohamat, S.A.; Amir, A.; Ghalib, A. (2012) The effect of gas metal arc welding (GMAW) processes on different welding parameters. *Procedia Engineering*, 41: 1502–1506.

Juang, S.C.; Tarng, Y.S. (2002) Process parameter selection for optimizing the weld pool geometry in the tungsten inert gas welding of stainless steel. *Journal of Materials Processing Technology*, 122: 33–37.

Kang, B.Y.; Prasad, Y.; Kang, M.J.; Kim, H.J.; Kim I.S. (2009) The effect of alternate supply of shielding gases in austenite stainless steel GTA welding. *Journal of Materials Processing Technology*, 209: 4722–4727.

Karadeniz, E.; Ozsarac, U.; Yildiz, C. (2007) The effect of process parameters on penetration in gas metal arc welding processes. *Materials and Design*, 28: 649–656.

Khanna O.P. (2011) A Text book of Welding Technology, Dhanpat Rai Publications, New Delhi. 2nd Edn.

Kobe Steel (2011) Essential factor in gas metal arc welding, Kobe Steel Ltd, Japan 4th edn.

Li, D.; Lu, S.; Li, Y. (2010) Weld pool shape variations and electrode protection in double shielded GTAW welding. *Advanced Materials Research*, 97–101: 3978–3981.

Lothongkuma, G.; Chaumbaib, P.; Bhandhubanyong, P. (1999) GTAW pulse welding of 304L austenitic stainless steel in at, vertical and overhead positions. *Journal of Materials Processing Technology*, 89–90: 410–414.

Lu, S.P.; Qin, M.P.; Dong, W.C. (2013) Highly efficient GTAW welding of Cr13Ni5Mo martensitic stainless steel. *Journal of Materials Processing Technology*, 213: 229–237.

Norrish, J. (2006) Advanced Welding Processes, Woodhead Publishing Limited, Cambridge, England. Ist Edn.

Palani, P.K.; Murugan, N. (2006) Selection of parameters of pulsed current gas metal arc welding. *Journal of Materials Processing Technology*, 172: 1–10.

Parmar R. S. (2011) Welding processes and technology, Khanna Publishers New Delhi.

Pires, I.; Quintino, L.; Miranda, R.M. (2007) Analysis of the influence of shielding gas mixtures on the gas metal arc welding metal transfer modes and fume formation rate. *Materials and Design*, 28: 1623–1631.

Ruan, Y.; Qiu, X.M.; Gong, W.B.; Sun, D.Q.; Li, Y.P. (2012) Mechanical properties and microstructures of 6082-T6 joint welded by twin wire metal inert gas arc welding with the SiO2 flux. *Materials and Design*, 35: 20–24.

Suban, M.; Tusek, J. (2001) Dependence of melting rate in GMAW/MAG welding on the type of shielding gas used. *Journal of Material Processing Technology*, 119: 185–192.

Tewari, S. P.; Gupta, A.; Prakash J (2010) Effect of welding parameters on the weldability of material. *International Journal of Engineering Science and Technology*, 2(4): 512–516.

TMR Stainless (2009) Practical Guidelines for the fabrications of duplex stainless steels, IMOA, London UK 2nd edn.

Web References

http:/www.lincolnelectric.com/gmawweldingguide, downloaded on dated- Dec 05, 2013.

http:/www.millerwelds.com-pdf-GMAW-Welding-Tips, downloaded on dated- Aug 10, 2013

http:/www.smt.sandvik.com/en/products/weldingproducts/shieldinggases/shielding-gases-for-GMAW, downloaded on dated- Aug 01, 2013

http:/www.boconline.co.uk/shielding-gas-brochure410_80125, downloaded on dated- Sep 06, 2013

http://www.twi.co.uk/technical-knowledge/job-knowledge/equipment-for-submerged-arc-welding-016, downloaded on dated Dec 07, 2013.

http://www.burnsstainless.com/weldingarticle1.aspx, downloaded on dated Dec 07, 2013.

http://www.nhml.com/martensite-in-austenitic-stainless-steel-welds.cfm downloaded on dated Dec 07, 2013.

http://www.corrosionist.com/Shielded_metal_arc_welding_(SMAW).htm downloaded on dated Dec 07, 2013

http://dc347.4shared.com/doc/RThV4o3P/preview.html downloaded on dated Dec 07, 2013

http://www.zirconium-tungsten-electrode.com/Advantages-of-Zirconium-Tungsten-Electrodes.html downloaded on dated Dec 07, 2013